MUTUAL DIFFUSION OF BINARY GAS MIXTURES

Peter John Carson, B.Sc.(Hons.)

A thesis presented for the degree of

Doctor of Philosophy

March 1974

Department of Physical and Inorganic Chemistry,

University of Adelaide.

Contents

Contents

List of Figures

List of Tables

ABSTRACT

This thesis reports the measurement of mutual binary diffusion coefficients of gases using an apparatus styled on that designed by Harned for diffusion studies of electrolyte solutions. It was unnecessary to calibrate this apparatus against any standard system in order to obtain absolute values.

The diffusion coefficients of the gas pairs He-Ar, He-Kr, He-$CClF_3$, H_2-Ar and H_2- N_2 were measured as a function of mole fraction at 300 K and near 1 atmosphere pressure. The He-Ar system was also studied as a function of temperature in the range 278 to 325 K at pressures near 1 atmosphere. The results from the temperature and composition dependences were discussed with reference to the Chapman and Enskog theories.

In addition, a pressure dependence study was attempted, also on the He-Ar system, but due to experimental difficulties, this was restricted to the range 1 to 5 atm.

This thesis contains no material which has been accepted for the award of any other degree or diploma in any University, and to the best of my knowledge and belief, contains no material previously published or written by another person, except where due reference is made in the text.

ACKNOWLEDGEMENTS

I wish to show my appreciation of my supervisor, Dr. P.J. Dunlop, for his guidance and his ready willingness to provide assistance throughout this project.

I take this opportunity to thank the staff of the electronics workshop, Mr. K. Shepherdson, Mr. J. Beard, and formerly Mr. R. Weste, and of the mechanical workshop, Mr. A. Bowers and Mr. J. Netting. I also thank my fellow students, particularly Mr. M. Yabsley, and a former student Dr. K. Harris.

INTRODUCTION

The Chapman and Enskog theories describe the transport properties i.e. viscosity, thermal conductivity, diffusion, by connecting the sizes of molecules and the forces between them with the values of the transport coefficients. These intermolecular parameters may be calculated from a set of values of only one coefficient and, in turn, the calculated parameters allow the estimation of the coefficient for both smoothing of the original data and extrapolation to experimentally inaccessible regions. In addition, other transport coefficients may be calculated from the results of a more easily measured coefficient. For example, mutual diffusion coefficients have been computed, with an accuracy similar to that from direct determinations, using the accurate measurements of the viscosity coefficient[59] of the same system.

It can be seen that the Chapman and Enskog theories are very useful for dealing with the transport properties of gases. However, there have been doubts cast upon some aspects of these theories, specifically, that the measured concentration dependence[18,65] (see also ref. 43, p. 83) of the diffusion coefficient for some systems did not correspond to the theoretical predictions. It is the purpose of this thesis to experimentally investigate this reported behaviour.

Because the diffusion coefficient changes by only about 4% max. over the entire mole fraction range for most binary gas systems, the precision of the method for such an investigation must be very high.

The majority of methods that have been used previously did not have a precision of better than, at best, about ± 1%[43] near room temperature. Accordingly, the concentration dependence of diffusion coefficients has not been experimentally examined by many workers.

Our method, reported here, is believed to have an accuracy of about ± 0.2% for individual determinations at almost any mole fraction. The method is in some ways similar to the classical Loschmidt method[21] but we are able to monitor concentrations throughout each experiment; also the diffusion coefficient obtained is specific to a known mole fraction. The possibility of leaks is also reduced because of the absence of any partition within the cell as is required in the Loschmidt technique.

Descriptions of other apparatuses used for measuring diffusion coefficients have been summarised in a thesis by Marrero.[43] His thesis also correlates all diffusion data published up to 1969. Since then, Hogervorst has presented measurements of most of the raregas binary systems using a rather different technique, involving cataphoretic segregation, which is very suitable for measuring the temperature dependence.

Chapter 1

APPARATUS AND METHOD

Fick's 2nd Law of Diffusion may be written as

$$\left(\frac{\partial c_i}{\partial t}\right)_{x,y,z} = \text{div}\,(D_i . \underset{\sim}{\nabla}\, c_i)_t \qquad (1.1)$$

where c_i is the concentration of the ith component,

t is the time variable,

x,y,z are the fixed spatial coordinates,

and D_i is the diffusion coefficient.

This expression can be considerably simplified for experimental use in determinations of the coefficient, D_i. Firstly, most experimental situations require that there is only a one-dimensional concentration gradient (e.g. along the x - direction). Secondly, if these gradients are small enough, the diffusion coefficients may be assumed to be independent of concentration for that particular experiment; this condition is readily met for gas mixtures since the D_i have only a slight dependence upon composition over the entire composition range. Furthermore, for two-component systems measured with respect to a volume-fixed frame of reference, $D_1 = D_2 = D_{12}$, as can be readily shown.[1] A volume-fixed frame of reference is one for which the nett flow of volume relative to it is zero. A system confined to fill a constant volume cell and containing no pressure gradients (e.g. the gas phase is a good approximation for such a system) has its cell-fixed and volume-fixed frames of reference identical. These conditions reduce equation

(1.1) to

$$\left(\frac{\partial c}{\partial t}\right)_x = D_{12} \left(\frac{\partial^2 c}{\partial x^2}\right)_t \qquad (1.2)$$

A cell of length, ℓ, and closed at both ends imposes the boundary conditions

$$\frac{dc}{dx} = 0, \quad \text{at} \quad x = 0 \text{ and } x = \ell, \qquad (1.3)$$

which simply means that the cell is impermeable to the diffusing material and so allows no flow through the ends of the cell. A solution is the Fourier series,[2]

$$c = a_o + \sum_{n=1}^{\infty} a_n . \exp\left(-\frac{n^2\pi^2}{\ell^2} D_{12} t\right) . \cos\frac{n\pi x}{\ell} \qquad (1.4)$$

This form of solution can be more useful than that employing error functions as was demonstrated by Harned[3] in a design of a cell for measuring diffusion coefficients of dilute electrolyte solutions. When differences of concentration are taken at sites equidistant from each end of the cell e.g. at $x = a$ and $x = \ell - a$, equation (1.4) becomes

$$c(a) - c(\ell - a) = 2.a'.\cos\frac{\pi a}{\ell} + 2.a_3'.\cos\frac{3\pi a}{\ell} + 2.a_5'.\cos\frac{5\pi a}{\ell} + .. \qquad (1.5)$$

where $a'_n = a_n . \exp\left(-\frac{n^2\pi^2}{\ell^2} D_{12} t\right)$, i.e. all the even terms disappear. Additionally, if these two sampling sites are at positions, $x = \ell/6$ and $x = 5\ell/6$, the 3rd, 7th, etc., terms also disappear to give

$$c(\ell/6) - c(5\ell/6) = 2/\sqrt{3} \left\{ a_1 . \exp\left(-\frac{\pi^2}{\ell^2} D_{12} t\right) + a_5 . \exp\left(-\frac{25\pi^2}{\ell^2} D_{12} t\right) + \ldots \right\} \quad (1.6)$$

Thus it can be seen that, since the a_n coefficients are similar in magnitude (see Appendix A), the series converges to the first term very rapidly with time yielding

$$\ln [c(\ell/6) - c(5\ell/6)] = -\left(\frac{\pi^2}{\ell^2}\right) D_{12} t + \text{constant.} \quad (1.7)$$

A plot of ln (concentration differences) versus time is a straight line graph, with the diffusion coefficient obtainable from the slope,

$$D_{12} = -(\ell/\pi)^2 \times \text{slope.} \quad (1.8)$$

By taking a large number of readings of concentration difference over an extended period of time, the error in the slope, and consequently in D_{12}, will be reduced. In addition, since these readings are taken towards the end of a run when the concentration differences are reduced, the value of D_{12} obtained approaches the value of the differential diffusion coefficient, i.e. the value of D_{12} corresponding to the composition of the final mixture.

Often, concentrations themselves are not measured directly but some sensitive physical property which varies with concentration is monitored instead. This was the case in Harned's study in which he used two pairs of electrodes which detected changes in ionic

conductance. This property is, however, not directly proportional to concentration, although this proportionality is the leading term in a polynomial-like series. By taking differences in the conductivities, some of the higher terms cancel exactly whilst the others are reduced in magnitude so that the difference in conductivities is nearly proportional to the difference in concentrations, and becoming more so with decreasing size of the differences (increasing time). It is this aspect which is particularly appealing for gas analysis since there are not many (inexpensive) detectors which give a proportionality to concentration.

Gover[4] also exploited this design in order to measure mutual binary gas diffusion coefficients at room temperature. His cell was a vertical metal cylinder with sampling ports at $\ell/6$ and $5\ell/6$; these ports were small holes sealed with rubber septa through which hypodermic syringes were pushed, simultaneously, at regular intervals and samples withdrawn to be analysed in a gas chromatograph. Although, for its purpose - a student experiment - it was very adequate, this method of sampling has several drawbacks for very accurate determinations. In addition to the pressure being lowered within the cell, the flow lines within the cell are disturbed as samples are drawn into the syringe. The sampling needs to be done simultaneously; besides, it also makes accurate thermostatting of the cell difficult. There is also a possibility of selective permeation (for low molecular weight gases) and adsorption (for polar molecules) at the septa.

The design of the cell used for obtaining the results reported here was similar to that used by Gover. The main difference involved the choice of concentration detectors; we used thermistors, one screwed into each of the ports at $\ell/6$ and $5\ell/6$ so that the progress of a diffusion run could be monitored continuously.

Thermistors are (physically) small resistors which have a large negative temperature coefficient of resistance, α, i.e. the resistance decreases rapidly with increasing temperature. Those chosen for this work were Fenwal[5] type G112 [Fig. 1], which are pairs matched to within 30, 25, 20, 20 mv of each other at 2, 5, 10 and 15 milliamperes in a helium environment, and their resistances (zero current flow) to within 2% of each other at 25°C. Thermistors with designations G112 H and G112 P with 2x and 3x, respectively, stricter specifications were also used, but the results obtained appear to be the same, within experimental error. The thermistor beads are composed of oxides of metals such as nickel, copper, cobalt, iron, manganese and uranium sintered together to make a ceramic mass and this is then covered with a layer of glass for protection. However, this is not sufficient protection against the effects of hydrogen[8] which is (apparently) able to diffuse through the glass and chemically react with the oxides which both changes the characteristics of the bead and generates heat as well. It was noted that van Heijningen[19] *et al.* used thermistors without any shielding in measurements of the N_2-H_2 system; this hydrogen attack[12,13] could account for what they ascribed to a constant temperature drift - this would make their procedure of calculating the asymptote rather suspect.

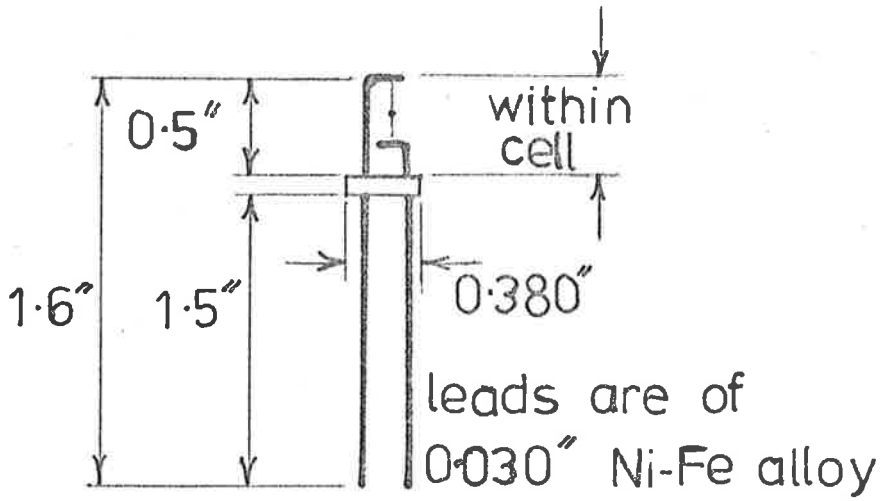

Fig. 2: Fenwal G 112 Thermistor

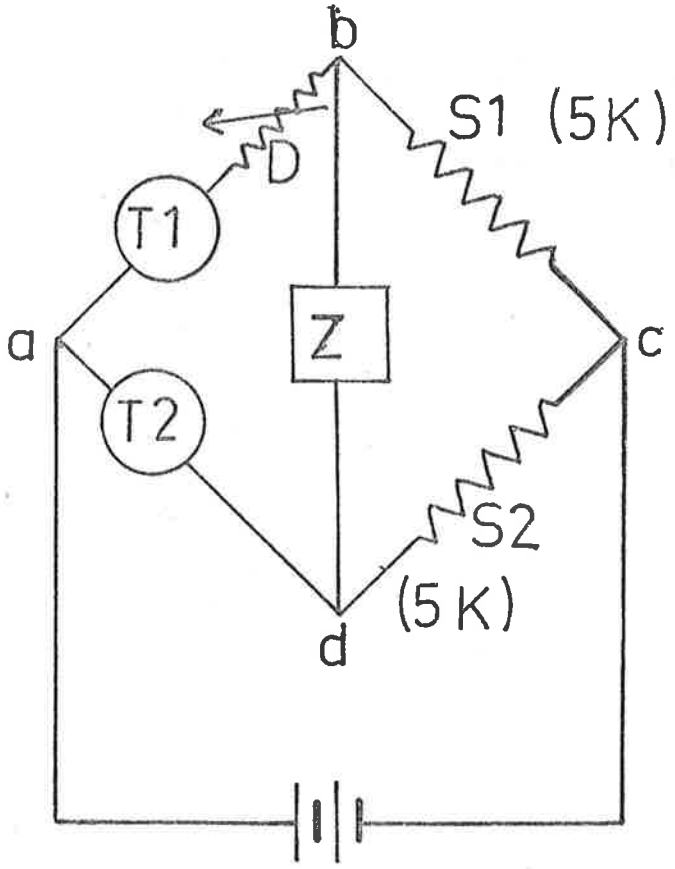

Fig. 2 : Measuring Circuit

Since α is so large, the resistance depends quite markedly upon the power, and hence upon the current, flowing through them so that a thermistor's intrinsic resistance is measured at zero current flow. Also, when a current is flowing, the resistance is dependent upon the thermal conductivity of its environment; a more highly conducting medium carries Joulean heat (I^2 R) from the thermistor more rapidly so that it is cooler and with a higher resistance than in a medium of low thermal conductivity. At a constant ambient temperature, it can be seen that a thermistor's resistance is a measure of the thermal conductivity of the medium, if a constant voltage is used.

By making each thermistor T_1, T_2, a separate arm of a Wheatstone bridge circuit [Fig. 2], with the other two arms S_1, S_2, each being a temperature - independent resistor and of the same resistance, the difference in resistance of the two thermistors can be recorded simultaneously. This can be done by adjusting the variable resistance, D, in series with T_1 so that there is no potential drop across b,d as indicated, for example, by an automatic recording potentiometer, Z. The difference in resistance, T_1-T_2, is given by-D, the value of the variable resistance.

The recorder, Z, used in this work was either a Philips PM 8100 or a Leeds & Northrup Speedomax XL681, with differences in the potential between b and d being monitored on the 1 millivolt full scale (10") range. The variable resistance box, D, used was either a Cambridge Instrument's L-426149 with a specified accuracy of 0.05% or an Electro Scientific Industry's Decabox DB 62 with a specified

accuracy of ± (.01% + 0.001 Ω)/year. The standard resistors were mica card resistors, nominally of 5 K Ω ± 0.05%, although the pair used here was matched to better than 0.001%. Fluctuations in voltage of the constant voltage power supply tend to cancel out if the bridge is at or near balance; by deliberately altering the voltage by 1 volt in the range 2-5 volts the balance is altered by only a few tenths of an inch. The power supply, constructed by the Department's electronics workshop, has a temperature variation in voltage of .003%/°C, and a load variation of 1 K Ω in series with the bridge circuit alters the voltage by less than 0.02%. The balance point of the bridge can be maintained to better than about ± 0.02 Ω if the thermistors are in the same thermostatted environment, as occurs before or after a diffusion run. This variation can be largely attributed to the random fluctuations in temperature of the thermostat bath.

The diffusion cell itself [Fig. 3] consists of a hollow stainless steel (type 316) cyclinder 102.0, 60.015 or 45.019 cm in height and 5 cm in outside diameter, with the cylinder walls being 0.25 cm in thickness. Each end-plate was attached by screws onto a flange which had been argon welded (to prevent small pinhole leaks) to the outside of each end of the cylinder. Viton O-rings were placed in an annular groove cut into each end-plate and clamped between the flange and the end-plate thus providing the vacuum seal. A similar technique was used to seal the other metal-metal interfaces. The end-plates, which were each 1 cm thick, had threaded holes drilled through the centre in order to take a hexagonal bolt which was in turn drilled and threaded. This

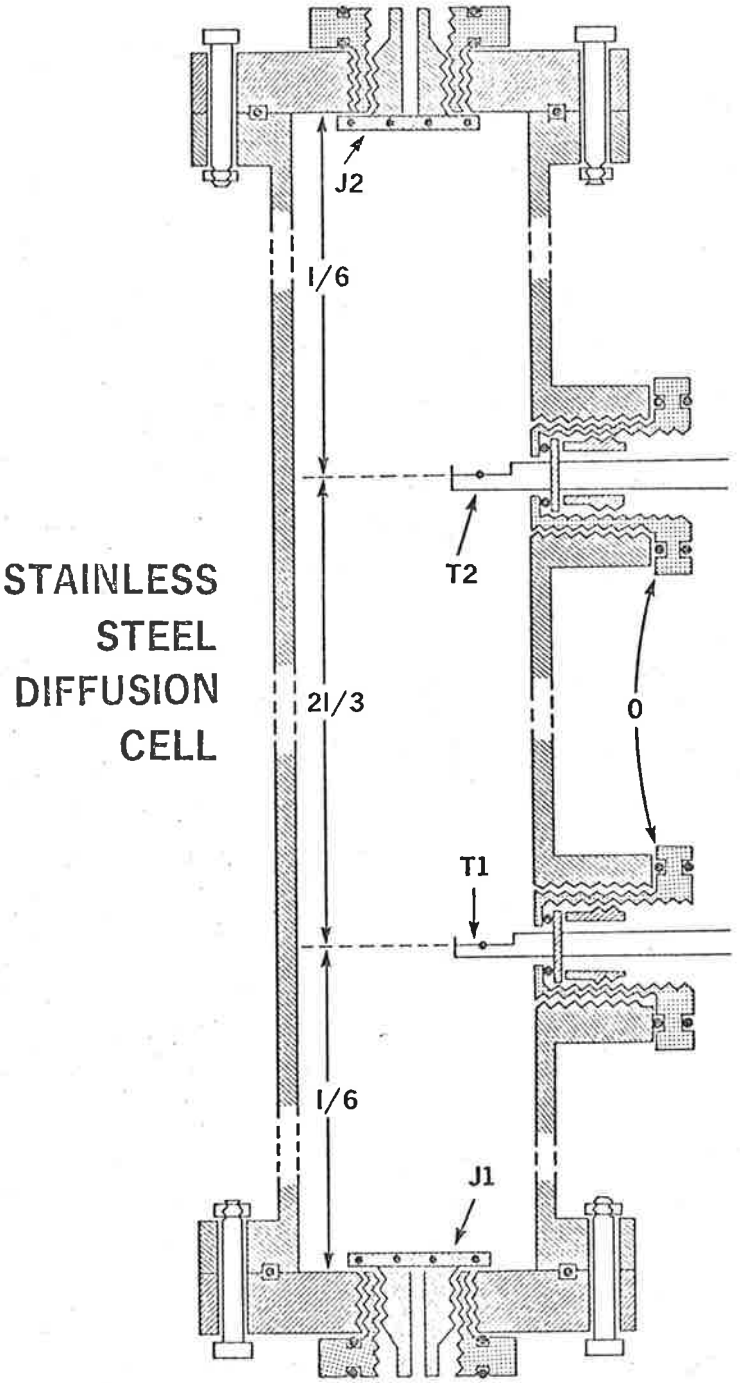

Fig. 3 : Diffusion Cell

bolt carries, on the internal side, a brass jet (J1, J2), and on the outer side, a Nupro bellows valve, B4H, not shown in the figure, which provides the gas inlet. The brass jets, which were of various sizes in order to determine the effect of their size, were used to both control the rate and direction of the gas flowing into the cell and to reduce the size of the volume between the valve and the cell (about 0.3 ml).

The sampling ports, shown in fig. 3, are also argon welded to the cylinder and take a hexagonal bolt, similar to those described above, which just fill the length of the port. These bolts allow a thermistor assembly to be positioned inside them, and this is then held securely with a hollow screw which is tightened behind it. These hexagonal bolts, and those in the end-plates, allow easy access to their attachments for replacement purposes.

A hollow brass box, with a removable lid, was screwed into each bolt behind the hollow screw. This box allows watertight electrical connections to be made to each thermistor. Shielded cable was used for leads to prevent spurious signals and the cell earthed with the shielding.

The cell was held at two positions by a clamp, and the clamp was positioned kinematically[6] so that the cell was supported vertically (checked with a sensitive box level) below the surface of a large glass-fronted water-bath containing about 500 kg of deionised water. The water was stirred vigorously (with a 1/3 H.P. motor) to reduce thermal

gradients and the temperature was maintained to better than ± 0.001°C by a combination of constant base and on/off heaters of stainless steel pyrotenax. The base heater, positioned at the end of the bath closest to the cell, was adjusted by rheostat to produce a slightly falling temperature and then the temperature was regulated with a thyratron control with a mercury-toluene regulator.[7] The temperature of the laboratory was maintained to ± 2°C throughout the year so that adjustments via the base heater were not usually required; it also reduced temperature fluctuations in the resistance elements of the measuring circuit.

The temperature fluctuations within the cell could be observed quite easily by replacing one of the thermistors in the bridge circuit with a resistor of a similar resistance (so that current conditions within the bridge were approximately the same). The fluctuations were displayed as variations in the recorder output with a spread of about 0.5" for 3 volt across the bridge. The temperature/resistance relation for thermistors is given by

$$R_{(T)} = R_{(1)} \cdot e^{\beta \left(\frac{1}{T} - \frac{1}{T_1}\right)} \qquad (1.9)$$

where $R_{(1)}$ is the resistance of the thermistor at T_1 °K

$R_{(T)}$ is the resistance of the thermistor at T °K

and β is a constant depending on the material from which the thermistor is made; $\approx$ 4000 for Fenwal material.

$$\therefore \qquad dT = -\frac{dR}{R_{(T)}} \cdot \left(\frac{T^2}{\beta}\right) \qquad (1.10)$$

Therefore, the temperature range can be calculated from the resistance range. Equation (1.10) also gives a means of calculating the temperature of the thermistor. By integration,

$$T_2 = \frac{\beta}{\ln\left(\frac{R_1}{R_2}\right) + \frac{\beta}{T_1}} \qquad (1.11)$$

It is found that the thermistors are less than 4° above ambient for the range of voltages used, at least when no diffusion is taking place.

Another advantage of using the difference in signal between two detectors is also demonstrated here. With only one thermistor in circuit, the "thermostat noise" amounts to about 0.5"; with both thermistors, this noise is reduced to about 0.05". This reduction is due to the tendency of temperature fluctuations to occur at the same time throughout the cell.

Since diffusion coefficients are, to a good first approximation, inversely proportional to the pressure, the accuracy of the D_{12} obtained, when referred to a particular pressure or density, is directly proportional to that of the pressure measurement. A Bourdon - type gauge,[9] the essential feature of which is an interchangeable quartz spiral for different ranges, is used to measure pressures. Each spiral had previously been calibrated by Texas Instruments with reference to a Primary standard Micrometer Barometer or to a dead-weight tester at

about twenty points for each range. The reproducibility of the gauge reading is similar to the calibration instruments' so that the gauge's accuracy is that of the calibration of about ± 0.05 mm. Pressures can be read very rapidly, and in digital form, without using liquids, which could possibly contaminate the system.

The block diagram of the apparatus is shown in Fig. 4. The connecting tubing is of 1/2" stainless steel with joins made using Swagelok[10] fittings; teflon front and brass back ferrules were used when pressures up to 1 atmosphere were to be used, and stainless steel or brass ferrules, depending if stainless steel or brass nuts, respectively, were used, for greater pressures. The metal ferrules required pre-swaging before use.[11] The advantage of using teflon ferrules is that the joint is readily broken and remade so that modifications or replacements can be carried out easily, whereas the metal ferrules form a semi-permanent joint; if these were re-made, the joint had to be carefully checked for leaks. Flexible braided metal tubing was used for joints requiring manoeuvrability but its use was kept to a minimum since it took a long time to de-gas when evacuating the apparatus. The whole system could be pumped out, right back to, and including, the gas cylinder heads, to give a pressure of 10^{-5} - 10^{-7} mm and a leak/degassing rate of about 10^{-4} mm/min. The vacuum pumps used were an Edwards (silicone) oil diffusion pump with an Edwards "Speedivac" two stage rotary oil pump.

An experiment was performed by (i) loading the cell (and pressure gauge so that pressure could be registered) with one gas, (ii) sealing

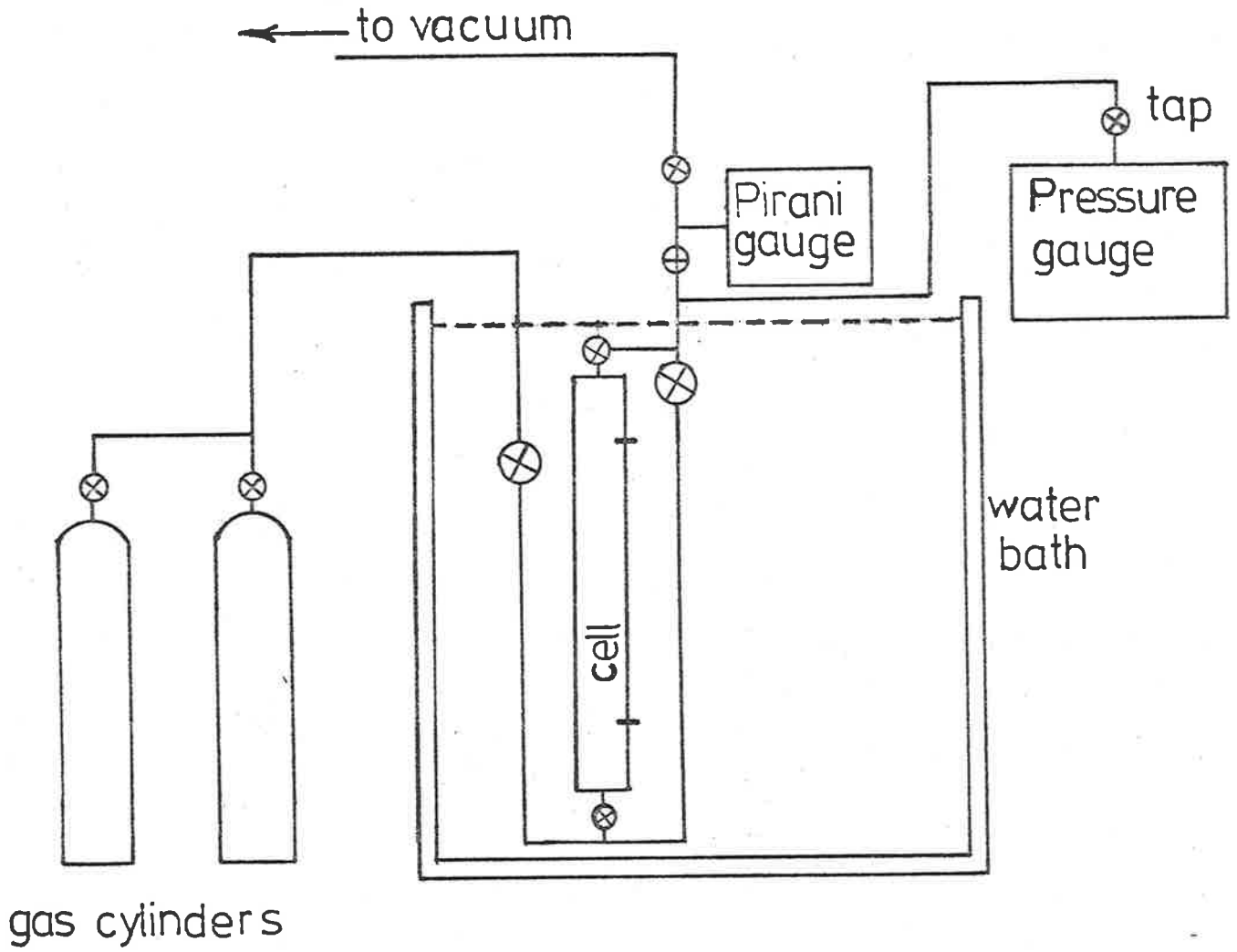

Fig.4: Block Diagram of Apparatus

off the cell and pumping out the gauge and all the connecting tubing, (iii) filling up the tubing and gauge with a second gas to a greater pressure than that within the cell, and then (iv) letting the gas into the cell slowly through either top or bottom Nupro valve, depending on whether the second gas is less or more dense, respectively, than the first; this time varied from one to four minutes. (v) Readings of the difference in resistance between the thermistors were taken as a function of time. Further experiments could be performed by withdrawing some of the gas mixture from the cell and repeating steps (ii) → (v).

The time required for a gas to reach the water bath temperature was shown, by using the thermistor circuit, to take, at most, two or three minutes, even if the gas is taken directly from the cylinder (at about 2000 p.s.i. pressure). The circuit is quite sensitive to temperature changes; it was shown that a shift in bath temperature of 0.2° altered the balance point by about 0.3" which is very easily seen compared to the noise. This indicates that temperature changes caused by the Joule-Thomson effect disappear rapidly and so will not cause any significant disturbance on a diffusion run after about five minutes.

Since, in general, all real gases are non-ideal at other than very low pressures, there is generally a pressure change when two gases are mixed. Therefore, the pressure measured just after letting in the second gas should differ from that at the end of the run. This was observed, although the difference only amounted to about 0.25% at pressures up to five atmospheres. The difference in pressure before mixing, P_b, and the pressure when mixing is complete, P_f, is given by

(see Appendix B)

$$P_f = \frac{P_b}{1 - x_1.x_2.P_b.[2B_{12} - (B_1 + B_2)]} \qquad (1.12)$$

if third, and higher, virial coefficients are neglected.

B_1, B_2 are the second virial coefficients of gases 1 and 2.

B_{12} is the (second) interaction virial coefficient.

x_1, x_2 are the mole fractions of gas 1 and 2 in the final mixture.

It can be seen that for a pair of gases at a given temperature, the pressure change is always of the same sign for all compositions. If $B_{12} = (B_1 + B_2)/2$ there will be no pressure change.

Decade box resistance and time measurements were taken at equal intervals of resistance, usually one ohm, for about 80 - 100 readings which usually spread over about 80 minutes. It was found that those readings taken before about 20 minutes from adding the second gas were systematically in error and had to be discarded. This is probably due to some after effects of convection caused by letting in the second gas. This puts a lower limit on the magnitude of the charge of the second gas to be added.

The stopwatch used was calibrated against an electronic timer which has an accuracy of 0.01%. Times were recorded at which the recorder pen passed a pre-set zero position indicating that the two

thermistor arms of the bridge were equal; these times were able to be observed with an accuracy of ± 0.3 sec. The final difference in resistance, RF, after diffusion is complete, was usually measured about five hours after the start.

All the gases used for this report had a purity of better than 99.9% except for the $CClF_3$ which was specified to be better than 99.0%. No further purifications were attempted before the gases were used.

Mercury-in-glass thermometers monitored the thermostat bath temperatures. These were calibrated annually against platinum resistance thermometers so that the temperature of the baths can be measured at about ± 0.001_5°.

By assuming a proportionality between the difference in thermal conductivity and difference in concentration at the two thermistor positions at any given time, for the period over which readings are taken, it can be shown that the difference in resistance, ΔR_t, of the thermistors is also proportional to the difference in concentration (Appendix C). The measured times were corrected to allow for the pressure change, indicated in equation (1.12), occurring during diffusion assuming that the pressure change occurs at the same rate as diffusion. (The value of P_b in (1.12) has also to be altered slightly for the same reason). The pressure differences indicated by (1.12) agreed with those obtained experimentally. Linear plots of $\ln(\Delta R_t - RF)$ versus time were usually obtained, although occasionally some (sometimes as many as 30)

of the initial points had to be rejected in order to obtain linearity. (The computer program for processing this data is listed in Appendix as RFFIXM). Most data obtained at slightly elevated pressures, i.e. greater than 1 atmosphere, were curved and the above procedure could not be applied very satisfactorily (see next Chapter).

To summarise, the advantages of this apparatus for measuring diffusion coefficients are:

i) The high sensitivity of the thermistors to concentration changes, particularly for gases of large thermal conductivity differences.

ii) This allows the diffusion coefficient to be measured towards the end of the run so that the differential diffusion coefficient is obtained. Disturbing influences due to letting gas into the cell are also reduced in this manner. Equation (1.7) is more closely followed at larger times too.

iii) No zero-point time is required as is required by some methods.[14,15,21]

iv) The precision can be increased by taking a large number of measurements of resistance difference.

v) The thermistors are physically small and monitor the diffusion continuously without disturbing the flow lines significantly. The heating of the gas by the thermistors has little effect upon the rate of mixing (by causing convection) as is demonstrated by the stability of the base-line trace given by the recorder.

vi) The method is one for determining absolute values of diffusion coefficient.

vii) There are no sliding surfaces, which need to be polished and which develop leaks rather readily, such as are needed in a Loschmidt-type apparatus. These surfaces also require some lubricant which could cause some problems with adsorption.[15]

viii) The complete range of compositions of a pair of gases can be studied.

Some disadvantages are:-

i) Relatively large amounts of gas are required so that the gas mixtures studied have to be fairly cheap.

ii) Large water baths are required to accommodate the large cells used.

iii) Close temperature control of the cell is required because of the high sensitivity of the thermistors to temperature changes (see equation C.2).

iv) The thermistors are also sensitive to temperature changes generated during diffusion such as heat of mixing and Dufour effect.[16,17] This is discussed in Chapter 2.

v) The method is not capable of high precision for measuring self-diffusion, or where the thermal conductivity difference between the two components is small. However, we were particularly interested in systems containing helium + noble gas since van Heijningen[18] *et al.* reported some discrepancies encountered in the concentration depen-

dence of such systems. Our method seems to be very appropriate for such an investigation.

vi) The small dead volumes associated with the Nupro valves at each end of the cell causes a little uncertainty with the correct length to be used in calculating the absolute value of the diffusion coefficients. However, this can be calculated for and also checked experimentally by using different sized jets; for the 102 cm cell the correction only amounts to about 0.03% for the jets used.

vii) Another difficulty encountered was the corrosion that occurred at the brass Nupro valves; the water tended to attack the union between the bellows and the main body of the valve where solder had been used, and the valves had to be replaced after about 12 months of use.

Chapter 2

Some Applications of the Chapman and Enskog Theories

Chapman and Enskog, in the period from about 1910-1917, independently proposed rather similar theories for describing non-equilibrium processes in gases. (These two theories will be referred to as the C-E theory in the remainder of this thesis). The C-E theory produces expressions for the transport coefficients, e.g. the coefficients of mutual and thermal diffusion, viscosity and thermal conductivity, as long as some limitations are fulfilled. These limitations are presented more fully in the text of Hirschfelder, Curtiss and Bird[22] (HCB), p. 18-21, but will be summarised here.

i) The gases must be sufficiently dilute, i.e. the pressure must be low enough, that only binary collisions between molecules of the gases need be considered. However, as has been shown experimentally[23,24] and predicted theoretically by an extension to the C-E theory proposed by Enskog himself (see later this chapter), the deviations from the theory caused by increased pressures are rather small. It is generally considered that pressures of up to a few atmospheres cause experimentally insignificant departures from theory.

ii) The pressure must not be so low that the mean free path is comparable to any of the dimensions of the containing apparatus so that collisions between the molecules and the cell walls need to be

considered. In this region, apparatus requires to be calibrated to allow for such collisions.[18,19]

iii) The C-E solution applies only to situations where gradients in physical properties are small (compared to the reciprocal of the mean free path). Thus, for pressures of greater than about one atmosphere, the C-E solution applies to all but extreme conditions, such as is found in shock waves.

iv) The theory strictly applies only to monatomic gases but it is found that thermal conductivity is the coefficient most affected by this restriction, the other coefficients not being greatly changed if the molecules are not too non-spherical[19,25] or polar.[26]

v) The theory was derived using classical mechanics so that for low molecular weight gases at lower temperatures, significant deviations will be observed. However, these quantum corrections may be largely allowed for by the use of suitably adjusted tables.[27,28]

The solutions given by the C-E theory for the transport coefficients take the form of an infinite series, the higher order terms becoming rapidly more complex but also being much smaller than the first term,[29] except for thermal diffusion (HCB, p. 480, 481). The convergence properties of the series has not been fully

established but it appears that only the first and second terms are required for processing the results of this thesis.

The expression obtained by the C-E theory for the mutual diffusion coefficient of a binary mixture is (HCB, p. 539)

$$[D_{12}]_m = \frac{0.0026280 \sqrt{\frac{T^3 (M_1 + M_2)}{2 M_1 M_2}}}{P . \sigma_{12}^2 . \Omega_{12}^{(1,1)*} (T_{12}^*)} \cdot f_D^{(m)} \qquad (2.1)$$

where $[D_{12}]_m$ is the diffusion coefficient for the gas pair 1,2 as calculated using the first m terms of the C-E series. Its units are $cm^2 . sec^{-1}$.

P is the pressure in atmospheres.

T is the temperature (°K).

M_1, M_2 are the molecular weights of species 1,2.

σ_{12} is a molecular size parameter (Å).

$f_D^{(m)}$ is a term representing the higher approximations and is a function of molecular weights and mole fractions, among other parameters discussed later. $f_D^{(1)} = 1$.

$\Omega_{12}^{(1,1)*}$ is known as the reduced collision integral, and is the dimensionless ratio of the collision integral divided ("reduced") by its corresponding rigid sphere value

i.e. $$\Omega_{12}^{(1,1)*} = \Omega_{12}^{(1,1)} / \Omega_{12}^{(1,1)} \quad \text{(rig. sph.)}$$

The $\Omega_{12}^{(1,1)*}$ contains the details of the collision process (compared to

the idealised model of a rigid sphere collision), and is a function of the reduced temperature, $T_{12}^* = kT/\varepsilon_{12}$ °K, where k is Boltzmann's constant and ε_{12} is a parameter representing the interaction energy between molecules 1 and 2.

Overall then, it can be seen, in the first approximation, that the diffusion coefficient is dependent only on the interaction between unlike molecules and contains no terms representing interactions between like molecules. The C-E expressions for the thermal conductivity and viscosity coefficients of pure gases are similar to (2.1) except that like molecule parameters only are present in the first approximation; even for mixtures, the like molecule terms are predominant. Therefore, the diffusion (both mutual and thermal) coefficient is particularly important for investigating unlike interactions.

Since $f_D^{(1)} = 1$, the first approximation is independent of composition of the gas mixture. Higher approximations given by

$$[D_{12}]_m = [D_{12}]_1 \cdot f_D^{(m)} \qquad (2.2)$$

are composition dependent since the $f_D^{(m)}$ $(m \geqslant 2)$ are complicated functions of mole fraction and other parameters.

It can be seen from (2.1) that the diffusion coefficient is directly dependent on the parameter σ_{12} and indirectly on ε_{12} through

$\Omega_{12}^{(1,1)*}$. Because the form of the relation between ε_{12} and the collision integral is not given specifically but only through an intermolecular potential energy function, the form of this function needs to be known before calculations using (2.1) can be made.

It has been found that the form of this potential function cannot be deduced unambiguously from determinations of the bulk properties of gases.[30,31] In addition, quantum mechanics has only been able to derive usable functions for the very simplest molecular systems.[32,33] Instead, what is usually done is to assume the form of the potential function, using a mixture of intuitive and theoretical reasoning, and testing this with experimental data from transport properties to discard unsuitable choices. Unfortunately, there are a large number of such potentials which fit the experimental data satisfactorily over rather large temperature ranges but not universally nor over all the temperature range[34,35] without using different parameter values. (HCB, p. 1110) Such potentials fall into several classes[35] the more common of which, in approximate order of increasing complexity, are the m-6, the Kihara, the Morse, and the exp.6. These all predict that the potential energy of interaction, V(r), [Figure 5], between a pair of molecules tends to zero, although remaining attractive (i.e. negative), as the distance of separation, r, approaches infinity; that it increases rapidly so that the molecules repel each other strongly at small values of r; and at some intermediate r, of the order of a few Å, there is an

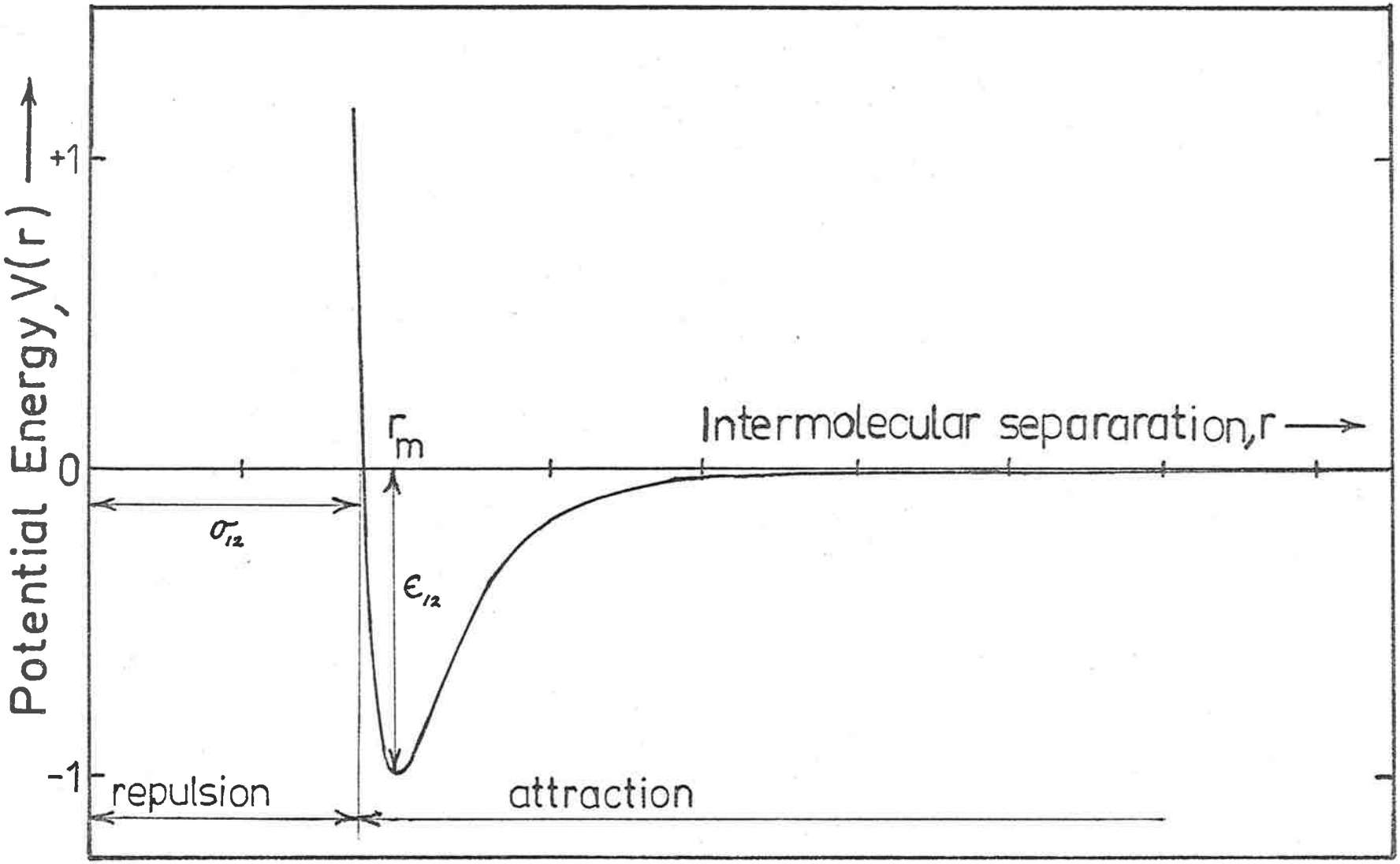

Fig. 5 : Intermolecular Potential Function, V(r).

attractive "potential well" at r_m of depth ε. At a distance $r = \sigma$, $V(r) = 0$.

The Lennard-Jones (12-6) potential, a member of the m-6 class, is usually written in the convenient form

$$V(r) = 4\varepsilon\left[\left(\frac{\sigma}{r}\right)^{12} - \left(\frac{\sigma}{r}\right)^{6}\right] \qquad (2.3)$$

which is the sum of an attractive potential, $-4\varepsilon\left(\frac{\sigma}{r}\right)^6$, which is predominant at large r, and a repulsive potential, $4\varepsilon\left(\frac{\sigma}{r}\right)^{12}$, predominant at small r. This potential, as well as the others mentioned above, is spherically symmetric and so is strictly applicable only to monatomic gases but it seems that small molecules are rather insensitive to this limitation.[26]

The inverse 6th power attractive term was deduced theoretically by London[36] (in 1930) and so this term is included in each of the above potentials (but the Morse which was designed particularly for regions about r_m). The repulsive part of the potential is rather less well known theoretically.[38] Experimentally, this region is best determined by very high temperature measurements, since this region is of high energy, or by high energy atomic beam scattering.[39] The inverse 12th power replusive term was introduced more out of mathematical convenience than theoretical backing[37] and several values other than 12 have been used, and this accounts for the family of m-6 potentials.

Because of i) its simplicity in having only two adjustable parameters, σ and ε, ii) the availability of collision integral tables,

particularly quantum corrected ones,[27] iii) its ability to reproduce the data about as well as other semi-empirical potentials even though they may contain more adjustable parameters, and iv) the abundance of data referred to it, the Lennard-Jones (12-6) potential is used in this thesis for correlating results. It has been found that by including an additional term proportional to the inverse 8th power or r, which is the next highest term for the attractive potential as calculated by London, better correlations of experimental data over more extended temperature ranges were possible. The value of m which best fitted the experimental data using this m-6-8 potential so formed was found to be 11 for each of the three noble gases (Ar, Kr, Xe) investigated.[34] However, this improved potential was not used since tabulations for it have yet to be published.

It can be seen that the C-E theory, through equation (2.1), predicts that the diffusion coefficient for a given system varies with temperature, pressure and, to a slight extent, with composition. Each of these dependences will now be examined individually.

Composition Dependence

The composition dependence is contained entirely in the factor $f_D^{(m)}$, and the form of this factor becomes rapidly more complex with increasing values of m. Kihara[40] gave a slightly simpler, and apparently more accurate, expression for this factor (denoted here by $g_D^{(m)}$ to distinguish it from the C-E factor $f_D^{(m)}$), and for m=2 this becomes

$$g_D^{(2)} = 1 + \Delta' \qquad (2.3)$$

where $$\Delta' = \frac{(6C_{12}^* - 5)^2}{10} \cdot \frac{x_1^2 P_1 + x_2^2 P_2 + x_1 x_2 P_{12}}{x_1^2 Q_1' + x_2^2 Q_2' + x_1 x_2 Q_{12}'} \cdot$$

x_1, x_2 are the mole fractions of the heavy and light components respectively. The P and Q are

$$P_1 = \frac{2 M_1^2}{M_2(M_1 + M_2)} \sqrt{\frac{2 M_2}{M_1 + M_2}} \left(\frac{\Omega_{11}^{(2,2)*}}{\Omega_{12}^{(1,1)*}}\right) \left(\frac{\sigma_{11}}{\sigma_{12}}\right)^2$$

$$P_{12} = 15\left(\frac{M_1 - M_2}{M_1 + M_2}\right)^2 + \frac{8 M_1 M_2 A_{12}^*}{(M_1 + M_2)^2}$$

$$Q_1' = \frac{2}{M_2(M_1 + M_2)} \sqrt{\frac{2 M_2}{M_1 + M_2}} \left(\frac{\Omega_{11}^{(2,2)*}}{\Omega_{12}^{(1,1)*}}\right) \left(\frac{\sigma_{11}}{\sigma_{12}}\right)^2 \cdot$$

$$(M_1^2 + 3M_2^2 + 1.6\, M_1 M_2 A_{12}^*)$$

$$Q'_{12} = 15\left(\frac{M_1 - M_2}{M_1 + M_2}\right)^2 + \frac{32\, M_1 M_2 A_{12}^*}{(M_1 + M_2)^2} + \frac{8(M_1 + M_2)}{5\sqrt{M_1 M_2}} \left(\frac{\Omega_{11}^{(2,2)*}}{\Omega_{12}^{(1,1)*}}\right) \cdot$$

$$\left(\frac{\Omega_{22}^{(2,2)*}}{\Omega_{12}^{(1,1)*}}\right) \left(\frac{\sigma_{11}}{\sigma_{12}}\right)^2 \left(\frac{\sigma_{22}}{\sigma_{12}}\right)^2$$

P_2, Q'_2 are obtained by interchanging subscripts in P_1, Q'_1. A_{12}^* and C_{12}^* are both ratios of collision integrals (HCB p. 528)

$$A^* = \Omega^{(2,2)*}/\Omega^{(1,1)*}$$

$$C^* = \Omega^{(1,2)*}/\Omega^{(1,1)*}$$

and are approximately equal to 1.

These complicated expressions for the composition dependence simplify considerably at the extremes of mole fraction. At $x_1 = 1$,

$$\Delta' = \frac{(6C_{12}^* - 5)^2}{10} \cdot \frac{1}{1 + 3\left(\frac{M_2}{M_1}\right)^2 + 1.6\left(\frac{M_2}{M_1}\right) A_{12}^*}$$

$$\rightarrow \frac{(6C_{12}^* - 5)^2}{10} \qquad \text{if } M_1 >> M_2$$

At $x_2 = 1$,

$$\Delta' = \frac{(6C_{12}^* - 5)^2}{10} \cdot \frac{(M_2/M_1)^2}{(M_2/M_1)^2 + 3 + 1.6\,(M_2/M_1)\, A_{12}^*}$$

$$\rightarrow 0 \qquad \text{if } M_1 >> M_2$$

It can be seen that the extent of the composition dependence is determined solely by the reduced temperature and almost completely by C_{12}^*. Therefore the value of ε_{12} can be calculated from the ratio of the diffusion coefficients at the two composition extremes. When this value is combined with the absolute value of the diffusion coefficients, the value of σ_{12} can also be obtained using (2.1).

Experimentally, the above procedure for obtaining the intermolecular potential parameters has to be modified since composition extremes are not accessible by our method of determining the diffusion coefficients but a large range of mole fractions is. These diffusion coefficients are fitted as a function of mole fraction by a least squares procedure (Program MMC, in appendix E) and the smoothed values of D_{12} at the lowest and highest mole fractions measured, together with the standard error of fit, are evaluated. With these smoothed values, together with literature values of σ_1, σ_2, ε_1, ε_2, the "best" values of σ_{12} and ε_{12} may be calculated using (2.1) and (2.3). From the fiducial limits[41] of both smoothed values of D_{12}, the corresponding fiducial limits of σ_{12}, ε_{12} may be calculated from the maximum and minimum ratios of the limiting D_{12}.

By taking measurements of D_{12} as close as possible to the intercepts, the values of σ_{12}, ε_{12} obtained are less dependent upon the pure parameter values assumed. Since quantum corrections are applied in such calculations (see Program CARKIH in appendix F),

a starting guess for the quantum parameter

$$\Lambda^* = \frac{h}{\sigma_{12}\sqrt{2\ \mu\ \varepsilon_{12}}}$$

(h is Plank's constant, μ is the reduced mass) is required so that the answers have to be re-iterated. No more than four iterations have ever been required to obtain convergence (a change in ε of less than 0.01% and in σ of less than 0.1%; the convergence occurs in an oscillatory manner so that the limit is assured to be in these limits). A wide variety of starting guesses of ε_{12}, σ_{12} always gives the same final result. Different values of σ_1, ε_1, σ_2, ε_2 have negligible effect even if they are poor estimates.

The function used to fit the diffusion coefficients as functions of mole fraction was of a form suggested by Amdur and Schatzki[42] and by Marrero and Mason[43]

$$D_{12} = a_1 + \frac{a_2\ x_1}{1 + a_3\ x_1} \qquad (2.4)$$

where a_1, a_2, a_3 are fitting parameters and x_1 is the mole fraction of the heavy component. It is found that this equation generally gives a better fit of the experimental data than does the polynomial

$$D_{12} = a_1 + a_2\ x_1 + a_3\ x_1^2 \qquad (2.5);$$

(2.4) also gives a lower intercept at $x_1 = 0$. It is because of this

slight ambiguity that extrapolations to the intercepts are not used in order to calculate the parameters $\varepsilon_{12}, \sigma_{12}$. By generating theoretical concentration dependences with the aid of (2.3) using an assortment of values of ε_{12}, σ_{12}, and fitting these dependences to both (2.4) and (2.5) it is invariably found that (2.4) gives the better fit and to within the accuracy of the generated data.

Temperature Dependence

Equation (2.1) may be rearranged to the form

$$D_{12} \cdot g_D^{(m)} \cdot P = \left(\sqrt{\frac{M_1 + M_2}{2 M_1 M_2}} \cdot \frac{0.0026280}{\sigma_{12}^2} \right) \left(\frac{T^3}{\Omega_{12}^{(1,1)*}} \right) \qquad (2.6)$$

i.e. $$Y_i = m X_i$$

The temperature dependence of the diffusion coefficient, at a given pressure, is given almost entirely by the X_i; there is only a slight dependence contained in $g_D^{(m)}$, and this contributes very little, especially at low mole fractions. This form of the equation suggests a simpler method of determining the potential parameters ε_{12}, σ_{12} than that used by, for example, van Heijningen *et al.*[18,19] and by Hogervorst.[44]

For a given set of D_{12}, T values, n sets of (X_i, Y_i) may be calculated by using n values of ε_{12}; a single value of σ_{12} needs

to be assumed also to evaluate the $g_D^{(m)}$ and Λ^* but since these have only a minor influence, the value of σ_{12} used is not particularly critical. Straight lines (which are fixed to pass through the origin) are fitted to each of these (X_i, Y_i) sets so that a "best" value of ε_{12} may be chosen from the fit of least standard error. This fit will also generate a best value of σ_{12} from the slope, m. By applying an F-test to the standard error of the best fit, the range of standard errors within the error limits, and hence the error limits of ε_{12} and σ_{12}, can be determined.

This method is very suitable for determining the potential parameters from a small temperature range since only one parameter, ε_{12}, needs to be adjusted to give the best fit; more parameters confuse the search when fitting a slight curve.

Pressure Dependence

It can be seen from (2.1) that for conditions of constant temperature and composition, the product $D_{12} \times P$ should be a constant. However, the C-E theory was derived for pressures where only binary collisions occur i.e. rather low pressures where the gases act as ideal gases with respect to their PVT properties. The use of (2.1) can be extended if account is taken of the change in density (from ideal) with pressure by using the product $D_{12} P (n/n_{ideal})$ so that the diffusion coefficient is still referred to the standard of 1

atmosphere pressure. If pressures are low enough (a few atmospheres) that only the second virial coefficient, B_M (atm^{-1}), need be considered, this product becomes

$$D_{12}\ P\ \left(\frac{n}{n_{id}}\right) = \frac{D_{12}\ P}{(1 + B_M.P)}\ , \qquad (2.7)$$

where n is the number density. It is this modification of the product D_{12} x P that is used in this thesis.

The original C-E theory, because it disregarded three-body and higher order collisions and it assumed the size of molecules were small compared to the average distance between them, was only correctly applied to dilute gases. Enskog extended the C-E theory by assuming that deviations caused by elevated pressures could be accounted for by assigning the molecules a rigid sphere diameter which was independent of pressure but different for each temperature. In effect, it is assumed that the intermolecular potential is unchanged by pressure variations since the collision cross-section, Ω, is held constant at its dilute gas value for that temperature. The influence of many-body collisions was disregarded due to theoretical difficulties,[45] although a recent article[46] describes a correction for a type of many-body encounter but which is applicable only for special conditions.

Enskog's theory was further extended by Thorne[47] to apply to binary mixtures, and this was combined with the Percus-Yevick approximation by McConalogue and McLaughlin[48] to yield an expression applicable

to diffusion up to very high pressures and all mole fractions. This expression can be written as

$$1-y = \frac{n\ D_{12}}{(n\ D_{12})^{\circ}} = \frac{(1-\S)^2}{(1-\S) + \left(\frac{3r\S}{1+r}\right)\left(\frac{x_1 + x_2\ r^2}{x_1 + x_2\ r^3}\right)} \qquad (2.8)$$

where $(n\ D_{12})^{\circ}$ is the value of the product $n\ D_{12}$ at zero density,

r is the ratio of the rigid sphere diameters $\frac{\sigma 2}{\sigma_1}$,

and § is the ratio of the volume of all the molecules to the volume of the system. If the ideal gas law is used for calculating the approximate number density of the system,

$$\S = \frac{\pi}{6}\ \frac{P\ \sigma_1^{\,3}}{k\ T}\ (x_1 + x_2\ r^3) \quad . \qquad (2.9)$$

It can be seen that § contains the pressure dependence. It was found[48] that (2.8) was able to reproduce the experimental data[49] within the estimated experimental error (for pressures up to 408 atmospheres).

For an example, the helium-argon system, using the Lennard-Jones (6-12) parameters as an approximation for the hard sphere diameters, the following values are obtained from (2.8):-

If $\left.\begin{aligned}\sigma_2 &= 2.56\ \text{Å}\\ \sigma_1 &= 3.42\ \text{Å}\end{aligned}\right\}$ $r = 0.749$

(He is component 2, Ar is 1),

then $\S = 5.04 \times 10^{-4} (x_1 + x_2 r^3) P$

[Note: the value of § for close packing is 0.74]

and	y equals	for	1 atm	5 atm
		at $x_2 = 0$	0.0012	0.0057
	and at	$x_1 = 0$	0.00057	0.0029 .

It can be seen, therefore, that at high mole fraction of Ar, the ratio $n D_{12}/(n D_{12})^\circ$ decreases in going from 1 atm. to 5 atm. by 0.45% for trace He, and by 0.23% for trace Ar.

It would appear that if the accuracy of the 1 atm. results was maintained, this decrease would be relatively easy to measure. However, it was found that for He-Ar diffusion runs at elevated pressures (of 3, 5, 6, 7, and 9 atm.), the output of RFFIXM using (1.7) became increasingly curved, particularly at higher mole fractions of argon. The only difference in experimental set-up between these runs was the length of the cell used in order to keep the runs to a suitable length of time; 102 cm cells were used for 1 atm. runs, 60 cm for 3 atm., and 45 cm for 5 atm. and higher. Using a 45cm cell, it was found that the other systems tried, N_2-Ar at 1.3 atm. and He-CO_2 at 4.2 atm., also gave similarly curved output.

It was suspected that temperature changes occurring with diffusion might be the cause of the difficulty. This was investigated by altering the thermistor circuit so that it was less dependent upon thermal con-

ductivity changes and relatively more responsive to temperature changes. The potential difference across the bridge circuit was reduced to about 0.05 volt (c.f. about 4 volt for usual diffusion run) - this reduces the sensitivity to changes in thermal conductivity differences (see (C.6)) relative to changes in temperature differences ((C.2) and (C.3)). It was not possible to use voltages much less than 0.05 volt due to the lowered signal/noise ratio. The output signal was amplified about 50 fold with a null detector (Leeds and Northrup, cat. no. 9834) before being fed to the recorder (Z in Fig. 2) so that a change of 1 ohm caused a change of about 0.6" in the recorder signal. For each diffusion run observed with this amplified signal, the signal rose sharply to a maximum of several ohms within 3 to 6 minutes and then returned to its original zero with approximately the same time constant as diffusion (half-time of approximately 16 minutes). This signal, therefore, behaved in much the same manner as that delivered by the usual bridge circuit except that it was of a smaller magnitude. In addition, the amplified signal was in the opposite direction from usual showing that the temperature differences produced by diffusion are such as to cool the lower region, containing the high molecular weight component, compared to the upper region of the cell.

For runs at 5 atm. (in the 45 cm cell), the maximum deflection of the amplified signal, for a 10% charge of the second gas, was about 7 ohms when helium was the added gas and about 4 ohms when it was argon. Using (C.2) and (C.3), this indicates that the difference in temperatures at the two thermistor positions were approximately 0.02° and 0.01°

respectively. However, this signal was found to be somewhat power dependent even though the b coefficients of (C.2) and (C.3) are negligibly dependent on the power at such low powers; if the voltage was doubled, the maxima were increased by a factor of less than 2. This indicates that the signal from thermal conductivity differences was still present. Results for 1 atmosphere (in the 102 cm cell) behaved similarly to the 5 atmosphere except that the magnitude of the maxima were reduced to less than one third.

Overall, these experiments demonstrated the presence of temperature changes accompanying diffusion, as well as their approximate rate of decay, but the size of these effects is in doubt. Kieselbach[53] demonstrated the use of screened thermistors for improved performance in gas chromatography. These screened thermistors, as used by Kieselbach, were for reducing the flow sensitivity but were used by us, in the 45 cm cell only, to conduct heat to or away from the vicinity of the thermistors. A screen of 48 mesh 0.005" silver wire was glued to each thermistor mounting so that the screen passed within a millimetre on each side of the thermistor bead. Using these screened thermistors, the output (from RFFIXM) of such diffusion runs were greatly improved in their linearity compared to those without screens. However, there still remained some non-linearity which increased as pressures greater than 5 atm. were used.

These experiments with amplified signals and screened thermistors indicated that interference was being caused by temperature differences being generated during diffusion, presumably by the

diffusion thermoeffect[54,55] (or Dufour[50] effect) and/or heat of mixing. The amplified signal experiments indicated that the temperature differences decayed at the same time constant, τ, as the diffusion since differences in temperature, $\Delta\theta$, between the two thermistors are directly proportional to differences in resistance, ΔR (see (C.2) and (C.3)). However, if this is the case, there should be no change in either diffusion coefficient or linearity of (1.7) for if

$$\Delta R \text{ (temp.)} = b.\Delta\theta = B\, e^{t/\tau}$$

and $$\Delta R \text{ (therm. cond.)} = a.\Delta K = A\, e^{t/\tau},$$

then $$\Delta R \text{ (total)} = (A + B)\, e^{t/\tau}$$

where b, B, a, A are proportionality constants, and ΔK is the difference in thermal conductivity. The experiments with screened thermistors, however, showed that if the temperature in the vicinity of the thermistor was maintained constant, or more nearly so than without the screens, the runs changed significantly indicating that there was at least a component of the temperature differences which did not decay with the time constant, τ. These two conflicting conclusions can be reconciled if it is assumed that the signal from temperature differences, as measured by the low power circuit, was greatly reduced by the signal from thermal conductivity differences so that a smaller component, with a time constant different from τ, would have been masked.

More complete investigations of the diffusion thermoeffect have been carried out by Waldmann[51] using a cell of variable length and sensitive thermometers which could be positioned anywhere along this length. He found that initially the temperature fell in the half-cell containing the heavier component but rose in the upper half; both temperatures then decayed, with time constant, τ, to the temperature of the cell walls.

Waldmann derived a differential equation to describe his results for which Ljunggren[52] gave the approximate solution for the temperature, ν, generated during diffusion (in a cell composed of two half-cells which are separated at the beginning of each run):-

$$\nu = F\left[\alpha.\Delta\gamma.\left(\sin\frac{\pi x}{l}\cdot e^{-t/\tau} + \sin\frac{3\pi x}{l}\cdot e^{-9t/\tau} + \ldots\ldots\right)\right.$$

$$+ \frac{4\,b^*}{\pi^2\,\tilde{V}}\cdot(\Delta\gamma)^2\cdot\left(\tfrac{1}{2}\,e^{-2t/\tau}\cdot\left(1+\cos\frac{2\pi x}{l}\right) + \text{terms disappearing}\right.$$

$$\left.\left.\text{faster than } e^{-9t/\tau}\right)\right] \qquad (2.10)$$

where x is the distance coordinate along the axis of the cylinder,

$\tilde{V}$ is the molar volume of the gas mixture,

$\Delta\gamma$ is the initial difference in mole fraction,

α is the thermal diffusion factor,

$b^* = B_{11}^* + B_{22}^* - 2\,B_{12}^*$,

$B_{ik}^* = B_{ik} + T\left(\frac{\partial B_{ik}}{\partial T}\right)$,

B_{ik} is the second interaction virial coefficient for components i,k,

and F is a collection of constants.

$$F = \frac{8}{\pi} \cdot \Phi(y) \cdot \frac{D}{\kappa} \cdot \left(\frac{d}{\ell}\right)^2 \cdot \left(\frac{R}{C_p}\right) \cdot T$$

where d is the diameter of the cell,

κ is the thermal diffusivity,

R is the gas constant,

C_p is the heat capacity at constant pressure,

T is the absolute temperature of the thermostat,

and $\Phi(y)$ is a function of position along the diameter of the cell.

It can be seen from (2.10) that ν is composed of two terms, the first, ν_i, which disappears at the same rate as diffusion and is present even for ideal systems, and the second, ν_r, which disappears at twice the rate of diffusion and is equal to zero for ideal systems since b* is then zero. In addition, ν_i is of opposite sign in each half-cell, due to $\Delta\gamma$, but ν_r is of the same sign ($(\Delta\gamma)^2$) so that when differences are measured, the contribution from ν_i is doubled but that from ν_r disappears; the ν_r term is also an order of magnitude smaller than ν_i[52] at low pressures. Because the circuit is sensitive to temperature changes, even though the temperature at both thermistors is equal (see Chapter 1), (2.10) indicates that there will still be a signal due to the ν_r term.

Equation (2.10) is compatible with the experiments using screened thermistors in that it suggests that, for a given diffusion cell, increases in pressure will give more discrepant results because b* in the ν_r term increases. The equation is also compatible with the low

power circuit experiments as it indicates that the temperature differences principally decay with a time constant τ.

The ν_i term is largely independent of pressure yet the temperature difference signal at 1 atm. is much smaller than that at 5 atm; this is due to the $(d/\ell)^2$ term in F of (2.10), which will similarly affect ν_r. It is expected that the size of any diffusion thermoeffect could have been reduced by using cells of smaller diameter.

The resistance difference, ΔR_i, time, t_i, data were fitted by weighted least squares[56] to an equation modified from (1.7) by the use of (2.10):-

$$\Delta R_i - RF = a_1 e^{a_2 t_i} + a_3 e^{a_4 t_i} \qquad (2.11)$$

where a_1, a_2, a_3 are fitting parameters, with $a_2 = (\frac{\pi}{\ell})^2 D_{12}$, and $a_4 = 2 \times a_2$. This equation did indeed give a better fit of the data than did equation (1.7), however, the fit was still not adequate for the majority of the diffusion runs done at 5 atm. or higher and the D_{12} values obtained were not always consistent. This indicates that other terms should also be included in (2.10). Equation (2.11) was also tried as a four parameter fitting equation by not fixing the value of a_4, but even more inconsistent D_{12} values were obtained and often convergence of the iterative least-squares procedure could not be achieved.

The diffusion thermoeffect can also have an effect on the results other than by changing the resistance of the thermistors. Firstly, from (2.1), it can be seen that D_{12} is quite temperature dependent; a change of 1°K causes a change in D_{12} of approximately 0.5%. However, since differences in signals from the warmer and cooler (i.e. upper and lower) sections of the cell were being taken, an average D_{12} is yielded which has a much reduced dependence on the temperature differences produced. Secondly, the temperature field set up by ν_i is such as to bring about thermal diffusion in the opposite direction from mutual diffusion so that mixing of the gases is slowed. This second consequence has not been accounted for in the derivation of (2.10) by Ljunggren who assumed the concentration gradients to be unaffected by the small temperature gradients.

Due to the apparent presence of a large number of interfering influences, and due to the lack of success in adequately fitting the departures of the data from (1.7), particularly for the higher pressures studied, with equations such as (2.11), it was necessary to apply some compromises.

i) For diffusion runs in the 102 cm and 60 cm cells, i.e. for 1 atm. and 3 atm. He-Ar runs respectively, the experimental arrangement was just as in Chapter 1 but the least-squares procedure was modified by the inclusion of a third parameter:

$$\Delta R_i - RF = a_1 e^{a_2 t_i} + a_3 \qquad (2.12)$$

If the departures from (1.7) are caused by an interference which could perhaps be represented by a series of exponential like terms, the first term of the expansion would be a constant. If these departures arise from the diffusion thermoeffect, it would be expected, from the low power circuit experiments, that the sign of a_3 would be opposite from that of a_1 (positive). For experiments with negligible interference from the diffusion thermoeffect, the value of a_3 may be looked upon as being a calculated correction to the experimental determination of RF. For 1 atm. He-Ar runs, a_3 was almost always in the range of $\pm$ 0.03 Ω, which is close to the experimental accuracy of RF, and also usually negative. The spread of a_3 increased to +0.03, -0.1 Ω for the 3 atm. (60 cm cell) runs indicating the increased prominence of the diffusion thermoeffect.

ii) It was found that (2.12) is not at all useful for processing the results from 5 atm. or higher (in the 45 cm cell). By choosing groups of approximately twenty successive points from a given run, it was possible to calculate D_{12} values with a spread of more than 3% and with no regular pattern to the variation; 1 atm. results, similarly treated, give a spread of only 0.1 - 0.2%. It was therefore necessary to use only the results using screened thermistors in conjunction with (2.12). Results from pressures greater than 5 atm. were still not sufficiently consistent to be useful in testing the pressure dependence of D_{12} and are not included in the results.

iii) In addition, since (2.12) is not a particularly good representation, it will not fit the data from a given run equally well over its entire length. The value of a_3 is a type of average of the departures from (1.7) occurring during the run. The initial data points, where $\Delta R_i - RF - a_3$ is large, are not greatly affected if a slightly incorrect value of a_3 is used. The final few points, where $\Delta R_i \to RF$, are greatly affected by the choice of a_3, in fact, a_3 should be zero for these points. To prevent bias from these last points, which also have the largest experimental error, those which are less than about 5 or 6 ohms from RF are omitted from the least squares fitting of the 3 and 5 atm. results.

In summary, equation (2.12) is the fitting equation used for all the data. The precision, and presumably the accuracy also, of the lower pressure results, i.e. those done in the 102 cm cell, is about ± 0.1 to 0.2% for individual D_{12} values. The 3 atm. He-Ar (from 60 cm cell) runs are fitted by (2.12) less well so that a few points near the end of each run and as many as 30 points at the beginning need to be dropped, leaving about 50 points to be least-squared. This drops the precision to about ± 0.2 - 0.3%. The 5 atm. results (45 cm cell) obtained by using screened thermistors are similar to the 3 atm. results.

Chapter 3

Results

Helium-Argon: The diffusion coefficient of this system was determined as a function of mole fraction, temperature and pressure. The results for the composition dependence at 300 K and corrected to 1 atm. pressure, using (2.7), are presented in Table 1.

The column headed "D_{12}" gives the values of the product, $D_{12} \cdot P \cdot \frac{n}{n_{id}}$, as in (2.7). The second virial coefficients of He (+ 4.58 x 10^{-4} atm.$^{-1}$) and of Ar (- 6.05 x 10^{-4} atm.$^{-1}$) were from the smoothed data presented by Dymond and Smith,[57] and that of the mixed virial (+ 7.54 x 10^{-4} atm.$^{-1}$) from Kalfloglou and Miller.[58] All pressures for these runs were within 0.3% of 1 atm. The "Difference" column gives the differences, $(D_{12})_{\text{experimental}} - (D_{12})_{\text{smoothed}}$. The smoothing equation is (2.4) as used in program MMC (Appendix E). The column headed "Volts" gives the potential difference across the bridge circuit of fig. 2.

The runs numbered 10, 16, 19, 21, 23, 24 were performed without jets being screwed into the Nupro valves so that there was an extra volume of 1.14 c.c. available within the cell which increased the effective length of the cell by 0.11%; these D_{12} values have therefore been increased by 0.22%. This assumes that the extra volume can be assumed to act as though evenly spread to produce an extra cylinder

No.	Volts	x_{Ar}	D_{12}	Difference
1	3.5	.08190	$.7339_8$	.00080
2	4.5	.08218	$.7330_9$	-.00011
3	5.5	.08230	$.7329_2$	-.00028
4	3.5	.08231	$.7336_6$	.00046
5	4.5	.08239	$.7328_5$	-.00036
6	5.5	.08243	$.7329_2$	-.00029
7	3.5	.1865	$.7365_2$	-.00083
8	3.5	.2783	$.7404_0$	-.00006
9	3.0	.3442	$.7429_1$	.00047
10	4.0	.3796	$.7441_0$	.00067
11	5.5	.3973	$.7442_3$	.00032
12	3.5	.4040	$.7439_1$	-.00017
13	3.0	.4649	$.7458_3$	.00021
14	3.5	.4973	$.7457_0$	-.00069
15	5.5	.4973	$.7470_8$	.00069
16	4.0	.5126	$.7469_9$	.00025
17	3.5	.5966	$.7480_0$	-.00056
18	3.0	.6281	$.7487_4$	-.00050
19	4.0	.6920	$.7500_2$	-.00039
20	3.5	.8136	$.7520_7$	-.00043
21	4.0	.8401	$.7527_2$	-.00019
22	3.0	.8485	$.7525_2$	-.00052
23	4.0	.8489	$.7535_6$	.00051
24	4.0	.8491	$.7534_8$	.00043

No.	Volts	x_{Ar}	D_{12}	Difference
25	3.5	.9178	$.7544_4$	.00036
26	3.0	.9178	$.7537_6$	-.00032
27	3.5	.9180	$.7537_7$	-.00031
28	4.5	.9220	$.7547_9$	.00065
29	4.0	.9323	$.7544_8$	.00020

TABLE 1: Helium-Argon. Diffusion Coefficients at 300 K, (cont.) 1 atm.

of length 0.112 cm, with the same diameter as the cell, added to each end. Similarly, run 29 has been decreased by 0.03% to allow for the jets used which protruded to decrease the cell volume by 0.016%. The remainder of these runs had jets which were flush with the ends of the cells.

It was found that the results were somewhat dependent upon the potential difference across the bridge circuit and were affected in two different ways.

i) Large potential differences yielded larger diffusion coefficients. This was presumably due to convection brought about by the larger power generating more heat than could be conducted away by the gas; this effect would be expected to be more prominent in gas mixtures of low thermal conductivity i.e. high mole fractions of argon. At mole fractions near $x_{Ar} = 0.9$, potential differences up to 4.5 volts yielded the same D_{12} but 5.0 volts caused a 0.3% increase. Larger voltages than about 5.0 volts were not able to be used at these mole fractions because of the possibility of "thermal runaway"[5] of the thermistors.

ii) Small potential differences yielded runs which fitted (2.12) rather poorly, particularly for small mole fractions of argon. This was possibly due to the decreased sensitivity of the thermistors to thermal conductivity changes compared to temperature changes (see Chapter 2). The sensitivity to thermal conductivity differences decreases with decreasing mole fraction of argon so that this effect

would be expected to be larger at these mole fractions for a given potential difference. At $x_{Ar} = 0.08$, the lower limit of the useful potential differences appeared to be 3.5 volts; at 3.0 volts, an increase of 0.4% in D_{12} was observed. At larger mole fractions, this effect was not observed at 3.0 volts, the lowest potential difference used.

The D_{12} values seem to be independent of the ranges of voltages quoted in the table.

The smoothing equation for this data is

$$D_{12} = 0.72935 + \frac{0.0505.x_{Ar}}{1 + 0.954.x_{Ar}} \qquad (3.1)$$

with the standard errors of the coefficients being 0.00035 (a_1), 0.0029 (a_2) and 0.099 (a_3), and the standard deviation of fit being 0.00049. From the smoothed values of D_{12} at $x_{Ar} = 0.08190$ (0.73319) and at $x_{Ar} = 0.9323$ (0.75428), together with their 95% fiducial limits, the intermolecular potential parameters

$$\varepsilon_{12}/k = 32.2 \begin{cases} +5.3 \\ -6.7 \end{cases} \text{ K} \qquad (3.2)$$

and

$$\sigma_{12} = 3.045 \begin{cases} +0.055 \\ -0.039 \end{cases} \text{ Å}$$

were obtained from CARKIH (Appendix F). Note: the minimum ratio of D_{12} values, 0.75398 and 0.73351, produced the values 37.5 K, 3.006 Å, and

x_{Ar}	D_{12} Equation (3.1)	"Best" Ratio Parameters - (3.1)	Min. Ratio - (3.1)	Max. Ratio - (3.1)
0.0	.72935	-.00109	-.00057	-.00159
.1	.73396	.00015	.00049	-.00017
.2	.73784	.00077	.00097	.00059
.3	.74113	.00104	.00113	.00097
.4	.74398	.00108	.00108	.00109
.5	.74646	.00098	.00091	.00107
.6	.74863	.00082	.00069	.00096
.7	.75056	.00059	.00041	.00078
.8	.75228	.00034	.00011	.00057
.9	.75382	.00007	-.00019	.00034
1.0	.75521	-.00020	-.00049	-.00011

TABLE 2: Comparison of Kihara 2nd Approximation with Experiment - Composition Dependence.

the maximum ratio 0.75459, 0.73286, the values 25.5 K, 3.100 Å.

The composition dependences predicted by these three sets of intermolecular parameters are compared to the smoothed results of (3.1) in Table 2. Columns 3, 4 and 5 give the D_{12} values of the 2nd Kihara approximation, using (32.2 K, 3.045 Å), (37.5 K, 3.006 Å), and 25.5 K, 3.100 Å) respectively, from which the values in the 2nd column are subtracted. It can be seen that the second approximation predicts a rather more curved dependence than has been obtained although the maximum departure is only about 0.15%. The values of the intermolecular parameters for the pure components that were used in generating the composition dependence are

$$\varepsilon_{Ar}/k = 121 \text{ K}, \sigma_{Ar} = 3.42 \text{ Å}$$

$$\varepsilon_{He}/k = 10.5 \text{ K}, \sigma_{He} = 2.56 \text{ Å}$$

These were taken from Table XXII, "Mean values from other sources" of reference 18. The composition dependence is virtually unaffected by poor choices of these parameters.

Marrero[43] presents an equation for correlating concentration dependences:

$$\Delta' \approx \zeta_{\bullet}(6C_{12}^* - 5)^2 \frac{a \cdot x_{Ar}}{1 + b \cdot x_{Ar}} \qquad (3.3)$$

with C_{12}^*, Δ' as defined in (2.3) and a,b determined from molecular parameters; ζ is a fitting parameter which should be 1.0 if the

Kihara 2nd approximation is followed. For the He-Ar system, Marrero obtains a = 0.18, b = 1.17, assuming ε_{12}/k = 40.2 K, and, based upon van Heijningen's[18] data, sets ζ = 1.67; (3.3) then gives a concentration dependence at 300 K, $\Delta' = [D_{12}\ (x_{Ar} = 1)/D_{12}\ (x_{Ar} = 0) - 1]$ = 0.0578 compared to that obtained from column 3, Table 2 of 0.0367 ± 0.0011. This is a fair comparison, even though we were not able to cover the entire composition range, since (3.3) is also based upon the Kihara 2nd approximation. However, if ζ is set to its theoretical value of 1.0, Δ' = 0.0346, which is much closer to our results, the small difference probably being due to the different ε_{12}/k parameters. The value of Δ' obtained from van Heijningen's[18] parameters, ε_{12}/k = 40.2 K and σ_{12} = 2.98 Å, when used in (2.3), is 0.0341. The a and b of (3.3), when calculated from (3.1), assuming ζ = 1.0, are 0.155 and 0.954 respectively.

The values of ε_{12}/k and σ_{12} obtained from the concentration dependence are rather insensitive to errors in the absolute values of D_{12}; a displacement of 0.2% in D_{12} causes a change of 0.05% in ε_{12}/k and of 0.1% in σ_{12}. However, an error in $[D_{12}\ (x_{Ar} = .1)/D_{12}\ (x_{Ar} = 0)]$ of 0.2% causes an error of 22% in ε_{12}/k and of 2% in σ_{12}.

The effect of pressure on the D_{12} values, other than via the virial coefficients, as in (2.7), is assumed to be insignificant at 1 atmosphere; any corrections would be rather difficult to make with sufficient accuracy, anyhow, because of the lack of knowledge of the correct rigid sphere diameters to be used in (2.8); the accuracy of the experimental determination of this dependence is also fairly low (see later in this chapter).

The results for the temperature dependence are presented in Table 3. Only the small temperature range of 48 K was attempted but the D_{12} from each end of the mole fraction scale were measured. A larger range of pressures was necessary in order to keep the experiments to similar lengths of time. A greater spread of voltages (Column 3) was also necessary so that the circuit sensitivity was approximately the same for each run. The "Difference" column gives the difference, D_{12} - (value calculated with the intermolecular parameters given below (in (3.4), and using Kihara's 2nd approximation).

Figure 6 plots the fit of (2.6) to the experimental data from both concentration ranges separately and together. The abscissae are the set of ε_{12}/k values used and the ordinates are the percentage errors of the slopes, m, which are given by 100 x (standard error of slope)/slope. Table 4 gives the values of σ_{12} corresponding to each ε_{12}/k value for the three sets of concentrations (A is argon-rich, $x_{Ar} = .02 \rightarrow .1$, H is helium rich, $x_{Ar} = .89 \rightarrow .98$, and C is the combined results).

Each of these plots has a series of minima giving rise to a multiplicity of possible potential parameters. Curve H has two almost exactly equal lowest minima at ε_{12}/k = 33 K and 44 K, which is close to the usual figure given by other references.[18,44] Curve A has minima at similar ε_{12}/k values but with a slight bias towards the smaller ε_{12}/k value. However, when combined, this smaller ε_{12}/k value minimum is decidedly favoured. Table 4 shows that A and H have rather different slopes, i.e. different σ_{12} values, near ε_{12}/k = 40 K whereas

Temp. (K)	Pressure (atm.)	Volts	x_{Ar}	D_{12}	Difference
325.877	1.15	2.3	.8904	.86683	.00040
319.186	1.09	2.5	.9062	.83672	-.00007
319.186	1.09	3.3	.09409	.81528	.00055
313.170	1.06	4.0	.9539	.80998	-.00096
313.170	1.07	3.5	.1054	.79052	.00080
313.170	1.06	3.5	.08002	.78827	-.00007
307.992	1.03	3.3	.9262	.78751	-.00070
307.992	1.04	4.0	.08308	.76635	-.00044
300.000	1.00		.9000	.75383	-.00011
300.000	1.00		.1000	.73426	-.00042
288.153	.980	4.3	.9309	.70624	.00099
288.153	.983	6.6	.06506	.68498	-.00037
283.129	.916	4.8	.9615	.68589	.00069
283.129	.916	7.8	.03857	.66411	-.00021
278.104	.885	4.9	.9810	.66537	.00009
278.104	.885	8.7	.01940	.64381	-.00011

TABLE 3: Helium-Argon. Temperature Dependence of D_{12}

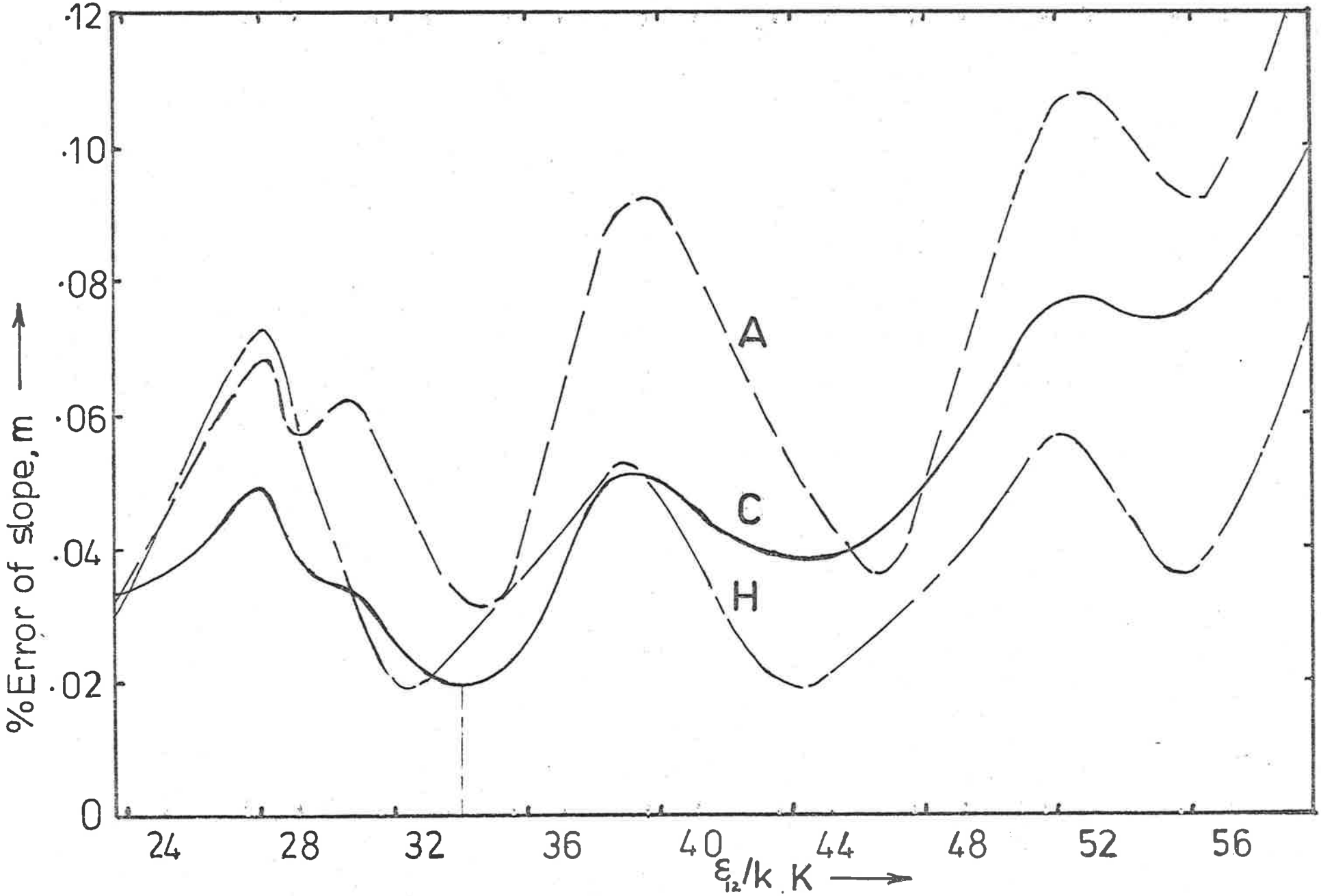

Fig 6: Fitting of Temperature Dependence Data

ε_{12}/k	σ_{12} (A)	σ_{12} (H)	σ_{12} (C)
25.25	3.0998	3.1024	3.1011
28.25	3.0746	3.0764	3.0755
31.25	3.0478	3.0480	3.0479
34.25	3.0235	3.0234	3.0234
37.25	3.0018	3.0006	3.0012
40.25	2.9806	2.9788	2.9797
43.25	2.9601	2.9573	2.9587
46.25	2.9426	2.9388	2.9407
49.25	2.9263	2.9215	2.9239
52.25	2.9107	2.9057	2.9079
55.25	2.8944	2.8883	2.8913
58.25	2.8790	2.8718	2.8754

TABLE 4: Values of σ_{12} generated from running parameter, ε_{12}/k - Temperature Dependence.

near 34 K the σ_{12} values become identical. The smaller-valued minimum of C provides

$$\varepsilon_{12}/k = 34.1 \begin{matrix}+2.5\\-2.7\end{matrix} \text{ K}$$

$$\sigma_{12} = 3.025 \begin{matrix}+0.022\\-0.019\end{matrix} \text{ Å} \qquad \text{(95\% fiducial limits)} \qquad (3.4)$$

in agreement with those obtained from the concentration dependence (3.2).

Since these parameters are rather different from those obtained from other workers, some comparisons with their results is necessary, and these are presented in Table 5. The D_{12} values are calculated at $x_{Ar} = 0$ using the Kihara 2nd approximation (except for the "M" results which are at $x_{Ar} = 0.5$) and may be as much as 0.15% low (see Table 2). The differences of (the second column derived D_{12} values) from (the reference workers' experimental or derived D_{12}) are given in the third column. "K" is calculated using the parameters derived from Kestin's viscosity data ($\varepsilon_{12}/k = 43.10$ K, $\sigma_{12} = 2.9667$ Å); these parameters also predict a lower concentration dependence of 0.0333. "V" are the experimental results of van Heijningen *et al.*[18] which have been corrected, using their experimentally determined concentration dependence, to $x_{Ar} = 0$. "M" are values calculated from Marrero's[43] equation for correlating all diffusion data that had been obtained (up to 1969). The remainder of the values in the table are the experimental D_{12} measured in the range 300 - 1400 K by Hogervorst[44]; his results are consistently ½ - 1% higher than our values calculated from (3.4), but this is within his estimated experimental error.

Temp. (K)	D_{12} from (3.4)	Difference
300	.7289	-.0026 K
90.2	.09211	.00056 V
169.3	.2783	-.0021 V
295	.7087	-.0023 V
400	1.174	.010 V
300	.729	.003
350	.943	.003
400	1.17	.01
450	1.43	.01
500	1.71	.01
550	2.00	.02
600	2.31	.02
650	2.63	.02
700	2.98	.02
750	3.34	.03
800	3.72	.03
850	4.11	.05
900	4.52	.04
950	4.94	.05
1000	5.38	.04
1050	5.83	.01
1100	6.29	.04
1150	6.77	.07
1200	7.26	.07

TABLE 5

Temp. (K)	D_{12} from (3.4)	Difference
1250	7.77	.10
1300	8.30	.08
1350	8.84	.06
1400	9.39	.06
90.2	.0931	.0021 M
300	.7475	.0085 M
800	3.815	.319 M
1400	9.637	1.328 M

TABLE 5: Comparisons of predicted temperature dependence with that from other workers.

It can be seen from Table 5 that our parameters, (3.4), are essentially able to duplicate the D_{12} obtained by Kestin, van Heijningen, and Hogervorst in the range 90.2 → 1400 K, but their intermolecular parameters are not able to reproduce our concentration dependence. Marrero's equation predicts a greatly different temperature dependence from (3.4), especially at elevated temperatures.

The effect of pressure upon the composition dependence of D_{12} for the He-Ar system is illustrated in Figure 7 . The 3 and 5 atmosphere results are listed in Tables 6 and 7 together with the differences of the smoothed data from the experimental. The smoothing equation for 3 atm. is

$$D_{12} = 0.72638 + \frac{0.0442 \cdot x_{Ar}}{1 + 0.64 \cdot x_{Ar}} \qquad (3.5)$$

with the standard errors of the coefficients being 0.00076 (a_1), 0.0070 (a_2) and 0.25 (a_3), and the standard deviation of the fit is 0.00082. For 5 atm., the equation is

$$D_{12} = 0.7262 + \frac{0.034 \cdot x_{Ar}}{1 + 0.55 \cdot x_{Ar}} \qquad (3.6)$$

with standard errors of 0.0011 (a_1), 0.0070 (a_2) and 0.28 (a_3), and the standard deviation of fit is 0.00096.

Although the pressure range amenable to measurement in our apparatus is not large, the essential features of (2.8) are shown. The rate of decrease of D_{12} at low x_{Ar} is seen to be less than that for

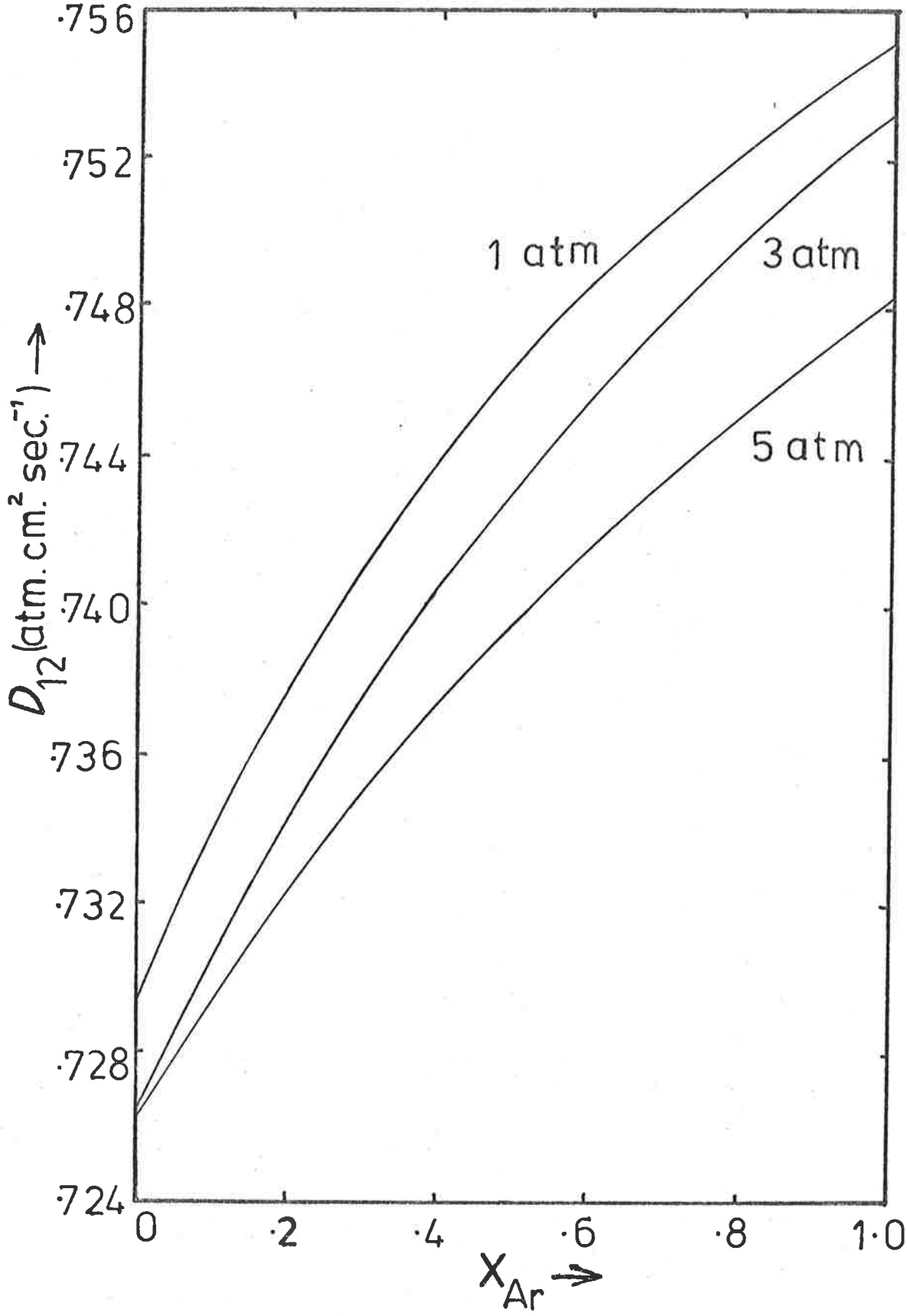

Fig. 7: Effect of Pressure on Composition Dependence

x_{Ar}	D_{12}	Difference (D_{12} - smoothed)
.06805	.7293	.0001
.06892	.7292	-.0001
.06918	.7295	.0002
.1511	.7324	-.0001
.3097	.7373	-.0005
.4920	.7438	.0009
.7901	.7483	-.0013
.8004	.7506	.0009
.8491	.7496	-.0011
.9136	.7524	.0006
.9137	.7522	.0004

TABLE 6: Helium-Argon. 3 Atmospheres pressure, 300 K .

x_{Ar}	D_{12}	Difference (D_{12} - smoothed)
.07208	.7289	.0003
.1074	.7293	-.0004
.2512	.7336	-.0001
.5104	.7403	.0005
.5122	.7396	-.0003
.5122	.7407	.0008
.7517	.7427	-.0016
.9130	.7479	.0009
.9304	.7464	-.0009
.9306	.7487	.0015
.9306	.7464	-.0008
.9312	.7473	.0001

TABLE 7: Helium-Argon. 5 atmospheres pressure, 300 K .

larger x_{Ar}, in accordance with (2.8), but the rate is a little larger than that calculated in the previous chapter. This could be due to either the inappropriate rigid sphere diameters chosen or to the scatter of the results. An insufficient number of pressures were able to be used to attempt a meaningful evaluation of the rigid sphere diameters to be used.

From our data, the calculated decrease of D_{12} from its zero pressure value is in the range of 0.1 to 0.24%/atm. with the smaller mole fractions of argon having the smaller decrease. Although there appears to be no data on the pressure dependence of D_{12} for the He-Ar system, there have been a number of other systems studied, among which are i) the Kr-trace^{85} Kr by Trappeniers and Michels,[60] who measured an initial decrease of about 0.06%/atm. at 25°C, ii) the^{3} He-4% O_2 system by Karra and Kemmerer,[61] using nuclear spin lattice relaxation rate, who found the large (compared to those of other systems) increase in D_{12} of about 7%/atm. at 23°C, and iii) ^{85}Kr trace through a number of gases, including ordinary Kr, by Durbin and Kobayashi[48,49]; they found that D_{12} increased with density by a similar amount for each system, increasing by about 0.1%/atm. at 35°C for the Kr-^{85}Kr which is in contrast to the results of Trappeniers and Michels. Our results are within the range of others studied.

The composition dependences of the systems H_2-N_2, H_2-Ar, He-Kr, He-$CClF_3$ (chlorotrifluoromethane, freon-13) at 300 K were measured and are presented in Tables 8-11. These systems were measured at approximately 1, 1, 0.88, 0.6 atm., respectively. The mixed virial coefficients of the latter two systems were not found in the literature[31] and so these diffusion coefficients were corrected to 1 atm. as the product $D_{12}.P$. The second virial coefficients of H_2 ($+6.01 \times 10^{-4}$ atm.$^{-1}$), N_2 (-4.1×10^{-4} atm.$^{-1}$) and Ar (-6.05×10^{-4} atm.$^{-1}$) were from the smoothed data of Dymond and Smith[57]; the mixed virial coefficients of H_2-N_2 ($+ 4.43 \times 10^{-4}$ atm.$^{-1}$) and H_2-Ar ($+1.10 \times 10^{-4}$ atm.$^{-1}$) were extrapolated from the data of Zandbergen and Beenakker.[63] The smoothing equation for the H_2-Ar, He-Kr, He-$CClF_3$ systems was equation (2.4), with the actual value of the fitting parameters presented in Table 12.

H_2-N_2: There were insufficient points to justify fitting them to (2.4) in order to determine the intermolecular parameters. The thermistors were affected by hydrogen during these runs so that this series had to be abandoned after only a few runs. H_2-Ar runs were similarly affected, using a new pair of thermistors, but several more runs were completed before the runs were affected significantly. Our D_{12} values range from 0.13% less, to 1.0% greater than, the value given by Marrero's correlation (at $x_{N_2} = 0.5$, 300 K); our values are also very similar to those obtained using a similar apparatus.[64]

x_{N_2}	D_{12}
.186	.7828
.187	.7822
.364	.7862
.689	.7889
.884	.7924
.884	.7921

TABLE 8: H_2-N_2. Diffusion Coefficients at 300 K, 1 atm.

x_{Ar}	D_{12}	Difference (D_{12} - Smoothed)
.115	$.8263_0$	.00023
.298	$.8281_2$	-.00013
.308	$.8283_3$	-.00005
.308	$.8287_3$	.00035
.422	$.8292_6$	-.00062
.459	$.8295_0$	-.00089
.540	$.8323_0$	.00074
.578	$.8323_3$	.00020
.692	$.8343_4$	.00041
.885	$.8371_1$	-.00024

TABLE 9: H_2-Ar. Diffusion Coefficients at 300 K, 1 atm.

x_{Kr}	D_{12}	Difference (D_{12} - smoothed)
.0340	.6332	.0012
.0735	.6342	-.0000
.1250	.6363	-.0005
.1313	.6357	-.0014
.2107	.6395	-.0009
.3520	.6456	.0006
.3924	.6465	.0005
.4393	.6469	-.0003
.4957	.6499	.0015
.6003	.6507	.0002
.6649	.6519	.0003
.7280	.6530	.0005
.8422	.6526	-.0015
.9011	.6538	-.0010
.9660	.6562	.0007

TABLE 10: He-Kr. Diffusion Coefficients at 300 K, 1 atm.

x_{CClF_3}	D_{12}	Difference (D_{12} - smoothed)
.0499	.4194	.0008
.0518	.4185	-.0002
.0547	.4191	.0002
.0793	.4186	-.0012
.1305	.4220	.0004
.1956	.4239	-.0001
.2910	.4256	.0004
.3975	.4265	-.0003
.5052	.4274	-.0006
.5385	.4281	-.0003
.5996	.4291	.0002
.6468	.4306	.0014
.8996	.4307	-.0000
.9495	.4311	.0001
.9754	.4304	-.0007

TABLE 11: He-$CClF_3$. Diffusion Coefficients at 300 K, 1 atm.

System	a_1	a_2	a_3	Std. Deviation
H_2-Ar	.82482 (.00069)	.011 (.024)	-0.29 (0.16)	.00056
He-Kr	.62981 (.00098)	.067 (.011)	1.57 (0.36)	.00097
He-$CClF_3$	.41620 (.00074)	.056 (.012)	2.72 (0.69)	.00068

TABLE 12: Values of Fitting Parameters - refer to (2.4). Values in parentheses are standard errors.

H_2-Ar: $\varepsilon_{12}/k = 107.4 \begin{smallmatrix}+9.9\\-8.8\end{smallmatrix}$ K, $\sigma_{12} = 2.966 \begin{smallmatrix}+.046\\-.045\end{smallmatrix}$ Å. The concentration dependence fitting parameters (Table 13) give very different a and b parameters (refer to (3.3)), 0.062 and -0.29 respectively, from those of Marrero's correlation, 0.17 and 0.85. Although the departure of the smoothed D_{12} values from those given by the Kihara 2nd approximation, as given in Table 13, is rather large, these are mostly within the error limits. There is a rather large range of intermolecular parameters found in the literature ranging from 66.7 K, 3.037 Å[63] to 155 K, 2.76 Å[65]. Our intermolecular parameters predict D_{12} values which are from 0.09% low at 295 K to 6.2% low at 1069 K when compared to Marrero's correlation; when compared to Westenberg and Frazier's [65] data, they are from 4.7% to 12.5% low in the same temperature range.

He-Chlorotrifluoromethane $CClF_3$[26] $\varepsilon_{12}/k = 48 \begin{smallmatrix}+12\\-13\end{smallmatrix}$, $\sigma_{12} = 3.83 \begin{smallmatrix}+.11\\-.09\end{smallmatrix}$. This system has apparently not been studied previously.[43] The smoothed D_{12} values closely follow the Kihara 2nd approximation curve (Table 13) even though $CClF_3$ is polyatomic and polar.

He-Kr $\varepsilon_{12}/k = 27 \begin{smallmatrix}+14\\-15\end{smallmatrix}$, $\sigma_{12} = 3.28 \begin{smallmatrix}+.14\\-.12\end{smallmatrix}$. (These parameters are different from those presented by us previously.[66] This is due to the previous values being calculated from the assumed intercepts, at $x_{Kr} = 0$ and $x_{Kr} = 1$, of the D_{12} *versus* x_{Kr} graph, rather than from the measured mole fraction range, as is done here). These parameters are still within the error limits of those of van Heijningen[18] and of Hogervorst,[44] as are the D_{12} at $x_{Kr} = 0$, 300 K. This demonstrates the negligible pressure dependence of this system, up to pressures of 0.9 atm, since the other

2nd Kihara Approximation - Smoothed D_{12}

x_{Heavy}	H_2-Ar	He-Kr	He-$CClF_3$
0	-.00190	-.00021	-.00039
.1	-.00019	.00043	.00023
.2	.00099	.00067	.00038
.3	.00173	.00073	.00036
.4	.00212	.00070	.00029
.5	.00229	.00061	.00021
.6	.00198	.00051	.00014
.7	.00153	.00049	.00006
.8	.00081	.00027	-.00001
.9	-.00015	.00015	-.00008
1.0	-.00134	.00008	-.00014

TABLE 13: H_2-Ar, He-Kr, He-$CClF_3$. Comparison of Theoretical Composition Dependence of D_{12} with Experimental (at 300 K, 1 atm.)

two groups obtained their results in the pressure range .007-.02 atm. The D_{12} predicted from our parameters for the temperature range 111.7-1100 K agree with those of van Heijningen and Hogervorst, with a maximum deviation of 1.6% (at 111.7 K). In this same range, our D_{12} are 0.89% (at 111.7 K) greater than to 10% less than (at 1100 K) the Marrero correlation. The a and b parameters, (3.3), determined from our concentration dependence, are 0.233 and 1.57 compared to 0.23 and 1.56 of Marrero's correlation (obtained from van Heijningen's data but with $\zeta = 1.65$).

Combination Rules: The rules usually used to determine the 1-2 interaction from the 1-1, 2-2 species interactions are (HCB 168)

$$\varepsilon_{12} = (\varepsilon_1 . \varepsilon_2)^{\frac{1}{2}} \tag{3.7}$$

$$\sigma_{12} = \tfrac{1}{2}(\sigma_1 + \sigma_2) \tag{3.8}$$

Although these rules have little foundation in theory (HCB 955-968) - (3.8) is derived from the rule for rigid spheres - these rules are often used for calculations, in the absence of suitable data. A comparison of the combination rules with the experimentally obtained values is shown in Table 14.

H_2-Ar does not follow either rule; this is in contrast to the conclusion reached by Zandbergen and Beenakker[63] but it is found that second virial coefficient determinations are not very sensitive to changes in the parameters if the area of the potential well, Fig. 5,

	ε/k (exp.) K	ε/k (C.R.)	σ (exp.) Å	σ (C.R.)
He-Ar	34.1	35.7	3.025	2.99
H_2-Ar	107.4	66.9	2.966	3.174
He-Kr	27	42.6	3.28	3.095
He-$CClF_3$	48	48.3	3.83	3.74
He[18]	10.5	-	2.56	-
Ar[18]	121	-	3.42	-
Kr[18]	173	-	3.63	-
H_2 (HCB 1110)	37	-	2.938	-
$CClF_3$ (HCB 1213)	222	-	4.92	-

TABLE 14: Comparison of Combining Rules with Experimental.

is kept constant (ref. 31, p. 179) by these changes.

The arithmetic mean rule (3.8) is approximately followed by the other systems studied, partly because the molecules involved do not differ greatly in size so that any type of average will give close to the correct value. In agreement with some other workers[19,63] it was found that the geometric mean rule (3.7) is followed very well; however, some other groups[18,62] found that other choices of the parameter values were more suitable for fitting their data. In summary, we agree with Marrero[43] (p. 34, 35) that these rules are useful in predicting most properties of a system, although it may be that the combination rules do not give the *best* values for some systems (e.g. H_2-Ar).

Chapter 4

Conclusions

This thesis describes the measurement of absolute values of the mutual diffusion coefficients of binary gas mixtures. The apparatus used was of simple design and operation; it was also reliable since it had no sliding surfaces so that sources of leaks were minimised. Under the most favourable circumstances, when the two components of the mixture have widely different thermal conductivities, and pressures are not too large, the precision, and presumably also the accuracy of measurement of individual diffusion coefficients is about ± 0.2%.

Because of the high degree of precision, the variation of diffusion coefficient with composition of several systems was able to be investigated. In contrast to the results of van Heijningen *et al.*[18], our composition dependences closely conformed to those predicted by the Chapman and Enskog theories. In addition, we were able to calculate intermolecular parameters from these composition dependences which, although sometimes being different from those determined by other workers, were approximately as efficient in the correlation of diffusion coefficients over large ranges of temperature.

The variation of diffusion coefficient with temperature over the range 278 → 326 K was measured for the He-Ar system. By using two mole fraction ranges, and with the application of a different calculation technique from that usually used, intermolecular parameters were calculated which agreed with those from our composition dependence but with

smaller error limits. Although our parameters differed from those presented by van Heijningen[18] and by Hogervorst,[44] we were able to predict their diffusion data within very small limits. If it is assumed that our predicted data is accurate, the correlation given by Marrero[43] is rather inaccurate, particularly at higher temperatures. This same conclusion holds true, but to a lesser extent, for the He-Kr and H_2-Ar systems.

A study of the variation of diffusion coefficient with pressure was attempted but was greatly hindered by the increased prominence of the diffusion thermoeffect so that pressures greater than 5 atmospheres were not feasible. The results that were obtained were not in disagreement with a theory presented by McConalogue and McLaughlin[48] but nor were they very conclusive. A slight modification to the apparatus geometry was suggested which would be expected to yield much better results so that a more extended pressure range might be examined.

The combining rules, used for calculating mixed interaction potential parameters, were found to be sufficiently accurate for predicting diffusion coefficients. The Lennard-Jones (12-6) potential function was used throughout and appeared adequate over large temperature ranges in spite of the crudeness of the inverse 12th power repulsive part of the potential; this may be due to the insensitivity of this repulsive region to all but extremely high energy collisions.

Appendix A

Evaluation of the coefficients of the Fourier series of (1.4),

$$c = a_o + \sum_{n=1}^{\infty} a_n . \exp\left(-\frac{n^2\pi^2}{\ell^2} Dt\right) . \cos\left(\frac{n\pi x}{\ell}\right)$$

The coefficients are constants and so are independent of t. At t = 0, (1.4) becomes

$$c(x) = a_o + \sum_{n=1}^{\infty} a_n . \cos \frac{n\pi x}{\ell} \qquad (A.1)$$

These coefficients may be obtained, using Euler's method,[20] by integration of both sides of (A.1), multiplied by the corresponding $\cos \frac{n\pi x}{\ell}$, over the period, 2ℓ, which is twice the length of the cell. Therefore, the experimental concentration profile has to be extended hypothetically over 2ℓ.

Let the concentration profile in the cell at some time, t' = 0, be

$$\begin{aligned} c(x) &= c_1 \quad , \quad 0 \leqslant x < \ell p, \\ &= c_2 \quad , \quad \ell p < x \leqslant \ell \end{aligned} \qquad (A.2)$$

where p is the proportion of the length of the cell filled by gas of concentration c_1 of one of the components; c_2 is the concentration of the same component in the remainder of the cell. This assumes that there is no mixing by either diffusion or by convection. Mixing does

occur, of course, but since the form of (1.4) is followed, this means that t in (1.4) has a different zero point from (A.2), i.e. the hypothetical situation of t' = 0 would occur at negative t. However, this does not affect the evaluation of the a_n since these are independent of time.

The conditions of (A.2) have to be extended to 2ℓ with boundary conditions

$$\begin{aligned} \text{average } [c(x)] &= c_1 \quad \text{at} \quad x = 0,\ 2\ell,\ 4\ell,\ \ldots. \\ &= c_2 \quad \text{at} \quad x = \ell,\ 3\ell,\ 5\ell,\ \ldots. \end{aligned} \tag{A.3}$$

This can be accomplished by defining

$$\begin{aligned} c(x) &= c_1 \quad , \quad -\ell p < x < \ell p, \\ &= c_2 \quad , \quad \ell p < x < \ell\,(2-p), \\ &= c_1 \quad , \quad \ell\,(2-p) < x < \ell\,(2+p), \text{ etc.}, \end{aligned}$$

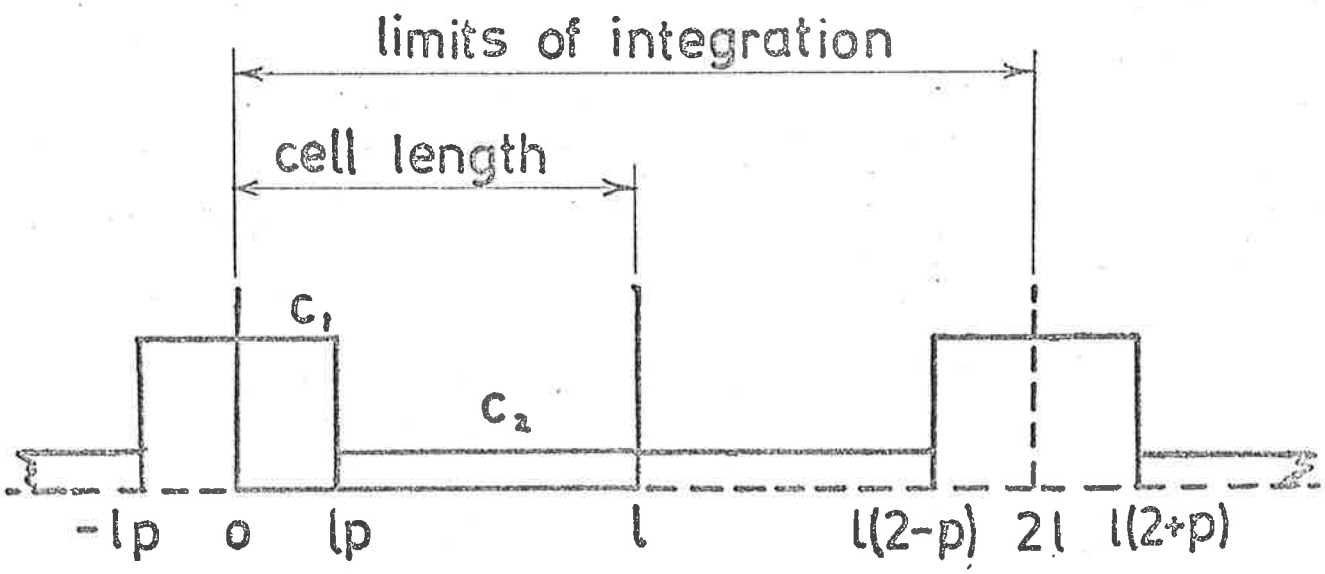

Then,[20]

$$a_o = \frac{1}{2\ell}\left\{\int_o^{\ell p} c_1.dx + \int_{\ell p}^{\ell\,(2-p)} c_2.dx + \int_{\ell\,(2-p)}^{2\ell} c_1.dx\right\}$$

$$\therefore \quad \underline{a_o = pc_1 + c_2\,(1-p)} \qquad (A.4)$$

which is the average concentration of the component over the length of the cell (and also over 2ℓ).

Similarly, the a_n may be determined over the same range.

$$a_n = \frac{1}{\ell}\left\{c_1\left(\int_o^{\ell p} \cos\frac{n\pi x}{\ell}\,.\,dx + \int_{\ell\,(2-p)}^{2\ell} \cos\frac{n\pi x}{\ell}\,.\,dx\right) + c_2\int_{\ell p}^{\ell\,(2-p)} \cos\frac{n\pi x}{\ell}\,.\,dx\right\}$$

$$= \frac{1}{n\pi}\left\{c_1(\sin n\pi p - \sin n\pi(2-p)) + c_2(\sin n\pi(2-p) - \sin n\pi p)\right\}$$

$$= \frac{1}{n\pi}\,(c_2 - c_1)\,(\sin n\pi(2-p) - \sin n\pi p)$$

$$\therefore \quad \underline{a_n = \frac{2\,(c_2 - c_1)}{n\,\pi}\,.\,\cos n\pi\,.\,\sin n\pi(1-p)} \qquad (A.5)$$

Combining (A.4) and (A.5),

$$\underline{c_x = pc_1 + c_2(1-p) + \frac{2(c_2 - c_1)}{\pi}\sum_{n=1}^{\infty}\left[\frac{(-1)^n}{n}\,.\,\sin n\pi(1-p)\right]\cos\frac{n\pi x}{\ell}} \qquad (A.6)$$

Note that

i) if $x/\ell = 1/6$ or $5/6$, $\cos 3n\pi\, x/\ell = 0$, and terms 3, 6, 9, etc., disappear.

ii) for a cell in which the size of the charge of gas added second is always equal to the size of the first, ie. $p = 1/2$, $\sin \frac{n\pi}{2} = 0$ for all even values of n.

It can be seen from (A.6) that none of the a_n can greatly exceed in magnitude the value of a_1 and so equation (1.6) converges rapidly enough to consider only the first term after only a short time.

Appendix B

To derive equation (1.12): The conditions are that initially gas 1 fills a cell of fixed volume, V, to a pressure P_1. Gas 2 is then added to the cell, but without mixing of the two gases, for example, if there is a flexible impermeable membrane between the two, so that there is a total pressure P_b. The final pressure, P_f, after complete mixing of the two gases is found from:-

(n_1, n_2 are the number of moles of gases 1, 2; B_1, B_2, B_{12}, are the second virial coefficients of gases 1, 2 and the "mixed gas" 12; B_M is the second virial coefficient of the gas mixture; R is the gas constant; T is the absolute temperature.)

$$P_1 V = n_1 RT (1 + B_1 P_1)$$ For gas 1 occupying entire cell.

$$P_b V_1 = n_1 RT (1 + B_1 P_b)$$
$$P_b V_2 = n_2 RT (1 + B_2 P_b)$$
} Before mixing.

where $V_1 + V_2 = V$.

When there is complete mixing,

$$P_f V = RT (n_1 + n_2) (1 + B_M P_f)$$

Now, substituting for V,

$$P_f \cdot \frac{RT}{P_b} [n_1 (1 + B_1 P_b) + n_2 (1 + B_2 P_b)] = RT (n_1 + n_2) (1 + B_M P_f)$$

$$\therefore \quad P_f\,[(n_1 + n_2) + P_b\,(n_1B_1 + n_2B_2)] = P_b\,(n_1 + n_2) + P_bB_MP_f\,(n_1 + n_2)$$

$$\therefore \quad (P_f - P_b)\,(n_1 + n_2) = P_fP_b\,[(n_1 + n_2)\,B_M - (n_1B_1 + n_2B_2)]$$

$$\therefore \quad \frac{P_f - P_b}{P_f\,P_b} = B_M - (x_1B_1 + x_2B_2)$$

Substituting for $B_M = x_1^2\,B_1 + x_2^2\,B_2 + 2x_1x_2B_{12}$ gives

$$\frac{P_f - P_b}{P_f.P_b} = x_1^2\,B_1 + 2x_1x_2B_{12} + x_2^2\,B_2 - x_1B_1 - x_2B_2$$

$$= x_1B_1\,(x_1 - 1) + x_2B_2\,(x_2 - 1) + 2x_1x_2B_{12}$$

$$= x_1x_2\,[2\,B_{12} - (B_1 + B_2)]$$

$$\therefore \quad P_f = \frac{P_b}{1 - x_1x_2P_b\,[2\,B_{12} - (B_1 + B_2)]}$$

Appendix C

It is shown here that the difference in resistance of the thermistors is directly proportional to the difference in concentration at these two positions, given the following assumptions:-

i) The difference in thermal conductivity is directly proportional to the difference in concentration for small concentration differences. Harned and French[3] showed that this assumption is very closely followed if the conductivity is a polynomial-like function of concentration.

ii) The variation in resistance of a thermistor, T, is given by

$$T = R_o \exp[B(\frac{1}{\theta_T} - \frac{1}{273})] \qquad (C.1)$$

where R_o is the resistance of the thermistor at 273°K, θ_T is the temperature of the thermistor in °K, and B is a constant depending on the material from which the thermistor is made - its value is about 4000 $(°K)^{-1}$ for Fenwal material.

iii) The value of B is assumed to be constant for each thermistor in a pair, but R_o is not necessarily the same since it is difficult to control the amount of material in each thermistor bead.

When a thermistor is heated, for example by passing a current,

the difference in temperature produced is proportional to the difference in resistance caused, if the temperature difference, Δ, is small. Using (C.1)

$$\frac{T_1 - R_1^f}{R_1^f} = [\exp(B \frac{1}{\theta_1 + \Delta_1}) - \exp(B \frac{1}{\theta_1})] / \exp(B \frac{1}{\theta_1})$$

$$= \exp(- \frac{B\Delta_1}{(\theta_1 + \Delta_1)\ \theta_1}) - 1$$

The subscript 1 refers to thermistor 1; R_1^f is the resistance of the thermistor at θ_1

$$\approx (1 - \frac{B\ \Delta_1}{\theta_1^2} + \ldots.) - 1$$

since $B\ \Delta_1/\theta_1^2$ is small, approximately $4000\ \Delta_1/90{,}000 \approx 0.05\ \Delta_1$.

$$\therefore \quad T_1 - R_1^f = \Delta_1 (- \frac{R_1^f\ B}{\theta_1^2}) = b_1\ \Delta_1 \qquad (C.2)$$

$$\text{Similarly,} \quad T_2 - R_2^f = \Delta_2 (- \frac{R_2^f\ B}{\theta_2^2}) = b_2\ \Delta_2 \qquad (C.3)$$

where subscript 2 refers to thermistor 2. For simplification, it is assumed that $\theta_1 = \theta_2 = \theta$, which is nearly exact. (It should also be noted that since the value of each $b \approx -300\ \Omega/°K$, and $R_1^f \approx R_2^f$, a difference $(T_2 - T_1)$ of 100 Ω represents a difference in temperatures

of about 1/3°, with T_1 above and T_2 below R_1^f and R_2^f respectively.)

From power considerations,

$$I_1^2 T_1 = a K_1 (\theta - \theta_w + \Delta_1) \qquad (C.4)$$

and

$$I_2^2 T_2 = a K_2 (\theta - \theta_w + \Delta_2) \qquad (C.5)$$

where $I_1 = I_2 = I$, the current flowing through each thermistor, since the bridge is balanced when a reading is taken; this current does, however, vary during the run. θ_w is the temperature of the cell walls and so remains constant throughout. K_1 and K_2 are the thermal conductivities at thermistor 1 and 2, and a is a cell constant depending on geometrical factors only.

By division of (C.4) and (C.5) and substituting $T_2 - D = T_1$,

$$K_2 (T_2 - D) (\theta - \theta_w + \Delta_2) = K_1 T_2 (\theta - \theta_w + \Delta_1)$$

Let $K_1 = K - \delta_1$, $K_2 = K + \delta_2$ where K is the thermal conductivity of the final mixture, then

$$T_2K (\theta - \theta_w) + T_2\delta_2 (\theta - \theta_w + \Delta_2) + T_2K\Delta_2 = T_2K (\theta - \theta_w)$$

$$+ T_2\delta_1 (\theta - \theta_w + \Delta_1) - DK (\theta - \theta_w) - D\delta_2 (\theta - \theta + \Delta_2) - DK\Delta_2$$

$$+ T_2K\Delta_1$$

$$\therefore \quad T_1\delta_2 (\theta - \theta_w + \Delta_2) + T_2\delta_1 (\theta - \theta_w + \Delta_1) - K (T_2\Delta_1 - T_1\Delta_2) = + DK (\theta - \theta_w)$$

Now substituting from (C.4) and (C.5) in first and second terms and from (C.2) and (C.3) in third term,

$$\frac{I^2T_1T_2}{a}\left(\frac{\delta_2}{K_2}+\frac{\delta_1}{K_1}\right)+\frac{K}{b_1b_2}\left[T_1T_2\,(b_1-b_2)+b_2T_2{R_1}^f-b_1T_1{R_2}^f\right]=DK\,(\theta-\theta_w)$$

$$\therefore\quad \frac{I^2T_1T_2}{a}\left[\frac{K\,(K_2-K_1)}{K_1\,K_2}\right]+\frac{K\theta^2}{B}\left[T_1T_2\,\frac{{R_2}^f-{R_1}^f}{{R_1}^f\,{R_2}^f}+(T_2-T_1)\right]=(T_2-T_1)$$

$$.K\,(\theta-\theta_w)$$

$$\therefore\quad (T_2-T_1)-\frac{T_1T_2\,\dfrac{{R_2}^f-{R_1}^f}{{R_1}^f\,{R_2}^f}\cdot K\,\dfrac{\theta^2}{B}\cdot}{K\left[(\theta-\theta_w)-\dfrac{\theta^2}{B}\right]}=(K_2-K_1)\,\frac{\dfrac{I^2T_1T_2}{a}\,\dfrac{K}{K_1\,K_2}}{K\left[(\theta-\theta_w)-\dfrac{\theta^2}{B}\right]}$$

$$\therefore\quad (T_2-T_1)-T_1T_2\,\frac{{R_2}^f-{R_1}^f}{{R_1}^f\,{R_2}^f}\,\frac{\theta^2/B}{(\theta-\theta_w)-\theta^2/B}=(K_2-K_1)\,\frac{I^2T_1T_2}{a}$$

$$\cdot\frac{1}{K_1\,K_2}\cdot\frac{1}{(\theta-\theta_w)-\theta^2/B}\qquad\qquad(C.6)$$

This is now of the form

$$\Delta\text{ (resistance) + term } = \Delta\text{ (thermal conductivity) x coefficient.}\qquad\qquad(C.7)$$

Taking the coefficient of the right-hand side first.

i) The term $a[(\theta-\theta_w)-\theta^2/B]$ is a constant.

ii) $I^2T_1T_2 = I^2T_1 (T_1 + D)$.

Then

$$\frac{d\ I^2\ (T^2 + TD)}{d\ D} = I^2 \left(\frac{dT^2}{dD} + D\ \frac{dT}{dD} + T\ \frac{dD}{dD}\right) + (T^2 + TD)\ \frac{dI^2}{dD}$$

(by the chain rule of differentiation, and dropping the subscript 1).

$$= -I^2\ (D + T) + 2IT\ (D + T)\ \frac{dI}{dD}$$

$$= I\ (D + T)\ \left(2T\ \frac{dI}{dD} - I\right).$$

It is found experimentally that the current changes by about + 0.01 ma for a decrease in D of 300 Ω when the current is about 0.80 ma; the value for T is in the range 6-7 K Ω. Taking the fractional change in $I^2T_1T_2$, i.e.

$$\frac{d\ (I^2T_1T_2)}{dD} \Big/ I^2T_1T_2 = \frac{2\ T_1\ \frac{dI}{dD} - I}{I\ T_1},$$

gives a percentage change of about 0.03%. Therefore the product $I^2T_1T_2$ may be considered to be constant within very small limits.

iii) K_1K_2.

By expanding the difference in conductivity as a polynomial in the difference in concentration at each point,

$$K_1\ K_2 = (K + \beta\ (c_1 - c) + \gamma\ (c_1 - c)^2 + \ldots)\ (K + \beta\ (c_2 - c) + \gamma\ (c_2 - c)^2 + \ldots)$$

$$= K\ [K + \beta\ (c_1 + c_2 - 2c) + \gamma\ (c_1 - c_2)\ (c_1 + c_2 - 2c) + \ldots]$$

where c is the concentration throughout the cell after complete mixing. From (1.4), it is seen that

$$c_1 + c_2 - 2c = 0 + 0 + a_2 \exp\left(-\frac{4\pi^2}{\ell^2} D_{12} t\right) + 0 +$$

$$\approx 0 \text{ for times during which readings are taken.}$$

$$\therefore \quad K_1 K_2 \approx K^2, \text{ a constant.}$$

Consider the term

$$T_1 T_2 \frac{R_2^f - R_1^f}{R_1^f R_2^f} \frac{\theta^2/B}{(\theta - \theta_w) - \theta^2/B},$$

which arises from the mismatching of the thermistors. The only variable is T_1T_2 and this varies closely as $1/I^2$ so that this term changes by about 2% (max.) over the range of measurement. The size of this term is also rather small; at the end of diffusion, it equals the value of the resistance box at balance, and this amounts to only a few ohms. Therefore, the variation of this term may be neglected and set as a constant, RF.

Overall, (C.7) may be written as

$$\Delta \text{ (resistance)} \propto \Delta \text{ (thermal conductivity)}$$

or, using assumption i),

$$\Delta \text{ (resistance)} \propto \Delta \text{ (concentration)}.$$

Appendix D

PROGRAM RFFIXM calculates the diffusion coefficient of a run from the difference in resistance, time data. It consists of the main program and this calls two subroutines, WLSQ3, which contains the fitting procedure,[56] and CALC, which prints most of the results. WLSQ3 calls the library subroutine, MATRIX, which performs the matrix inversion.

The function fitted is the 3 parameter equation (2.12) but it can be converted to the 2 parameter fit, with $a_3 = 0$, by changing the "M = 3" card to "M = 2" in line 5 of the main program.

INPUT

1st card:

is a heading card and contains identification information. The first column should be left blank.

2nd card:

IATE , I6. The date in numerical form

N , I3 The number of (resistance, time) values taken, 150 maximum

1X

RZ, F10. The value of the resistance difference when only the first gas is in the cell. This is not used in any calculations but is printed out.

RF , F10. This is the final value of the resistance difference at completion of diffusion. This is necessary for the calculation.

R(1) , F10. is the first value of the resistance difference taken.

AR , F10. is the (equal) increment of resistance difference, usually 1 ohm.

TT,F10. is the dial reading on the pressure gauge corresponding to the pressure after the second gas is added to begin the diffusion.

TI , F10. is the dial reading corresponding to the pressure of the first gas by itself.

XP , F10. is the initial mole fraction of heavy component of the first gas in the cell. If XP > 1, the initial mole fraction is taken to be that value already present in the computer. This allows several diffusion runs to be calculated at one run of the program. If XP < 0, the final mole fraction is that of the previous set of data.

3rd card:

K(I),NB(I),I3(I3,I3). These are the numbers of the first and last data points to be processed. This allows as many as 9 separate sections of the data to be examined individually.

$$1 \leqslant K(I) < NB(I) \leqslant N.$$

4th card:

LH , I1. If the second gas added is the smaller molecular weight species, LH = 1.

T1 , F9. is the approximate time, in minutes, that readings were taken after the addition of the second gas.

IØ , I1. This is an option parameter which allows the data to be taken in three different ways.

IØ blank or zero. The readings are taken at equal intervals of resistance difference, time is in seconds.

IØ = 1. As above, but time is in minutes and seconds.

IØ = 2. Resistance readings are taken at equal intervals of time in minutes. AR is the interval of time.

DØHM , F10. Applies only if IØ = 2 when DØHM represents the sensitivity of the circuit. Specifically, this is the deflection on the recorder caused by a 1Ω change on the resistance box.

5th → (4 + N/8)th card:

If IØ = 0,

S(I) , 8F10.6, are the time values, in seconds

If IØ = 1,

MT(I), S(I), 8(I3,F3.1,4X), are the time values in minutes and seconds.

IØ = 2,

R(I),8F10. are the values on the resistance box at equal intervals of time (minutes). To obtain the exact resistance at each interval one also requires the extra resistance represented by the deflection of the recorder, DELTA(I), from zero, which, when divided by DØHM, represents a small resistance value to be (algebraicly) added to R(I). These require a further N/8 cards, 8F10. format.

In addition to this formal input data, there are other parameters at present in this program which are specific to our apparatus and to the He-Ar system. Lines 6-11 contain information about the He-Ar system at 300 K. B1, B2, B12 are the second virial coefficients of He, Ar and He-Ar respectively, all in atm.$^{-1}$; RT is the product of the gas constant by 300 K; W1 and W2 are the molecular weights of He and Ar respectively.

The calibration of the Texas Instruments pressure gauge to convert dial reading to pressure in mm. is given in the lines beginning PI = and PT = . The calibration of the stopwatch is given in the line S(I) = S(I)*(1. and S(I)*0.00000015). The factor $(L/\Pi)^2$ for the 60 cm cell is already included, in the line D = -SLOPE* 364.939, in both the main program and CALC.

More than one data set may be processed in one run of the program as long as the N parameter is not equal to zero; therefore, to terminate the program, two blank cards need to be inserted after the last data set to be processed. (The first blank card corresponds to the header card.)

```
      PROGRAM RFFIXM  (INPUT,OUTPUT)
      DIMENSION R(150)           ,K(9),MT(150),NB(9),S(150),DELTA(150),
     $C(5,5),S2(5)
      COMMON RL(150),TIME(150),A(6)   ,FF
      M=3
      B1= 4.576E-04
      B2=-6.051E-04
      B12= 7.544E-04
      RT=2.46175E+04
      W1=4.0026
      W2=39.948
 2    READ 220
 220  FORMAT(80H
     $                                                          )
      READ 3,IATE,N ,      RZ,RF,R(1),AR,TT,TI,XP
 3    FORMAT(I6,I3,1X,7F10.)
      IF(N .EQ.0)GO TO 50
      PRINT 35
 35   FORMAT(1HI)
      PRINT 220
      READ 36, (K(I),NB(I) ,I=1,13)
 36   FORMAT(13(I3,I3))
C
      READ 39,LH,T1,IO,    DOHM
 39   FORMAT( I1,F9.,I1,    9X, F10.)
      IF(XP.LT.0) GO TO 7
      PI=TI*(TI*2.56633E-05+0.656378)*51.7149
      PT=TT*(TT*2.56633E-05+0.656378)*51.7149
      PD=PT-PI
      IF(XP.GT.1.)GO TO 6
      XH=XP
 6    IF(LH.EQ.1) GO TO5
      BS=B1
      BA=B2
      PR=PI*(1.+BA*PT/760.)/(PD*(1.+BS*PI/760.))
      XH=(1.+XH*PR)/(1.+PR)
      XL=1.-XH
      GO TO 71
 5    BA=B1
      BS=B2
      XL=1.-XH
      PR=PI*(1.+BA*PT/760.)/(PD*(1.+BS*PI/760.))
      XL=(1.+XL*PR)/(1.+PR)
      XH=1.-XL
 71   PTF=PT/(1.-PT*XL*XH*(2.*B12-B1-B2)/760.)
 7    CONTINUE
C
      IF(IO.EQ.2) GO TO 102
      IF(IO.EQ.1) GO TO 117
      READ 118,( S  (I),I=1,N )
 118  FORMAT(8F10.6)
      DO 121 I=1,N
      S(I)=S(I)*(1.+S(I)*0.00000015)
 346  TIME(I)= S  (I)+T1*60.
 121  R(I+1)=R(I)-AR
      GO TO 307
```

```
117   READ 8,(MT(I),S(I),I=1,N )
8     FORMAT(8(I3,F3.1,4X))
      DO 9 I=1,N
      R(I+1)=R(I)-AR
9     TIME(I)=60.*MT(I)+S(I)+T1*60.
      GO TO 307
102   TIME(1)=R(1)
      READ 103,(R(I),I=1,N )
      READ 103,(DELTA(I),I=1,N )
103   FORMAT (8F10. )
      DO 105 I=1,N
      TIME(I)=(I*AR+11)*60.
105   R(I)=R(I)-DELTA(I)/DOHM
307   CONTINUE
      SLOPE=ALOG((R(1)-RF)/(R(N )-RF))/(TIME(1)-TIME(N ))
      DO 967 I=1,N
      RL(I)=R(I)-RF
967   TIME(I)=TIME(I)*((PTF-(PTF-PT)*EXP(SLOPE*(TIME(I)-90.)))/PTF)
      PT=PTF
      PA=PT/760.
      AC1 =(R(2)-RF)/EXP(SLOPE*TIME(1))
      BM=XL*XL*B1+XH*XH*B2+XL*XH*B12*2.
      DM=PA/(RT*(1.+BM*PA))
      DN=DM*6.02252E+23
      Dw=DM*(XL*w1+XH*W2)
      DMRT=DM*RT
      PRINT 510,BM
510   FORMAT(5X*MIXTURE B=*E14.4*ATM*)
      IF(N .LE.5) GO TO 2
      I=0
      A(3)=A(4)=A(5)=0
      PRINT543
543   FORMAT(5X*F=Y-A1.EXP(A2.X)-A3     *)
98    I=I+1
      KK=K(I)
      N =NB(I)
      IF(N .EG.0)GO TO 2
      A(6)=0
      A(2)=SLOPE
      A(1)=AC1
      PRINT1085,(A(J),J=1,M),M ,RF
1085  FORMAT(/5X*ESTIMATES=* 3E13.2/7X,I2* PARAMETERS  RF=*F6.2)
      CALL WLSQ3              (N ,KK,S2,M,C)
      IF(A(6).EQ.1) GO TO 2
      A3=A(3)
556   R1=R(KK)-RF
      R2=R(N )-RF
      NU=N -KK+1
      SLOPE=A(2)
      SS=S2(2)
      B=A(1)
```

```
      D=-SLOPE*364.939
      DDM=D*DM
      DDN=D*DN
      DDW=D*DW
      D1P=D  *DMRT
      PRINT 303,DM,DDM,DN,DDN,DW,DDW,DMRT,D1P
303   FORMAT(15X*D X *E12.4* MOLES.CM(-3)=*E12.4/
     $       15X*D X *E12.4*        CM(-3)=*E12.4/
     $       15X*D X *E12.4*     GM.CM(-3)=*E12.4/
     $       15X*D X *E12.4*     ATM       *E12.4*CM2/SEC  *)
      PRINT 30,IATE,RZ,PT,RF,PI,PD,PA,XH,R1,R2,KK,N ,NU,T1,LH
30    FORMAT(/20X*DATE*I6/20X*R(ZERO)=*F10.3,3X*P(TOTAL)=*F8.3/
     $20X*R(INF) =*F10.3,3X*P(INIT.)=*F8.3/35X*SIZE OF CHARGE=*F8.3/
     $20X*P(ATM)=*F8.6,3X*X(HEAVY)=*F8.6/20X*RESISTANCE RANGE=*F7.3
     $* TO *F7.3/20X*NO. OF POINTS USED=*I3* TO *I3*= *I3/20X*READINGS
     $TAKEN*F5.1* MINS. AFTER ADDING GAS *I1/)
      CALL CALC (SLOPE,PA,SS,B ,TIME,R,RF,KK,N ,A3)
      GO TO 98
5     CONTINUE
      END
```

```
      SUBROUTINE CALC (SLOPE,PA,UA,PE,TIME,R,RF,KK,NR,A3)
      DIMENSION TIME(150),R(150),RC(150),CT(150),DT(150),V(150)
      NU=NR-KK+1
      NM3=NU-3
      DEVS=DEVR=DEVT=0
      DO 115 J=KK,NR
      RE=RF+A3
      RC(J)=PE*EXP(SLOPE*TIME(J))+RE
      ALD=ALOG((R(J)-RE)/PE)
      CS=ALD/ TIME(J)
      CT(J)=ALD/SLOPE
      V(J)=R(J)-RC(J)
      DT(J)=TIME(J)-CT(J)
      DEVS=(SLOPE-CS)**2+DEVS
      DEVR=V(J)*V(J)+DEVR
  115 DEVT=DT(J)*DT(J)+DEVT
      DEVR=SQRT(DEVR/NM3)
      DEVT=SQRT(DEVT/NM3)
      DEVS=SQRT(DEVS/NM3)
      D=-SLOPE*364.939
      D1=D*PA
      PC=-100.*UA/SLOPE
      ED=.01*D1*PC
      F1=D1+ED
      F2=D1-ED
      PRINT 15,PA,D,D1,ED,PC,F1,F2
   15 FORMAT(//15X*D(*F10.6*ATM, T K)=*F10.6/15X*D(1ATM, T K)=*F10.6,
     $12X*+/-* F7.5/50X*PC  *F6.4/17X*LIMITS *F9.6/21X*TO *F9.6)
      PRINT 401,DEVR,DEVT,DEVS
  401 FORMAT(/10X*STD. DEV.   R*15X*T* 15X*SLOPE*/12X,E15.6,3X,E15.6,
     $ 3X,E15.6/)
      PRINT 31
   31 FORMAT(20X*TIME      R(T)      CALC R    DIFF.    CALC T    DIFF.*/
     $48X*RES.*15X*TIME*)
      PRINT33,(TIME(J),R (J),RC(J),V(J),CT(J),DT(J),J=KK,NR)
   33 FORMAT(17X F8.2,F10.3,F10.3,F9.3,2F10.2)
      RETURN
      END
```

```
      SUBROUTINE WLSQ3        (N,KK,S2,M,C)
      DIMENSION       AA(5),AC(5),V(5),FA(5),S2(M),CONV(5),C(M,M)
      COMMON Y(150),X(150),A(6) ,FF
      G=1.
      FA(3)=-1.
      L=N-KK+1
      NI=0
      PRINT 2    ,(K,K=1,M)
2     FORMAT(/3X,3(*A(*I1*)*8X*STD.DEV.*4X))
1     NI=NI+1
      FF=ADC=S=0
      DO 96 J=1,M
      DO 95 K=1,M
95    C(J,K)=0
96    V(J)=0
      DO 150 I=KK,N
      FA(1)=-EXP(A(2)*X(I))
      FA(2)=A(1)*X(I)*FA(1)
      FX= A(1)*A(2)*FA(1)-A(3)
      F=Y(I)+A(1)*FA(1)-A(3)
      FF=FF+F*F
      DL=2.5E-05+4.0E-02*FX*FX
      DO 155 K=1,M
155   V(K)=V(K)+FA(K)*F/DL
      S=S+F*F/DL
      DO 150 J=1,M
      DO 150 K=1,M
150   C(J,K)=C(J,K)+FA(J)*FA(K)/DL
      CALL MATRIX(10,M,M,0,C,M,CINV)
      DO 166 K=1,M
      AA(K)=0
      DO 165 J=1,M
165   AA(K)=AA(K)+C    (J,K)*V(J)
      S2(K)=SQRT(ABS(S/(L-M)*C(K,K)))
8     A(K)=A(K)-AA(K)/G
      IF(A(K).NE.0 ) GO TO 190
      AC(K)=0
      GO TO 166
190   CONV(K)=AA(K)/(A(K)*G)
      AC(K)=ABS(CONV(K))
166   ADC=ADC+AC(K)
      FF=SQRT(FF/(N-M))
      PRINT 3,(A(K),S2(K),K=1,M),FF
3     FORMAT(10E12.3,E13.4 )
      IF(FF    .GE.1000  .AND.NI.GT.5) GO TO 700
11    IF(ADC  .LE..0001.AND.NI.GT.1)  GO TO 168
      IF(NI.LT.20) GO TO 1
700   A(6)=1
      PRINT 167
167   FORMAT(/10X*CONVERGENCE DOES NOT OCCUR*)
168   CONTINUE
      RETURN
      END
```

Appendix E

PROGRAM MMC calculates the fitting parameters, along with their corresponding standard errors, of equation (2.4). The program has one subroutine, WLSQ3M, which is very similar to WLSQ3 of Appendix D and requires the library subroutine, MATRIX, to perform matrix inversion. The program also prints out the predicted values of the diffusion coefficients at increments of mole fraction of 0.05. The routine sometimes does not converge if the data is very scattered or if poor estimates of the parameters are read in.

INPUT

1st card:

is a header card and contains identification information. The first column must be left blank.

2nd card:

A1 , F10. is the estimated value of a_1

A2 , F10. is the estimated value of a_2

A3 , F10. is the estimated value of a_3.

The A2 and A3 columns may be left blank which will cause these estimates to be calculated from the data. However, it may be necessary to specify these estimates if the data is scattered.

N , I3 is the number of (mole fraction, diffusion coefficient) pairs which are present in the data. Up to 90 pairs may be used.

3rd → (2 + N/8)th card:

X(I) , 8F10.10 are the mole fractions (heavy component) used.

(3 + N/8)th → (2 + N/8 + N/8)th card:

Y(I) , 8F10.10 are the diffusion coefficients corresponding to the X(I).

The program is terminated by two blank cards after the last set of data.

```
      PROGRAM MMC (INPUT,OUTPUT)
      COMMON X(90),Y(90)
1     READ 2
2     FORMAT(80H
     $                                                              )
      READ 3,A1,A2,A3,N
3     FORMAT(3F10.,I3)
      IF(N.EQ.0) GO TO 11
      READ 4,(X(I),      I=1,N)
      READ 4 ,(Y(I),I=1,N)
4     FORMAT(8F10.10)
      PRINT 102
102   FORMAT(1H1)
      PRINT 2
      IF(A2.NE.0) GO TO 123
      L=N/2+1
      Y3=Y(L)-A1 $ Y2=Y(N)-A1
      A3=(Y3*X(N)-Y2*X(L))/(X(N)*X(L)*(Y2-Y3))
      A2=Y2*(1.+A3*X(N))/X(N)
123   SX=V=DX=0
      DO 5 I=1,N
5     SX=SX+X(I)
      AX=SX/N
      KK=1
      CALL WLSQ3M (A1,A2,A3,N,KK)
      IF(A2.EQ.0) GO TO 1
      PRINT 107
107   FORMAT(10X * X* 11X* Y * 14X * CY * 10X*Y-CY*)
      DO 6 I=1,N
      CY=A1+A2*X(I)/(1.+A3*X(I))
      DY    =Y(I)-CY
      V=V+DY*DY
      D=X(I)-AX
      DX=DX+D*D
6     PRINT 7,X(I),Y(I),CY,DY
7     FORMAT(4F15.6)
      DIV=N-3
      V=SQRT(V/DIV)
      PRINT 8,DX,V,AX,N
8     FORMAT(* SUM OF X DEVIATIONS (X-X AV)2= * F15.6/
     $                                        * S.ERROR OF CURVE=*F15.6 /
     $* AVERAGE X =*F15.6/ * NO. OF VALUES= *  13)
      PRINT 110
110   FORMAT(//12X* X*9X*PREDICTED Y*)
      DO 9 I=1,21
      X(I)=(I-1)*.05
      Y(I)=A1+A2*X(I)/(1.+A3*X(I))
9     PRINT 10,X(I),Y(I)
10    FORMAT(10X,F4.2,5X,F15.6)
      GO TO 1
11    CONTINUE
      END
```

```
      SUBROUTINE WLSQ3M (A1,A2,A3,N,KK)
      DIMENSION A(3),C(3,3),AA(3),AC(3),V(3),FA(3),S2(3),CONV(3),S3(3)
      COMMON X(90),Y(90)
C   THIS FITS DIFFUSION DATA AS A FUNCTION OF CONCENTRATION
      A(1)=A1 $ A(2)=A2 $ A(3)=A3
      M=3
      N=N-KK+1
      PRINT 2    ,(K,K=1,M)
    2 FORMAT(10X,3(6X*A(*I1*)      STD. DEV. *))
      PRINT 91,A1,A2,A3
   91 FORMAT(10X,3(E13.4,12X)/)
      NI=0 $ G=1.
    1 NI=NI+1
      S=0 $ ADC=0
      DO 96 J=1,M
      DO 95 K=1,M
   95 C(J,K)=0
   96 V(J)=0
      FA(1)=-1.
      DO 150 I=KK,N
      B=1.+A(3)*X(I)
      F=Y(I)-A(1)-A(2)*X(I)/B
      FA(2)=-X(I)/B
      FX=-A(2)/B**2
      FA(3)=-FX*X(I)*X(I)
      DL=1.+FX*FX
      DO 155 K=1,M
  155 V(K)=V(K)+FA(K)*F/DL
      S=S+F*F/DL
      DO 150 J=1,M
      DO 150 K=1,M
  150 C(J,K)=C(J,K)+FA(J)*FA(K)/DL
      CALL MATRIX(10,M,M,0,C,M,CINV)
      DO 166 K=1,M
      AA(K)=0
      DO 165 J=1,M
  165 AA(K)=AA(K)+C    (J,K)*V(J)
      S2(K)=SQRT(ABS(S/(N-M)*C(K,K)))
    8 A(K)=A(K)-AA(K)/G
      CONV(K)=AA(K)/(A(K)*G)
      AC(K)=ABS(CONV(K))
  166 ADC=ADC+AC(K)
      PRINT 3,(A(K),S2(K),K=1,M)
    3 FORMAT(10X,3(E13.4,E12.3))
      IF(ADC  .LE..0001.AND.NI.GT.1)  GO TO 168
      IF(NI.LT.20) GO TO 1
      PRINT 167
  167 FORMAT(/10X*CONVERGENCE DOES NOT OCCUR*)
      A(2)=0
  168 CONTINUE
      A1=A(1) $ A2=A(2) $ A3=A(3)
      N=N+KK-1
      RETURN
      END
```

Appendix F

PROGRAM CARKIH calculates the intermolecular potential parameters, ε_{12}/k and σ_{12}, from the values of the mutual diffusion coefficient at two different mole fractions at the specified pressure and temperature. It also prints out the predicted diffusion coefficients at 0.05 mole fraction increments. Subroutine LINT contains the quantum corrected collision integrals[27] for the Lennard-Jones 12-6 potential; interpolation is performed linearly.

INPUT

1st card:

is a header card and contains identification information. The first column must be left blank.

2nd card:

DS , F10. is the value of the diffusion coefficient at the low mole fraction (of heavy component).

DB , F10. is the value of the diffusion coefficient at the large mole fraction (of heavy component).

T , F10. is the temperature in degrees Kelvin.

P , F10. is the pressure in atmospheres.

E , F10. is the estimated value of ε_{12}/k K

S , F10. is the estimated value of σ_{12} Å

L , I2 is an option parameter. If L $\neq$ 0, the third card of data must be omitted and the values that this card normally contains will be assumed to be those from the previous data

set. L must be set to zero (or blank) for the first set of data of a particular run of the program.

2X

IFD(1) and IFD(2),2I2. These are set to 1 if the components are Fermions, otherwise they are left blank.

3rd card: (only if L = 0)

E1 , F10. is ε_1/k K of the heavier molecular weight species.

S1 , F10. is σ_1 Å of the heavier component.

M1 , F10. is the molecular weight of the heavier component.

X , F10. is the mole fraction of heavy component corresponding to DS.

E2, S2, M2, 3F10. are the lighter component analogues of E1, S1 and M1.

Y , F10. is the mole fraction corresponding to DB.

The program is terminated by two blank cards after the last set of data.

```
      PROGRAM CARKIH(INPUT,OUTPUT)
      DIMENSION C2(2),IFD(2),TE(2),R(2),B(2)
      REAL M12,M21,M1,M2,M11,M22
2     READ 12
12    FORMAT(80H
     $                              )
      READ 1,DS,DB,T,P,E,S,L,   IFD(1),IFD(2)
1     FORMAT(6F10.,  I2,2X,2I2)
      IF(DS.EQ.0) GO TO 21
      PRINT 5
5     FORMAT(1H1)
      PRINT 12
      IF(L.NE.0) GO TO 17
      READ 2,E1,S1,M1,X ,E2,S2,M2,Y
2     FORMAT(8F10. )
      IF(E.NE.0)GO TO 16
      E=SQRT(E1*E2)
      S=.5*(S1+S2)
16    PM=M1*M2
      SM=M1+M2
      RM=PM/SM
      M12=M1/M2
      M21=M2/M1
      SM1=M12*M12
      SM2=M21*M21
      TS=T/E
17    DR=DS/DB
      PRINT 18,DS,DB,E1,S1,E2,S2
18    FORMAT(10X*D(SMALL)=*F8.6,1X*D(BIG)=*F8.6/
     $       10X*E1/K=*F7.3* K*4X*SIGMA1=*F7.4* A*/
     $       10X*E2/K=*F7.3* K*4X*SIGMA2=*F7.4* A*/)
      PRINT 501,X,Y
501   FORMAT(10X* MOLE FRACTIONS USED*/10X,2F12.6)
      CX=1.-X $ CY=1.-Y
      R(1)=S1 $ R(2)=S2 $ B(1)=E1 $ B(2)=E2
      TE(1)=T/E1
      TE(2)=T/E2
      DO 19 J=1,2
      IF(IFD(J).EQ.1) GO TO 23
      K=500
      GO TO 22
23    K=660
22    CONTINUE
      QP=30.9439/(R(J)*SQRT(B(J)*RM))
      CALL LINT(K,QP,TE(J),C2(J))
19    CONTINUE
      ED=E $ SD=S
      M11=M1*M1
      M22=M2*M2
      FS=.0026280*SQRT(T**3/(2.*RM))/P
      SF=FS/DS
      I=-1
3     I=I+1
      QP=30.9439/(S*SQRT(E*RM))
      K=20
      CALL LINT (K,QP,TS,AS)
      K=340
      CALL LINT (K,QP,TS,CI11)
      PRINT 4,I,ED,SD,QP,AS ,CI11
4     FORMAT(/10X*ITERATION*I2/12X*E/K=*F7.3* K*/10X*SIGMA=*F7.4* A*/
     $11X*Q.P.=*F7.5/12X,4H A*=,F7.5/10X*OMEGA=*F7.4 )
      SS1=(S1/S)**2
```

```
      SS2=(S2/S)**2
      RC1=C2(1)/CI11
      RC2=C2(2)/CI11
      AM=PM*AS
      F0=2.*SQRT(2.*M2/SM)*RC1*SS1/(M2*SM)
      FT=2.*SQRT(2.*M1/SM)*RC2*SS2/(M1*SM)
      P1=M11*F0
      P2=M22*FT
      Q1=F0*(M11+3.*M22+1.6*AM)
      Q2=FT*(M22+3.*M11+1.6*AM)
      F3=15.*((M1-M2)/SM)**2
      F4=8.*AM/(SM*SM)
      P12=F3+F4
      Q12=F3+4.*F4+1.6*SM/SQRT(PM)*RC1*RC2*SS1*SS2
      XL=(X*X*P1+CX*CX*P2+X*CX*P12)/
     $   (X*X*Q1+CX*CX*Q2+X*CX*Q12)
      XH=(Y*Y*P1+CY*CY*P2+Y*CY*P12)/
     $   (Y*Y*Q1+CY*CY*Q2+Y*CY*Q12)
      CS=(SQRT((10.*(DR-1.))/(XL-XH*DR))+5.)/6.
      K=180
      CALL LINT (K,QP,CS,TS)
      K=340
      CALL LINT (K,QP,TS,CI11)
      DF=.1*(6.*CS-5.)**2
      GD=1.+DF*XL
      SD=SQRT(SF*GD/CI11)
      ED=T/TS
      SR=100.*ABS(SD/S-1.)
      PRINT15,CS,CI11,TS,ER,SR
15    FORMAT(12X,4H C*=,F7.5/10X,13H OMEGA(1,1)*=,F7.5/12X,4H T*=,F7.5/
     $ 10X*PER CENT DIFFERENCE BETWEEN*/14X*E/K(N+1) AND E/K(N) =*F6.3/
     $ 14X*SIGMA(N+1) AND SIGMA(N) =*F6.3//)
      ER=100.*ABS(ED/E-1.)
      IF(SR.LE..01.AND.ER.LE..1) GO TO 8
      IF(I.GE.5) GO TO 6
      E=ED
      S=SD
      GO TO 3
 6    PRINT 7
      GO TO 10
 7    FORMAT(10X*FIVE CYCLES HAVE BEEN RUN WITHOUT SUCCESS*)
 8    PRINT 9
 9    FORMAT(10X *...FINAL.....LIMITS HAVE BEEN SATISFIED*)
 10   QP=30.9439/(SD*SQRT(ED*RM))
      PRINT 4,I,ED,SD,QP,AS ,CI11
      D=FS/(CI11*S*S)
      PRINT 13,D
 13   FORMAT(/10X *CALCULATION OF THEORETICAL COMPOSITION DEPENDENCE*/
     $ 20X *D1=*F8.5*(CM2/SEC)*//
     $          10X*MOLE FRACTION   KIHARA      D(CM2/SEC)*/
     X 12X*      1 *8X*DELTA*/ )
      DO 24 I=1,21
      X1=(I-1)/20.
      X2=1.-X1
      DELTA=DF*(X1*X1*P1+X2*X2*P2+X1*X2*P12)/
     X          (X1*X1*Q1+X2*X2*Q2+X1*X2*Q12)
      GD=1.+DELTA
      D2=D*GD
      PRINT14,X1,DELTA,D2
14    FORMAT( 16X,F4.2,6X,F7.5,4X,F8.5)
 24   CONTINUE
      GO TO 20
 21   CONTINUE
      END
```

```
     $.63854,.62146,.59512,.57524,.55936,.53498,.51665/
      DATA(X(L),L=501,660)/  1.79296,1.68473,1.59503,1.31569,1.17549,
     $1.03813,.96926,.92624,.89575,.8535,.82415,.77558,.74357,.71972,
     $.70076,.67169,.6498,.63232,.60546,.58522, 1.78232,1.67147,1.58074,
     $1.30428,1.16816,1.03507,.96782,.92549,.89532,.85334,.82407,.77556,
     $.74356,.71972,.70076,.67169,.64980,.63232,.60546,.58522,  1.71724,
     $1.60767,1.52034,1.26386,1.1403,1.01945,.95819,.91932,.89131,.85164
     $,.8234,.77562,.74369,.71983,.70084,.67173,.64982,.63233,.60546,
     $.58523, 1.55776,1.47046,1.4017,1.20165,1.10433,1.00508,.95111,
     $.91503,.88821,.84946,.82165,.77467,.74325,.71965,.70079,.67176,
     $.64986,.63236,.60548,.58524,  1.3753,1.31909,1.27415,1.13784,
     $1.06636,.98743,.94127,.9191,.88451,.84794,.82095,.77426,.74277,
     $.71917,.70036,.67147,.64967,.63223,.60542,.58521,  1.24116,1.2074,
     $1.17985,1.09043,1.03818,.97461,.93431,.90496,.88191,.84678,.82035,
     $.77398,.74251,.71894,.70017,.67134,.64959,.63218,.6054,.58519,
     $1.18449,1.15509,1.13272,1.06402,1.02228,.96755,.93074,.90309,
     $.88096,.84665,.82045,.77403,.74246,.71884,.70007,.67127,.64954,  .
     $63215,.60538,.58519,  1.22174,1.17607,1.14315,1.05991,1.01896,
     $.96692,.93133,.90424,.88242,.84858,.82284,.77716,.74551,.72145,
     $.70216,.67255,.65033,.63265,.60561,.5853 /
      DATA(X(L),L=661,820)/ 1.79296,1.68473,1.59503,1.31569,1.17549,
     $1.03813,.96926,.92624,.89575,.85350,.82415,.77558,.74357,.71972,
     $.70076,.67169,.6498,.63232,.60546,.58522,  1.77711,1.66761,1.57784
     $,1.30342,1.16783,1.03499,.96760,.92547,.89531,.85333,.82407,.77556
     $,.74356,.71972,.70076,.67169,.64980,.63232,.60546,.58522,  1.71724
     $,1.60764,1.5203,1.26381,1.14021,1.01929,.95790,.91886,.89068,
     $.85078,.82249,.77494,.74326,.71956,.70067,.67165,.64976,.63231,
     $.60545,.58522,  1.55747,1.47030,1.40160,1.20165,1.10439,1.00528,
     $.95140,.91535,.88852,.84966,.82170,.77438,.74281,.71920,.70039,
     $.67149,.64968,.63224,.60542,.58521,  1.37658,1.31991,1.27470,
     $1.13796,1.06642,.98746,.94129,.90912,.88453,.84797,.82100,.77434,
     $.74283,.7192),.70039,.67148,.64967,.63224,.60542,.58521,  1.23757,
     $1.20582,1.17912,1.09039,1.03813,.97452,.93423,.90491,.88188,.84681
     $,.82043,.77414,.74269,.71910,.70030,.67142,.64964,.63221,.60541,
     $.58520,  1.13668,1.12774,1.11650,1.06200,1.02183,.96762,.93089,
     $.90324,.88109,.84677,.82059,.77423,.74268,.71904,.70023,.67137,
     $.64960,.63219,.60540,.58520,  1.03436,1.05388,1.06242,1.04678,
     $1.01560,.96627,.93103,.90403,.88227,.84850,.82279,.77714,.74551,
     $.72145,.70216,.67255,.65033,.63265,.60561,.58530 /
      I=1
      IQ=2*QP
      NQ=20*IQ
40    IF(K.EQ.180) GO TO 1
      N1=0
      N2=K+NQ
      GO TO 3
1     N1=K+NQ
      N2=0
3     J=1
4     IF(VG-X(J+N1))33,32,31
31    J=J+1
      GO TO 4
32    V(I)=X(J+N2)
      GO TO 100
33    V(I)=(VG-X(J-1+N1))*(X(J+N2)-X(J-1+N2))/(X(J+N1)-X(J-1+N1))+
     $ X(J-1+N2)
100   I=I+1
      IF(I.GE.3) GO TO 101
      NQ=NQ+20
      GO TO 40
101   QN=(NQ-20)/40.
      Vw=V(1)+2.*(V(2)-V(1))*(QP-QN)
      RETURN
      END
```

```
      SUBROUTINE LINT (K,OP,VG,VW)
      DIMENSION X(900) ,V(2)
      DATA(X(L),L=1,160)/ .8,.9,1.,1.5,2.,3.,4.,5.,6.,8.,10.,15.,20.,
     $25.,30.,40.,50.,60.,80.,100.,
     $1.11003,1.10807,1.10573,1.09660,1.09213,1.09248,1.09575,1.09917,
     $1.10220,1.10700,1.11054,1.11631,1.11982,1.12223,1.12401,1.12650,
     $1.12820,1.12945,1.13121,1.13241, 1.10997,1.10706,1.10425,1.09498,
     $1.09207,1.09326,1.09659,1. 9988,1.10277,1.10736,1.11078,1.11641, 1
     1.11987,1.12226,1.12403,1.12651,1.12820,1.12946,1.13121,1.13242,
     $1.09107,1.08934,1.08799,1. 8518,1.08554,1.08946,1.09435,1.09875,
     $1.10241,1.10789,1.11171,1.11747,1.12073,1.12292,1.12453,1.12681,
     $1.12839,1.12958,1.13128,1.13245, 1.06865,1.07121,1.07342,1.08159,1
     1.08728,1.09486,1.09957,1.10283,1.10531,1.10910,1.11201,1.11723,
     $1.12069,1.12308,1.12482,1.12717,1.12873,1.12987,1.13147,1.13258,
     $1.07468,1.07817,1.08100,1.08901,1.09522,1.10162,1.10572,1.10869,
     $1.11095,1.11417,1.11633,1.11970,1.12195,1.12369,1.12508,1.12717,
     $1.12866,1.12979,1.13141,1.13254, 1.09945,1.10098,1.10217,1.10575,
     $1.10792,1.11096,1.11319,1.11493,1.11632,1.11830,1.11956,1.12150,
     $1.12300,1.12433,1.12551,1.12739,1.12880,1.12988,1.13146,1.13257,
     $1.12720,1.12646,1.12577,1.12336,1.12221,1.12156,1.12174,1.12214,
     $1.12254,1.12310,1.12334,1.12363,1.12428,1.12517,1.12610,1.12773,
     $1.12902,1.13004,1.13155,1.13263 /
      DATA(X(L),L=161,309)/                1.15080,1.14888,1.14711,1.14057,
     $1.13672,1.13275,1.13094,1.13003,1.12957,1.12926,1.12930,1.12964,
     $1.12981,1.12984,1.12987,1.13010,1.13053,1.13103,1.13202,1.13288,
     $.82676,.83112,.83623,.86300,.88411,.90987,.92344,.93124,.93609,
     $.94149,.94422,.94702,.94792,.94824,.94834,.94831,.94818,.94803,
     $.94776,.94754,                      .82409,.82934,.83528,.86456,
     $.88634,.91182,.92484,.93224,.93681,.94189,.94447,.94711,.94797,
     $.94827,.94836,.94831,.94818,.94803,.94776,.94754,
     $.81323,.82268,.83183,.86847,.89165,.91655,.92855,.93510,.93903,
     $.94328,.94543,.94768,.94839,.94861,.94863,.94849,.94830,.94812,
     $.94781,.94756,                      .82373,.83645,.84754,.88533,
     $.90597,.92627,.93535,.94036,.94277,.94555,.94685,.94809,.94850,
     $.94865,.94869,.94860,.94843,.94824,.94791,.94764,
     $.86704,.87740,.88595,.91241,.92543,.93743,.94263,.94532,.94687,
     $.94844,.94911,.94955,.94951,.94936,.94919,.94885,.94856,.94831,
     $.94793,.94764,                      .91774,.92267,.92660,.93804,
     $94329,.94780,.94956,.95036,.95075,.95099,.95095,.95058,.95018,
     $.94984,.94955,.94908,.94871,.94842,.94799,.94768,
     $.95452,.95487,.95513,.95566,.95564,.95519,.95466,.95417,.95374/
      DATA(X(L),L=310,470)/
     $95303,.95246,.95144,.95076,.95027,.94989,.94931,.94888,.94854 ,
     $.94806,.94773,          .97266,.97084,.96938,.96485,.96235,.95947,
     $.95777,.95659,.95570,.95443,.95354,.95212,.95125,.95065,.95019,
     $.94949,.94900,.94863,.94813,.94775,
     $1.61524,1.52043,1.44252,1.20038,1.07633,.95025,.88456,.84267,
     $.81269,.77101,.74211,.69477,.66400,.64133,.62345,.59627,.57596,
     $.55984,.53523,.51679,  1.60338,1.50808,1.43019,1.19075,1.06953,
     $.94673,.88256,.84144,.81188,.77060,.74188,.69469,.66397,.64131,
     $.62344,.59626,.57596,.55984,.53523,.51679,   1.57390,1.47580,
     $1.39737,1.16463,1.05040,.93567,.87544,.83649,.80823,.76831,.74025,
     $.69378,.66339,.64091,.62315,.59610,.57586,.55978,.53519,.51678,
     $1.45756,1.37263,1.30577,1.11100,1.01571,.91809,.86511,.82986,
     $.80372,.76599,.73892,.69326,.66301,.64056,.62285,.59585,.57566,
     $.55962,.53519,.51672,  1.28032,1.22383,1.17893,1.04393,.97368,
     $.89635,.85128,.81999,.79018,.76107,.73543,.69153,.66206,.64003,
     $.62251,.59572,.57561,.55968,.53510,.51672, 1.12726,1.09594,1.07015
     $,.98612,.93703,.87722,.83928,.81165,.79000,.75722,.73278,.69020,
     $.66127,.63951,.62215,.59552,.57549,.55953,.53506,.51670,  1.02962,
     $1.01327,.99896,.94627,.91075,.86271,.82980,.80486,.78485,.75390/
      DATA(X(L),L=471,500)/  .73043,.68895,.66048,.63896,.62175,.59528,
     $.57534,.55942,.53501,.51666,      .96023,.97049,.96136,.92352,
     $.89493,.85332,.82337,.80010,.78113,.75141,.72861,.68796,.65986,
```

Appendix G

PROGRAM TEMPDEP calculates the fit of equation (2.6) for a series of values of specified ε_{12}/k along with the corresponding values of σ_{12}. Any mole fractions may be used since all diffusion coefficients are corrected to zero mole fraction (of heavier component) using the Kihara 2nd approximation. The main program calls the subroutine LlN which is very similar to LINT of Appendix F and also uses the same quantum corrected collision integrals.[27] The main program calls the one parameter linear least-squares program FIXLSQ1 which fixes the straight line to pass through the origin.

INPUT

1st card:

is a header card and contains identification information. The first column must be left blank,

2nd card:

E1 , F10. is ε_1/k K of the heavier component.

S1 , F10. is σ_1 of the heavier component.

M1 , F10. is the M.W. of the heavier component.

10X.

E2, S2, M3, 3F10. are the lighter component analogues of E1, S1, M1.

IFD(1) and IFD(2), 2I2 These are set to 1 if the components are Fermions, otherwise they are left blank.

3rd card:

EF , F10.10 is the first value of ε_{12}/k K to be used to generate the X_i and Y_i values of (2.6).

RN , F10.10 is the increment by which EF is increased each iteration.

S , F10.10 is the approximate value of σ_{12} that is assumed in the calculations.

NØI , I3 is the number of iterations that are required.

N , I3 is the number of points to be fitted.

4th → (3 + N)th card:

D, X1, T, 3F10.10 are the values of the diffusion coefficient, D_{12}, the mole fraction, and the temperature of each point.

This program is terminated by two blank cards after the last data set.

```
      PROGRAM TEMPDEP (INPUT,OUTPUT)
      DIMENSION C2(2),IFD(2),TE(2),R(2),B(2),C(50),D4(30,30),T0(50),
     $ CD(30),DD(30),G(30),XT(30,30)
      REAL M12,M21,M1,M2,M11,M22
20    READ 12
12    FORMAT(80H
     $                              )
      READ 2,E1,S1,M1,    E2,S2,M2,IFD(1),IFD(2)
2     FORMAT(3F10.,10X,3F10.,2I2)
      IF(E1.EQ.0) GO TO 314
      PRINT 5
5     FORMAT(1H1)
      PRINT 12
16    PM=M1*M2
      SM=M1+M2
      RM=PM/SM
      M12=M1/M2
      M21=M2/M1
      SM1=M12*M12
      SM2=M21*M21
      M11=M1*M1
      M22=M2*M2
17    F3=15.*((M1-M2)/SM)**2
      READ 110,EF,RN,S,NOI,N
110   FORMAT(3F10.10,2I3)
      DO 214 L=1,N
      READ 100,D,X1,T
100   FORMAT(3F10.10)
      G(L)=T
      DO 214 JJ=1,NOI
      RIN=JJ-1 $ E=EF+RIN*RN
      TS=T/E
      QP=30.9439/(S*SQRT(E*RM))
      K=20
      CALL LIN  (K,QP,TS,AS)
      K=180
      CALL LIN (K,QP,TS,CS)
      K=340
      CALL LIN  (K,QP,TS,CI11)
      TE(1)=T/E1
      TE(2)=T/E2
      R(1)=S1 $ R(2)=S2 $ B(1)=E1 $ B(2)=E2
      DO 19 J=1,2
      IF(IFD(J).EQ.1) GO TO 23
      K=500
      GO TO 22
23    K=660
22    CONTINUE
      QB=30.9439/(R(J)*SQRT(B(J)*RM))
      CALL LIN (K,QB,TE(J),C2(J))
19    CONTINUE
      SS1=(S1/S)**2
      SS2=(S2/S)**2
      RC1=C2(1)/CI11
      RC2=C2(2)/CI11
      AM=PM*AS
```

```
      FO=2.*SQRT(2.*M2/SM)*RC1*SS1/(M2*SM)
      FT=2.*SQRT(2.*M1/SM)*RC2*SS2/(M1*SM)
      P1=M11*FO
      P2=M22*FT
      Q1=FO*(M11+3.*M22+1.6*AM)
      Q2=FT*(M22+3.*M11+1.6*AM)
      F4=8.*AM/(SM*SM)
      P12=F3+F4
      Q12=F3+4.*F4+1.6*SM/SQRT(PM)*RC1*RC2*SS1*SS2
      DF=.1*(6.*CS-5.)**2
      XT(L,JJ)=T**1.5/C111 $ X2=1.-X1
      DELTA=DF*(X1*X1*P1+X2*X2*P2+X1*X2*P12)/
     X          (X1*X1*Q1+X2*X2*Q2+X1*X2*Q12)
      GD=(1.+DELTA)
      D4(L,JJ)=D/GD
  214 CONTINUE
      RM=SQRT(0.5*SM/PM)
      DO 199 J=1,NOI
      TOT=DT=SED=0
      RIN=J-1
      E=EF+RIN*RN
      PRINT 18,E,S
   18 FORMAT(//5X*TEMP.    X        (D)1      CD        D-CD*/
     $8X*E/K=*F5.2*    S=*F7.4/)
      DO 102 I=1,N
      C(I)=D4(I,J) $ TO(I)=XT(I,J)
  102 TOT=TOT+TO(I)
      AT=TOT/N
      CALL FIXLSQ1(TO,C,SL,ERS,N,SE)
      DO 7 I=1,N
      CD(I)=TO(I)*SL
      DT=DT+TO(I)*TO(I)
    7 DD(I)=C(I)-CD(I)
      PRINT 8,(G(I),TO(I),C(I), CD(I),DD(I),I=1,N)
    8 FORMAT(F9.3,F10.2,3F9.5)
      SIGMA=SQRT(0.002628 *RM/SL) $ P=ERS/SL
      PC=ABS(100.*P    )
      TD=1.
      UL=SIGMA*(1.+P*TD/2.)
      ZL=SIGMA*(1.-P*TD/2.)
      PRINT 399,SE
  399 FORMAT(10X*S.D. OF POINTS=*E12.4)
  105 PRINT 9,        SL,ERS,PC,AT,DT,        UL,SIGMA,ZL
    9 FORMAT(/1X *                SLOPE          ERROR            P.C. ERROR*/
     $ 6X    ,2E15.4,F10.4/10X*AV.X=*F8.2,3X*SUM(X  SQ ) =*E15.7//
     $18X,F7.4/5X*SIGMA=* F7.4,7X,*A*/18X,F7.4 )
  199 CONTINUE
      GO TO 20
  314 CONTINUE
      END
```

```
      SUBROUTINE FIXLSQ1(X,Y,S,ES,N,SE)
      DIMENSION X(50),Y(50)
      SY=SX=XX=XY=YY=0
      DO 1 I=1,N
      SY=SY+Y(I) $ SX=SX+X(I)
      XX=XX+X(I)*X(I) $ YY=YY+Y(I)*Y(I)
1     XY=XY+X(I)*Y(I)
      S=XY/XX
      SE=SQRT((YY-S*XY)/(N-2))
      ES=SE/SQRT(XX)
      RETURN
      END
```

```
      SUBROUTINE LIN  (K,OP,VG,VW)
      DIMENSION X(900) ,V(2)
      DATA(X(L),L=1,160)/ .8,.9,1.,1.5,2.,3.,4.,5.,6.,8.,10.,15.,20.,
     $25.,30.,40.,50.,60.,80.,100.,
     $1.11003,1.10807,1.10573,1.09606,1.09213,1.09248,1.09575,1.09917,
     $1.10220,1.10700,1.11054,1.11631,1.11982,1.12223,1.12401,1.12650,
     $1.12820,1.12945,1.13121,1.13241, 1.10997,1.10706,1.10425,1.09498,
     $1.09207,1.09326,1.09659,1.09988,1.10277,1.10736,1.11078,1.11641, 1
     1.11987,1.12226,1.12403,1.12651,1.12820,1.12946,1.13121,1.13242,
     $1.09107,1.08934,1.08799,1.08518,1.08554,1.08946,1.09435,1.09875,
     $1.10241,1.10789,1.11171,1.11747,1.12073,1.12292,1.12453,1.12681,
     $1.12839,1.12958,1.13128,1.13245, 1.06865,1.07121,1.07342,1.08159,1
     1.08728,1.09486,1.09957,1.10283,1.10531,1.10910,1.11201,1.11723,
     $1.12069,1.12308,1.12482,1.12717,1.12873,1.12987,1.13147,1.13258,
     $1.07468,1.07617,1.08100,1.09001,1.09522,1.10162,1.10572,1.10869,
     $1.11095,1.11417,1.11633,1.11970,1.12195,1.12369,1.12508,1.12717,
     $1.12866,1.12979,1.13141,1.13254, 1.09945,1.10098,1.10217,1.10575,
     $1.10792,1.11096,1.11319,1.11493,1.11632,1.11830,1.11956,1.12150,
     $1.12300,1.12433,1.12551,1.12739,1.12880,1.12988,1.13146,1.13257,
     $1.12720,1.12646,1.12577,1.12330,1.12221,1.12156,1.12174,1.12214,
     $1.12254,1.12310,1.12334,1.12363,1.12428,1.12517,1.12610,1.12773,
     $1.12902,1.13004,1.13155,1.13263 /
      DATA(X(L),L=161,309)/                 1.15080,1.14888,1.14711,1.14057,
     $1.13672,1.13275,1.13094,1.13003,1.12957,1.12926,1.12930,1.12964,
     $1.12981,1.12984,1.12987,1.13010,1.13053,1.13103,1.13202,1.13288,
     $.82676,.83112,.83623,.86300,.88411,.90987,.92344,.93124,.93609,
     $.94149,.94422,.94702,.94792,.94824,.94834,.94831,.94818,.94803,
     $.94776,.94754,                        .82409,.82934,.83528,.86456,
     $.88634,.91182,.92484,.93224,.93681,.94189,.94447,.94711,.94797,
     $.94827,.94836,.94831,.94818,.94803,.94776,.94754,
     $.81323,.82268,.83183,.86847,.89165,.91655,.92855,.93510,.93903,
     $.94328,.94543,.94768,.94839,.94861,.94863,.94849,.94830,.94812,
     $.94781,.94756,                        .82373,.83645,.84754,.88533,
     $.90597,.92627,.93535,.94006,.94277,.94555,.94685,.94809,.94850,
     $.94865,.94869,.94860,.94843,.94824,.94791,.94764,
     $.86704,.87740,.88595,.91241,.92543,.93743,.94263,.94532,.94687,
     $.94844,.94911,.94955,.94951,.94936,.94919,.94885,.94856,.94831,
     $.94793,.94764,                        .91774,.92267,.92660,.93804,
     $94329,.94780,.94956,.95036,.95075,.95099,.95095,.95058,.95018,
     $.94984,.94955,.94908,.94871,.94842,.94799,.94768,
     $.95452,.95487,.95513,.95566,.95564,.95519,.95466,.95417,.95374/
      DATA(X(L),L=310,470)/
     $95303,.95246,.95144,.95076,.95027,.94989,.94931,.94888,.94854 ,
     $.94806,.94773,          .97266,.97084,.96938,.96485,.96235,.95947,
     $.95777,.95659,.95570,.95443,.95354,.95212,.95125,.95065,.95019,
     $.94949,.94900,.94863,.94810,.94775,
     $1.61524,1.52043,1.44252,1.20038,1.07633,.95025,.88456,.84267,
     $.81269,.77101,.74211,.69477,.66400,.64133,.62345,.59627,.57596,
     $.55984,.53523,.51679,  1.60338,1.50808,1.43019,1.19075,1.06953,
     $.94673,.88256,.84144,.81188,.77060,.74188,.69469,.66397,.64131,
     $.62344,.59626,.57596,.55984,.53523,.51679,   1.57390,1.47580,
     $1.39737,1.16463,1.05040,.93567,.87544,.83649,.80823,.76831,.74025,
     $.69378,.66339,.64091,.62315,.59610,.57586,.55978,.53519,.51678,
     $1.45756,1.37263,1.30577,1.11100,1.01571,.91809,.86511,.82986,
     $.80372,.76599,.73892,.69326,.66301,.64058,.62285,.59585,.57566,
     $.55962,.53510,.51672,  1.28032,1.22383,1.17893,1.04393,.97368,
     $.89635,.85128,.81999,.79618,.76107,.73543,.69153,.66206,.64003,
     $.62251,.59572,.57561,.55960,.53510,.51672, 1.12726,1.09594,1.07015
     $,.98612,.93703,.87722,.83928,.81165,.79000,.75722,.73278,.69020,
     $.66127,.63951,.62215,.59552,.57549,.55953,.53506,.51670,  1.02962,
     $1.01327,.99896,.94627,.91075,.86271,.82980,.80486,.78485,.75390/
```

```
      DATA(X(L),L=471,500)/  .73043,.68695,.66048,.63896,.62175,.59528,
     $.57534,.55942,.53501,.51665,     .98023,.97049,.96136,.92352,
     $.89493,.85332,.82337,.80010,.78113,.75141,.72861,.68796,.65986,
     $.63854,.62146,.59512,.57524,.55936,.53498,.51665/
      DATA(X(L),L=501,660)/  1.79296,1.68473,1.59503,1.31569,1.17549,
     $1.03813,.96926,.92624,.89575,.8535,.82415,.77558,.74357,.71972,
     $.70076,.67169,.6498,.63232,.60546,.58522, 1.78232,1.67147,1.58074,
     $1.30428,1.16816,1.03507,.96782,.92549,.89532,.85334,.82407,.77556,
     $.74356,.71972,.70076,.67169,.64980,.63232,.60546,.58522,  1.71724,
     $1.60767,1.52034,1.26386,1.1403,1.01945,.95819,.91932,.89131,.85164
     $,.8234,.77562,.74369,.71983,.70084,.67173,.64982,.63233,.60546,
     $.58523,  1.55776,1.47046,1.4017,1.20165,1.10433,1.00508,.95111,
     $.91503,.88821,.84946,.82165,.77467,.74325,.71965,.70079,.67176,
     $.64986,.63236,.60548,.58524,  1.3753,1.31909,1.27415,1.13784,
     $1.06636,.98743,.94127,.9091,.88451,.84794,.82095,.77426,.74277,
     $.71917,.70036,.67147,.64967,.63223,.60542,.58521,  1.24116,1.2074,
     $1.17985,1.09043,1.03818,.97461,.93431,.90496,.88191,.84678,.82035,
     $.77398,.74251,.71894,.70017,.67134,.64959,.63218,.6054,.58519,
     $1.18449,1.15509,1.13272,1.06402,1.02228,.96755,.93074,.90309,
     $.88096,.84665,.82045,.77403,.74246,.71884,.70007,.67127,.64954,
     $63215,.60538,.58519,  1.22174,1.17607,1.14315,1.05991,1.01896,
     $.96692,.93133,.90424,.88242,.84858,.82284,.77716,.74551,.72145,
     $.70216,.67255,.65033,.63265,.60561,.5853 /
      DATA(X(L),L=661,820)/ 1.79296,1.68473,1.59503,1.31569,1.17549,
     $1.03813,.96926,.92624,.89575,.85350,.82415,.77558,.74357,.71972,
     $.70076,.67169,.6498,.63232,.60546,.58522,  1.77711,1.66761,1.57784
     $,1.30342,1.16783,1.03499,.96780,.92547,.89531,.85333,.82407,.77556
     $,.74356,.71972,.70076,.67169,.64980,.63232,.60546,.58522,  1.71724
     $,1.60764,1.5203,1.26381,1.14021,1.01929,.95790,.91886,.89068,
     $.85078,.82249,.77494,.74326,.71956,.70067,.67165,.64978,.63231,
     $.60545,.58522,  1.55747,1.47030,1.40160,1.20165,1.10439,1.00528,
     $.95140,.91535,.88852,.84966,.82170,.77438,.74281,.71920,.70039,
     $.67149,.64968,.63224,.60542,.58521,  1.37658,1.31991,1.27470,
     $1.13796,1.06642,.98746,.94129,.90912,.88453,.84797,.82100,.77434,
     $.74283,.71921,.70039,.67148,.64967,.63224,.60542,.58521,  1.23757,
     $1.20582,1.17912,1.09039,1.03813,.97452,.93423,.90491,.88188,.84681
     $,.82043,.77414,.74269,.71910,.70030,.67142,.64964,.63221,.60541,
     $.58520,  1.13668,1.12774,1.11650,1.06200,1.02183,.96762,.93089,
     $.90324,.88109,.84677,.82059,.77423,.74268,.71904,.70023,.67137,
     $.64960,.63219,.60540,.58520,  1.03436,1.05388,1.06242,1.04678,
     $1.01560,.96627,.93103,.90403,.88227,.84850,.82279,.77714,.74551,
     $.72145,.70216,.67255,.65033,.63265,.60561,.58530 /
      I=1
      IQ=2*QP
      NQ=20*IQ
      N1=0
      N2=K+NQ
      J=1
4     IF(VG-X(J+N1))33,32,31
31    J=J+1
      GO TO 4
32    V(I)=X(J+N2)
      GO TO 100
33    V(I)=(VG-X(J-1+N1))*(X(J+N2)-X(J-1+N2))/(X(J+N1)-X(J-1+N1))+
     $ X(J-1+N2)
100   I=I+1
      IF(I.GE. 3) GO TO 101
      NQ=NQ+20
      GO TO 4
101   QN=(NQ-20)/40.
      VW=V(1)+2.*(V(2)-V(1))*(QP-QN)
      RETURN
      END
```

References

1. Bearman, R.J. J.Phys.Chem., 65, 1961 (1961).
2. Jost, W. "Diffusion in Solids, Liquids, Gases" Academic Press (1952).
3. Harned, H.S. and French, D.M. Ann. N.Y. Acad.Sci., 46, 267 (1945).
4. Gover, T.A. J.Chem.Ed., 44, 409 (1967).
5. Fenwal Electronics, Framingham, Massachusetts. Thermistor Manual EMC-5.
6. Strong, J.D. "Procedures in Experimental Physics." Prentice-Hall (1938), p. 585.
7. Stokes, R.H. N.Z. J.Sci.Technol., 27, 75 (1945).
8. Schupp, O.E. III. "Technique in Organic Chemistry, Vol. XIII, Gas Chromatography", A. Weissberger, ed. Interscience (1968), p. 135.
9. Precision Pressure Gage, Model 145 of Texas Instruments Inc., Houston, Texas.
10. Trademark of Crawford Fitting Company, Solon 39, Ohio. These fittings allow tubes to be joined without torsion on the tubes.
11. Callahan, F.J. "Swagelok Tube Fitting and Installation Manual", Crawford Fitting Co., Cleveland, Ohio.
12. Heftmann, E. "Chromatography" Reinhold (1967), p. 203.
13. Johns, T. and Sternberg, J.C. in "Instrumentation in Gas Chromatography", Krugers, J. ed., Centrex Publishing Co. (1968), p. 189.
14. Malinauskas, A.P. J.Chem.Phys., 42, 156 (1965).
15. Manner, M. Ph.D. thesis University of Wisconsin (1967). Available from University Microfilms, Inc., Ann Arbor, Michigan.

16. Mason, E.A.,Miller, L., and Spurling, T.H. J.Chem.Phys., 47, 1669 (1967).

17. Clusius, K. and Waldmann, L. Die Naturwiss. 30, 711 (1942).

18. van Heijningen, R.J.J., Harpe, J.P., and Beenakker, J.J.M. Physica, 38, 1 (1968).

19. van Heijningen, R.J.J., Feberwee, A., van Oosten, A., and Beenakker, J.J.M. Physica, 32, 1649 (1966).

20. Any standard applied mathematics text e.g. Kreyszig, E. "Advanced Engineering Mathematics." 2nd ed., J. Wiley (1967), p. 434.

21. Loschmidt, J. Sitzber.Akad.Wiss.Wien, 61, 367 (1870).

22. Hirschfelder, J.O., Curtiss, C.F., and Bird, R.B. "Molecular Theory of Gases and Liquids", Corrected edition. J. Wiley (1964).

23. Hanley, H.J.M., McCarty, R.D., and Cohen, E.G.D. Physica, 60, 322 (1972).

24. Iwasaki, H. and Kestin, J. Physica, 29, 1345 (1963).

25. Kestin, J. and Yata, J. J.Chem.Phys., 49, 4780 (1968).

26. Yabsley, M.A. Carson, P.J., and Dunlop, P.J. J.Phys.Chem., 77, 703 (1973).

27. Munn, R.J., Smith, F.J., Mason, E.A., and Monchick, L. J.Chem.Phys., 42, 537 (1965).

28. Imam-Rahajoe, S., Curtiss, C.F., and Bernstein, R.B. Jr. J.Chem.Phys., 42, 530 (1965).

29. Mason, E.A. J.Chem.Phys., 22, 169 (1954).

30. Ferziber, J.H. and Kaper, H.G. "Mathematical Theory of Transport Properties in gases." North-Holland (1972), p. 265.

31. Mason, E.A. and Spurling, T.H. "The Virial Equation of State." Pergamon Press (1969).

32. Smith, F.T. in "VII International Conference of the Physics of Electronic and Atomic Collisions." North-Holland (1972).

33. Hirschfelder, J.O. ed. "Intermolecular Forces", Vol.12 of Advances in Chemical Physics. J. Wiley (1967).

34. Hanley, H.J.M. and Klein, M. J.Chem.Phys., 76, 1743 (1972).

35. Hanley, H.J.M. and Klein, M. NBS Tech. Note 360 (1967).

36. Margenau, H. and Kestner, N.R. "Theory of Intermolecular Forces." Pergamon Press (1969). Chapter 2.

37. Brush, S.G. "Kinetic Theory", Vol.3. Pergamon Press (1972), Chapter 3.

38. Ref. 36, Chap. 3.

39. Amdur, I. and Jordan, J.E. in "Molecular Beams", Vol.10 of Advances in Chemical Physics. J. Wiley (1966).

40. Mason, E.A. J.Chem.Phys., 27, 75 (1957).

41. Bennett, C.A. and Franklin, N.L. "Statistical Analysis in Chemistry and the Chemical Industry." J. Wiley (1954), p. 228-232.

42. Amdur, I. and Schatzki, T.F. J.Chem.Phys., 29, 1 (1958).

43. Marrero, T.R. Ph.D. thesis, Univeristy of Maryland (1970). Some of this material is also in AIChE Journal, 19, 498 (1973) by Marrero, T.R. and Mason, E.A. J.Phys.Chem.Ref. Data, 1, 3 (1972), and Adv.Atom.Mol.Phys., 6, 155 (1970), also by the same authors.

44. Hogervorst, W. Physica, 51, 59 (1971).

45. Cohen, E.G.D. "Transport Phenomena in Dense Gases" in Proceedings of Int. Seminar on the Transport Properties of Gases. Brown University (1964), p. 125.

46. Wakeham, W.A. J.Phys.(B), 6, 372 (1973).

47. Thorne, H.H. in "The Mathematical Theory of Non-Uniform Gases" 3rd ed. by Chapman, S. and Cowling, T.G. Cambridge University Press (1970), p. 311.

48. McConalogue, D.J. and McLaughlin, E. Molecular Phys., 16, 501 (1969).

49. Durbin, L. and Kobayashi, R. J.Chem.Phys., 37, 1643 (1962).

50. Dufour, L. Pogg.Ann., 148, 490 (1873).

51. Waldmann, L. in "Encyclopedia of Physics" Vol.12. Springer-Verlag (1958).

52. Lunggren, S. Arkiv För Kemi, 24, 1 (1965).

53. Kieselbach, R. Analytical Chem., 32, 1749 (1960). My thanks to Dr. K.R. Harris, formerly of this Department, for bringing this to my attention.

54. Miller, L. and Mason, E.A. Phys. of Fluids, 9, 711 (1966).

55. Grew, K.E. and Ibbs, T.L. "Thermal Diffusion in Gases." Cambridge University Press (1952). Chapter VI.

56. Wolberg, J.R. "Prediction Analysis" Van Nostrand (1967).

57. Dymond, J.H. and Smith, E.B. "The Virial Coefficients of Gases." Oxford University Press (1969).

58. Kalfloglou, N.K. and Miller, J.G. J.Phys.Chem., 71, 1256 (1967).

59. Dipippo, R. Kestin, J., and Oguchi, K. J.Chem.Phys., 46, 4986 (1967).

60. Trappeniers, N.J. and Michels, J.P.J. Chem.Phys.Lett., 18, 1 (1973).

61. Karra, J.S. and Kemmerer, G.E. Jr. Phys.Lett., 334, 105 (1970).

62. Hogervorst, W. Physica, 51, 77 (1971).

63. Zandbergen, P. and Beenakker, J.J.M. Physica, 33, 343 (1967).

64. Carson, P.J., Dunlop, P.J., and Bell, T.N. J.Chem.Phys., 56, 531 (1972).

65. Westenberg, A.A. and Frazier, G. J.Chem.Phys., 36, 3499 (1962).

66. Carson, P.J. and Dunlop, P.J. Chem.Phys.Lett., 14, 377 (1972).

Reprinted from:

THE JOURNAL OF CHEMICAL PHYSICS VOLUME 56, NUMBER 1 1 JANUARY 1972

Precise Method for Measuring Absolute Values of Diffusion Coefficients of Binary Gas Mixtures*

P. J. CARSON AND PETER J. DUNLOP

Department of Physical and Inorganic Chemistry, University of Adelaide, Adelaide, South Australia

AND

T. N. BELL

Chemistry Department, Simon Fraser University, Burnaby 2, British Columbia, Canada

(Received 25 May 1971)

An apparatus is described for determining binary diffusion coefficients of gases as a function of temperature, pressure, and concentration. Binary diffusion coefficients are reported for the systems H_2–N_2 and He–Ar at 300°K and 1 atm. The data are believed to be precise to *approximately* 0.2%, and show a linear dependence on concentration for the system H_2–N_2.

I. INTRODUCTION

This article describes an apparatus for measuring absolute values of the diffusion coefficients of binary gas mixtures which are undergoing "restricted diffusion".[1] The method incorporates suggestions made in 1945 by Onsager[1] to Harned and co-workers, who built a diffusion cell and, using a conductance bridge to monitor concentration changes, measured diffusion coefficients for many binary systems of strong electrolytes in water.[2] Their data provided the first test of the Onsager–Fuoss theory[3] which predicts for such systems the limiting slope of the curve of the diffusion coefficient versus the square root of the concentration. In 1967 Gover[4] reported that students at the University of Virginia, Charlottesville, had utilized the above technique to measure binary diffusion coefficients of gaseous systems with a precision of 1%. We believe that we have improved the method to yield data with a precision of *approximately* two-tenths of a percent, and intend to use the technique to study the dependence of the diffusion coefficients of binary gaseous systems on concentration, on temperature, and on pressure. Data for two binary systems at one atm pressure and 300°K were obtained to test the apparatus and are reported below and compared with similar data obtained by Beenakker and co-workers[5,6] who used the "two-bulb technique" of Ney and Armistead.[7] A brief comment is made on the agreement between the data and the Chapman–Enskog theory[8–10] for predicting the variation of the binary diffusion coefficient with concentration.

II. THEORY

Restricted diffusion may be defined as unidirectional relative transport of components in a cell of constant cross section and of finite length so that concentration changes take place at both ends of the cell. For a binary mixture the concentration distribution in such a vertical cell is obtained by solving Fick's second law

$$(\partial\rho_2/\partial t)_{T,p}=D_{12}(\partial^2\rho_2/\partial x^2)_{T,p} \qquad (1)$$

subject to the physical restriction that there is no transport through both ends of the cell

$$(\partial\rho_2/\partial x)=0 \qquad \text{at } x=0 \text{ and } l. \qquad (1')$$

In the above relationships ρ_2 is the mass density of the *heavier* component, t is the time, T is the absolute temperature, p the pressure, D_{12} is the binary diffusion coefficient, l is the length of the cell, and x is the distance along the direction of transport.

The required solution of Eq. (1) for the variation with time of ρ_2 in the cell is the Fourier series[11,12]

$$\rho_2=A_0+\sum_{n=1}^{\infty}A_n\exp\left(\frac{-n^2\pi^2D_{12}t}{l^2}\right)\cos\left(\frac{n\pi x}{l}\right), \qquad (2)$$

where A_0 and A_n are constants. This relation is best utilized, as suggested by Onsager, if a cell is designed so that *differences* in concentration are measured at two planes at right angles to the direction of transport and equidistant from the cell center, for then all the even terms in Eq. (2) vanish to give

$$[\rho_2(x)-\rho_2(l-x)]=2A_1\exp(-\pi^2D_{12}t/l^2)\cos(\pi x/l)+2A_3\exp(-9\pi^2D_{12}t/l^2)\cos(3\pi x/l)+2A_5\exp(-25\pi^2D_{12}t/l^2)\cos(5\pi x/l)+\cdots. \qquad (3)$$

In addition, if x is chosen to be $(l/6)$, Eq. (3) simplifies to

$$\Delta\rho_2(t)\equiv[\rho_2(l/6)-\rho_2(5l/6)]=2A_1\exp(-\pi^2D_{12}t/l^2)+2A_5\exp(-25\pi^2D_{12}t/l^2)+\cdots \qquad (4)$$

and for large values of t the second and all higher terms of Eq. (4) may be neglected, and the differential diffusion coefficient is obtained from

$$\ln[\Delta\rho_2(t)]=\text{const}-(\pi^2D_{12}t/l^2) \qquad (5)$$

by determining the variation with time of the difference function $\Delta\rho_2(t)$.

We have measured a quantity which is directly proportional to $\Delta\rho_2(t)$ by first inserting matched thermistors T_1 and T_2 into the diffusion cell (see Fig. 1) at positions $x=l/6$ and $x=5l/6$ and then

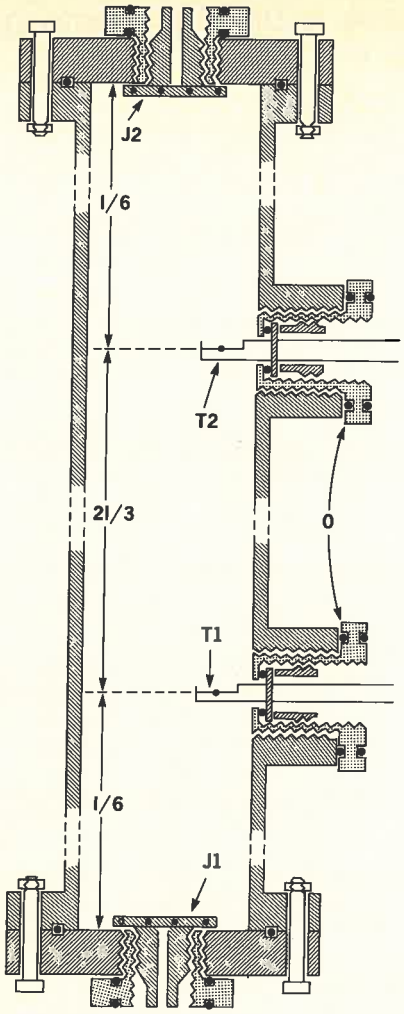

FIG. 1. Stainless steel diffusion cell in section; T_1 and T_2 are the thermistors, each positioned at a distance ($l/6$) from the ends of the cell; J_1 and J_2 are multijets to control the direction of flow of the gases while they are being introduced into the cell; O indicates some of the O rings used for both water and vacuum seals.

making them two of the arms of a sensitive Wheatstone bridge (see Fig. 2). D_{12} is then simply obtained by a linear least-squares procedure.

III. EXPERIMENTAL

A diagram of the diffusion cell is shown in Fig. 1. The cell for use at one atm pressure was 102.00 cm in length and was fabricated from type 316 stainless steel tubing with a thickness of 0.25 cm and an outside diameter of 5 cm. The end plates of the cell were bolted into position and made vacuum tight with viton O rings (indium O rings could easily be incorporated for use at low temperatures). Nupro bellows valves (Nupro Co., Cleveland, Ohio) which screwed directly into these end plates were used to control the gases entering and leaving the cell. The matched thermistors T_1 and T_2 (Fenwal Electronics, Framingham, Massachusetts) were also sealed into position with O rings. Plastic-coated, shielded cables were used to connect the thermistors to the Wheatstone bridge. O rings, which surrounded the cables where they entered the cell, sealed the thermistors from the water in the thermostat bath. The remaining features of the cell are illustrated in Fig. 1.

The cell was first kinematically suspended[13] in the thermostat bath which was filled with approximately 500 kg of water and then adjusted to a vertical position with a sensitive box level. The bath was stirred vigorously with a propellor blade 6 in. in diameter which was attached directly to the extended shaft of a $\frac{1}{3}$ hp motor. The bath temperature was maintained by means of an "on-off" mercury-toluene regulator which controlled the current passing through a stainless steel pyrotenax heater. When in operation the temperature of the bath varied by less than ± 0.001°K over a period of 8 h.

The cell and the adjacent vacuum lines were evacuated by means of an Edwards oil diffusion pump. Pressures of 10^{-6} torr were easily attainable. All the gases used in this study had purities greater than 99.99% and were used to form binary mixtures by introducing them into the diffusion cell from a stainless steel manifold which was situated in the thermostat bath and positioned directly below the cell. Pressures were measured by means of a Bourdon Tube (Texas Instruments, Houston) attached by means of flexible metal hosing to the manifold. As indicated in Fig. 1, gases could be introduced from the top and bottom of the cell. Small "multijets," situated at both ends of the cell, served to direct the gases in a horizontal direction and also to reduce the small "dead space" in the side of the Nupro valve facing the cell (see Fig. 1).

An experiment was performed by first introducing a mixture of known composition into the cell (the gas mixture was prepared by using the cell, the adjacent manifold, and the Texas Bourdon Gauge), and then one of the pure gases at a somewhat higher pressure than the mixture into the manifold. After the system had reached equilibrium the gas in the manifold was very slowly introduced into the cell by means of one of the Nupro bellows valves situated at each end of the cell. The variable resistance (e.s.i., Portland, Oregon) in the Wheatstone bridge (see

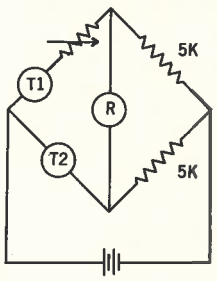

FIG. 2. Circuit used to measure the *difference* in resistance between the thermistors T_1 and T_2. The two 5K resistors are essentially identical.

TABLE I. Results obtained from a least-squares treatment of data for a diffusion experiment in which argon diffused into helium. $P=1.018_5$ atm; $T=300.0$°K; $R^{\infty}(\infty)=34.81\ \Omega$; $x_2=0.081_9$ [a]; Cell length = 102.00 cm; No. exp. points = 88.

Time[b] (min)	$[R(t)]_{exp}$	$[R(t)]_{calc}$	Time[b] (min)	$[R(t)]_{exp}$	$[R(t)]_{calc}$
24	131.47_1	131.56_8	71	48.84_3	48.82_3
25	127.60_8	127.66_6	72	48.28_1	48.25_8
26	123.86_9	123.92_6	73	47.75_8	47.71_7
27	120.26_1	120.33_6	74	47.19_0	47.19_7
28	116.83_0	116.89_2	75	46.73_9	46.69_8
29	113.52_3	113.58_6	76	46.22_9	46.21_9
30	110.36_6	110.41_3	77	45.73_9	45.75_8
31	107.32_7	107.36_8	78	45.34_0	45.31_8
32	104.39_2	104.44_5	79	44.88_2	44.89_5
33	101.55_6	101.64_1	80	44.47_7	44.48_9
34	98.91_5	98.94_9	81	44.10_5	44.09_9
35	96.32_7	96.36_6	82	43.71_9	43.72_5
36	93.82_4	93.88_6	83	43.38_6	43.36_6
37	91.47_1	91.50_7	84	43.01_3	43.02_1
38	89.19_6	89.22_3	85	42.69_9	42.69_1
39	87.03_3	87.03_2	86	42.34_0	42.37_3
40	84.91_5	84.92_8	87	42.07_2	42.06_9
41	82.90_2	82.91_0	88	41.79_1	41.77_6
42	80.98_7	80.97_2	89	41.54_2	41.49_6
43	79.05_5	79.11_3	90	41.23_5	41.22_6
44	77.31_4	77.32_9	91	40.94_8	40.96_8
45	75.60_8	75.61_6	92	40.73_9	40.72_0
46	73.96_1	73.97_3	93	40.47_1	40.48_2
47	72.40_5	72.39_5	94	40.24_8	40.25_3
48	70.91_5	70.88_1	95	40.07_2	40.03_4
49	69.43_8	69.42_9	96	39.82_4	39.82_4
50	68.08_5	68.03_4	97	39.70_6	39.62_2
51	66.70_6	66.69_6	98	39.40_5	39.42_8
52	65.40_5	65.41_2	99	39.22_9	39.24_2
53	64.20_3	64.17_9	100	39.05_2	39.06_4
54	63.01_3	62.99_6	101	38.88_2	38.89_2
55	61.88_9	61.86_1	102	38.73_9	38.72_8
56	60.75_8	60.77_2	103	38.59_5	38.57_0
57	59.72_5	59.72_6	104	38.39_9	38.41_9
58	58.72_5	58.72_2	105	38.26_1	38.27_3
59	57.77_8	57.75_9	106	38.11_8	38.13_4
60	56.85_6	56.83_5	107	37.99_3	38.00_0
61	55.94_8	55.94_8	108	37.88_9	37.87_1
62	55.08_5	55.09_6	109	37.72_5	37.74_8
63	54.27_5	54.27_9	110	37.60_8	37.63_0
64	53.49_0	53.49_5	111	37.51_0	37.51_6
65	52.75_2	52.74_3			
66	52.03_3	52.02_0			
67	51.32_7	51.32_7			
68	50.66_7	50.66_2			
69	50.03_9	50.02_3			
70	49.38_6	49.41_1			

Slope of $\ln\Delta R(t)$ versus $t=-4.111_1\times10^{-2}$
Standard error in slope $=1.32\times10^{-5}$
$D_{12}(1\text{ atm}; 300\text{°K})=0.735_8\ \text{cm}^2\ \text{sec}^{-1}$
Percentage error in $D_{12}=0.03\%$
(Standard error in slope/slope) $\times 100$

[a] x_2 denotes the mole fraction of the heavy component in the equilibrium mixture.

[b] Time after commencing the experiment.

Fig. 2) was then used to balance the circuit (except for a second-order correction which was obtained with the aid of the recorder) every minute, and a final reading, $R^{\infty}(\infty)$, was taken after the system had come to equilibrium. The binary diffusion coefficient was obtained from the *difference* between the resistance reading at each time $R(t)$ and the final equilibrium value.

With a power dissipation by each thermistor of approximately 0.5 mW, it was quite easy to obtain an initial "bridge signal" of 150–200 Ω by introducing into the cell a final quantity of pure component suf-

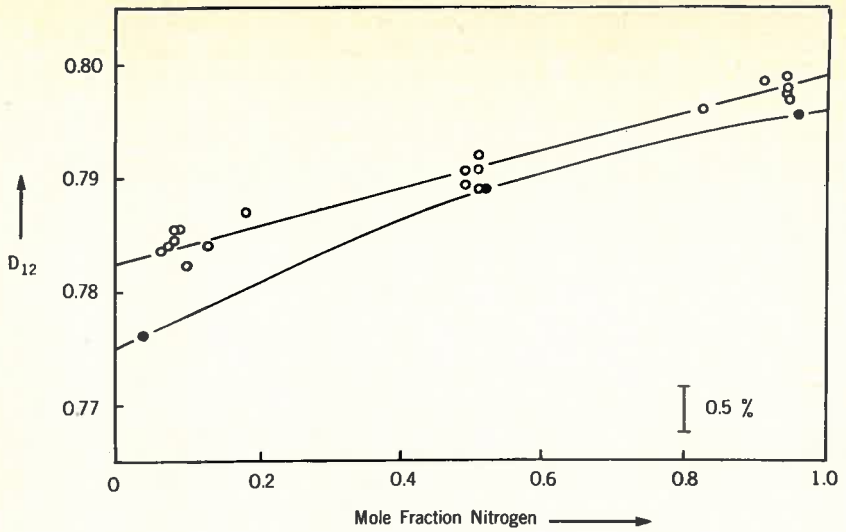

FIG. 3. Diffusion coefficients for the system H_2–N_2 at 300°K and 1 atm; –O–, experimental points; –●–, *smoothed* data of Beenakker *et al.* corrected to 300°K (not all experimental points are shown on the graph).

ficient to change the initial pressure by about 10%. Measurements were recorded during the period that the bridge signal decreased from 100 to 5 Ω. Experiments were designed to permit the value of $R^\infty(\infty)$ to be measured approximately 3 to 4 hours after commencing the experiment. It is believed that the $R^\infty(\infty)$ values are known to ±0.02 Ω.

IV. TREATMENT OF DATA

Although the two thermistors in the cell were specially selected to have absolute values and temperature coefficients which were as close as possible, they were nevertheless not perfectly "matched." As a result the resistances required to balance the bridge before and after an experiment changed by as much as 0.5 Ω. While diffusion was taking place the bridge signal was thus due to (a) differences in the thermal conductivities of the gas mixtures surrounding each thermistor, and (b) the *slight* difference in the temperature coefficients of the thermistors. The following procedure was used to treat the experimental data.

TABLE II. Binary diffusion coefficients for the system H_2–N_2 at 1 atm and 300°K.

x_{N_2}	D_{12} (cm² sec⁻¹)	x_{N_2}	D_{12} (cm² sec⁻¹)
0.065_2	0.783_5	0.511_2	0.789_1
0.076_1	0.784_0	0.511_5	0.791_8
0.081_2	0.784_4	0.512_3	0.790_8
0.081_4	0.785_4	0.823_6	0.796_0
0.081_9	0.785_2	0.911_0	0.798_5
0.099_7	0.785_4	0.941_7	0.797_3
0.111_1	0.782_1	0.942_0	0.798_9
0.128_4	0.783_9	0.942_8	0.798_1
0.180_2	0.786_9	0.946_2	0.797_1
0.491_1	0.789_6	0.947_3	0.797_7
0.492_1	0.790_8		

Let $R(t)$ be the resistance required to balance the bridge at time t, and $R^\infty(\infty)$ the resistance to balance the bridge at infinite time. Then, because the thermistors are not perfectly matched, the reference resistance which should be used to form "differences" proportional to $\Delta\rho_2(t)$ is a function of time and only becomes equal to $R^\infty(\infty)$ at equilibrium. Thus we define an effective reference point $R^\infty(t)$ at time t by the series expansion

$$R^\infty(t)=R^\infty(\infty)+a_1[\Delta\rho_2(t)]+a_2[\Delta\rho_2(t)]^2+\cdots, \quad (6)$$

where a_1 and a_2 are constants which depend on the *differences* between the characteristics of the thermistors ($a_1=a_2=\cdots=0$ for percent matching). Then in order to use Eq. (5) and the values of $R(t)$ and $R^\infty(\infty)$ to obtain the binary diffusion coefficient, we assume the quantity $[R(t)-R^\infty(t)]$ may be expressed as a series expansion in the concentration difference $\Delta\rho_2(t)$

$$[R(t)-R^\infty(t)]=b_1[\Delta\rho_2(t)]+b_2[\Delta\rho_2(t)]^2+\cdots, \quad (7)$$

where b_1 and b_2 are constants for a given experiment, and require that the experiments be allowed to proceed for times long enough so that the second-order terms in Eqs. (6) and (7) are negligible. With this restric-

TABLE III. Binary diffusion coefficients for the system He–Ar at 1 atm and 300°K.

x_{Ar}	D_{12} (cm² sec⁻¹)	x_{Ar}	D_{12} (cm² sec⁻¹)
0.081_9	0.735_6	0.559_6	0.751_6
0.086_4	0.737_5	0.751_9	0.754_4
0.087_1	0.737_5	0.938_0	0.756_8
0.272_3	0.743_7	0.945_0	0.756_5
0.557_2	0.750_8		

tion these two equations may be combined to yield

$$\Delta R(t) \equiv [R(t) - R^{\infty}(\infty)]$$
$$= (a_1 + b_1)[\Delta\rho_2(t)]. \quad (8)$$

Thus Eq. (5) may be used to obtain D_{12} either by graphing $\ln[\Delta R(t)]$ versus t or by using the method of least squares. The slope will be linear for times great enough so that the higher terms in Eqs. (4), (6), and (7) are negligible. Table I summarizes the results obtained in an experiment in which a small quantity of argon was introduced into the bottom of a diffusion cell (Fig. 1) containing pure helium. The mole fraction of argon, x_2, in the cell at the end of the experiment was 0.0819 and the total pressure 1.018_5 atm. It was not possible to detect a change in pressure in the cell by taking measurements before and after the experiment. The percentage error in the diffusion coefficient calculated from the standard error in the slope of $\ln[\Delta R(t)]$ versus t was usually less than that caused by an error in $R^{\infty}(\infty)$ of 0.01 Ω. It is believed that this latter error accounts for most of the error in D_{12} and, depending on the number of experimental points used, varies from 0.05 to 0.1%. The agreement between the values of $[R(t)]_{\text{exp}}$ and $[R(t)]_{\text{calc}}$ in Table I indicates that the assumptions made in using Eqs. (5) and (8) to obtain D_{12} are not unreasonable.

V. DISCUSSION

Tables II and III list the diffusion coefficients obtained for the systems H_2–N_2 and He–Ar, respectively, at 300°K and 1 atm. The results for both systems are compared in Figs. 3 and 4 with similar "smoothed" data obtained by Beenakker *et al.*[5,6] The latter data were corrected to 300°K to make a direct comparison possible. In both cases the diffusion coefficients obtained in this study show a considerably lower concentration dependence than that obtained by the former workers,[5,6] who were unable to explain the high concentration dependence they obtained for binary

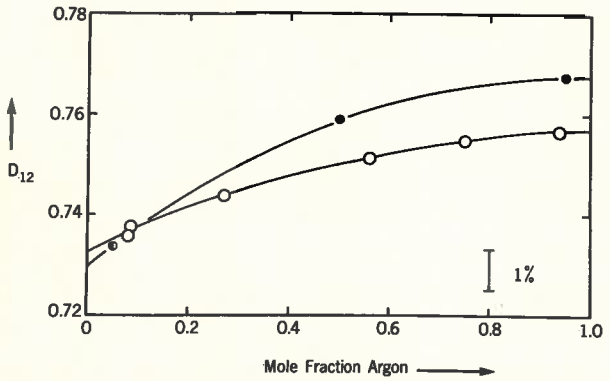

FIG. 4. Diffusion coefficients for the system He–Ar at 300°K and 1 atm: –○–, experimental points; –●–, *smoothed* data of Beenakker *et al.* corrected to 300°K (not all experimental points are shown on the graph).

TABLE IV.[a] Data for the system He–Ar for comparison with the results in Table III and Fig. 4.

x_2	D_{12} (cm² sec⁻¹)	Ref.
~0	0.734	14
~0	0.734	15
0.37	0.745	16
0.5	0.741	17
0.5	0.737	18
0.5	0.764	19
0.5	0.735	20
0.5	0.747	21
0.5	0.761	22
0.5	0.737	23
~1.0	0.763	14

[a] All values have been corrected to 300°K.

rare gas systems containing helium. We believe the concentration dependence of the H_2–N_2 system to be linear within the experimental error (Fig. 3). In addition, although the data for He–Ar certainly do not indicate a linear concentration dependence at 1 atm, our recent diffusion studies as a function of pressure for this system indicate that the concentration dependence *may* well be linear at lower pressures. Should this prove to be the case, it would seem that the second approximations of Chapman[8,10] and of Kihara[9,10] *may* well be unsuitable for predicting the concentration dependence of the binary diffusion coefficients of mixtures of rare gases. Since diatomic molecules do not have radial symmetry, the system H_2–N_2 is not expected to obey the Chapman–Enskog theory.[8] Certainly by assuming reasonable potential parameters the concentration dependence of the diffusion coefficient of the system H_2–N_2 reported here is considerably lower than that predicted by the above theory for a system which is Lorentzian[10] at one extreme ($x_2 \simeq 1$) and quasi-Lorentzian[10] at the other ($x_2 \simeq 0$).

Most of the more recent diffusion data for the system He–Ar have been corrected to 300°K and listed in Table IV.[14–23] All these results agree with the data in Table III within ±2%.

ACKNOWLEDGMENTS

The authors wish to compliment Arthur Bowers of Adelaide University, South Australia, Frank Wick of Simon Fraser University, British Columbia, and their staff for the excellent work done in constructing the stainless steel diffusion cells.

* This work was supported in part by the Australian Research Grants Committee and the National Research Council.

[1] H. S. Harned and D. M. French, Ann. N.Y. Acad. Sci. **46**, 267 (1945).
[2] H. S. Harned, Chem. Rev. **40**, 461 (1947).
[3] L. Onsager and R. M. Fuoss, J. Phys. Chem. **36**, 2689 (1932).
[4] T. A. Gover, J. Chem. Educ. **44**, 409 (1967).

[5] R. J. J. Van Heijningen, A. Feberwee, A. van Oosten, and J. J. M. Beenakker, Physica **32,** 1649 (1966).
[6] R. J. J. Van Heijningen, J. P. Harpe, and J. J. M. Beenakker, Physica **38,** 1 (1968).
[7] E. P. Ney and F. C. Armistead, Phys. Rev. **71,** 14 (1946).
[8] S. Chapman and T. G. Cowling, *The Mathematical Theory of Non-Uniform Gases* (Cambridge U. P., New York, 1952).
[9] T. Kihara, *Imperfect Gases* (Asakura Bookstore, Tokyo, 1949); Rev. Mod. Phys. **25,** 831 (1953).
[10] E. A. Mason, J. Chem. Phys. **27,** 75, 782 (1957).
[11] J. Crank, *The Mathematics of Diffusion* (Oxford U. P., London, England, 1956).
[12] H. S. Carslaw and J. C. Jaeger, *Conduction of Heat in Solids* (Oxford U. P., New York, 1959), 2nd ed.
[13] J. D. Strong, *Procedures in Experimental Physics* (Prentice-Hall, Englewood Cliffs, N.J., 1938).
[14] R. E. Walker and A. A. Westenberg, J. Chem. Phys. **31,** 519 (1959).
[15] S. P. Wasik and K. E. McCulloch, J. Res. Natl. Bur. Std. **A73,** 207 (1969).
[16] K. P. Srivastava, Physica **25,** 571 (1959).
[17] B. A. Ivakin and P. E. Suetin, Zh. Tekh. Fiz. **34,** 1115 (1964). [Sov. Phys. Tech. Phys. **9,** 866 (1964)].
[18] J. N. Holsen and M. R. Strunk, Ind. Eng. Chem. Fundam. **3,** 143 (1964).
[19] S. C. Saxena and E. A. Mason Mol. Phys. **2,** 379 (1959).
[20] B. P. Mathur and S. C. Saxena, Appl. Sci. Res. Sect. A **18,** 325 (1968).
[21] A. A. Strehlow, J. Chem. Phys. **21,** 2101 (1953).
[22] A. P. Malinauskas, J. Chem. Phys. **42,** 156 (1965).
[23] S. L. Seager, L. L. Gurtson, and J. C. Giddings, J. Chem. Eng. Data **8,** 168 (1963).

THE COMPOSITION DEPENDENCE OF THE DIFFUSION COEFFICIENT OF THE SYSTEM HELIUM–KRYPTON AT 300°K AND 1 ATMOSPHERE PRESSURE

P.J. CARSON and P.J. DUNLOP

Department of Physical and Inorganic Chemistry, University of Adelaide, South Australia

Received 25 February 1972

Values of binary diffusion coefficients, $\mathcal{D}_{12}$, measured for the system helium–krypton at 300°K and 1 atm pressure, may be represented by a second order polynomial in mole fraction, and agree well with the predictions of the Kihara second approximation of the Chapman–Enskog theory.

We report here experimental diffusion coefficients, $\mathcal{D}_{12}^{\exp}$, for the system He–Kr as a function of the mole fraction of krypton, x_2. Using an apparatus which has been previously described [1], the measurements were performed at known pressures close to 0.88 atm. The thermostat temperature was maintained at 300°K with a precision better than ± 0.001°. The thermometer used to adjust the thermostat temperature was calibrated with a platinum resistance thermometer. The krypton was supplied by Matheson Gas Products and the helium by Canadian Helium Ltd. Both gases had purities better than 99.9%, and no attempt was made to purify them further.

The fifteen experimental values of $\mathcal{D}_{12}^{\exp}$, together with diffusion coefficients, $\mathcal{D}_{12}$, calculated for one atmosphere pressure by assuming a linear dependence of $\mathcal{D}_{12}^{\exp}$ on the reciprocal of the total pressure, P, are presented in table 1 as a function of x_2. These values of $\mathcal{D}_{12}$ may be represented by the parabola

$$\mathcal{D}_{12} = 0.6308_8 + 0.0480_0 x_2 - 0.0242_1 x_2^2,$$

with a standard error of 0.0009. This functional form is not in disagreement with that suggested by Mason and Marrero [2].

Using a two-bulb technique [3], van Heijningen et al. [4] measured both the temperature and composition dependences of $\mathcal{D}_{12}$ for all the binary mixtures of noble gases. They found that their measured composition dependences for mixtures containing helium were considerably greater than those predicted using the potential parameters obtained from their measured temperature dependences. The difference between their experimental and predicted values of $[\mathcal{D}_{12}(x_2 = 1)/\mathcal{D}_{12}(x_2 = 0)]$ for the system He–Kr was + 2.2%. Hogervorst [5], using a cataphoretic technique for his temperature depen-

Table 1
Binary diffusion coefficients (in $cm^2\ sec^{-1}$) for the system He–Kr at 300°K

x_2	P (atm)	$\mathcal{D}_{12}^{\exp}$	$\mathcal{D}_{12}$
0.0340	0.8801	0.7195	0.6332
0.0735	0.8716	0.7278	0.6342
0.1250	0.8800	0.7231	0.6363
0.1313	0.8934	0.7115	0.6357
0.2107	0.8541	0.7487	0.6395
0.3520	0.8806	0.7330	0.6456
0.3924	0.8808	0.7338	0.6465
0.4393	0.8800	0.7351	0.6469
0.4957	0.8792	0.7391	0.6499
0.6003	0.8812	0.7384	0.6507
0.6649	0.8753	0.7447	0.6519
0.7280	0.8789	0.7429	0.6530
0.8422	0.8350	0.7815	0.6526
0.9011	0.8578	0.7622	0.6538
0.9660	0.8798	0.7459	0.6562

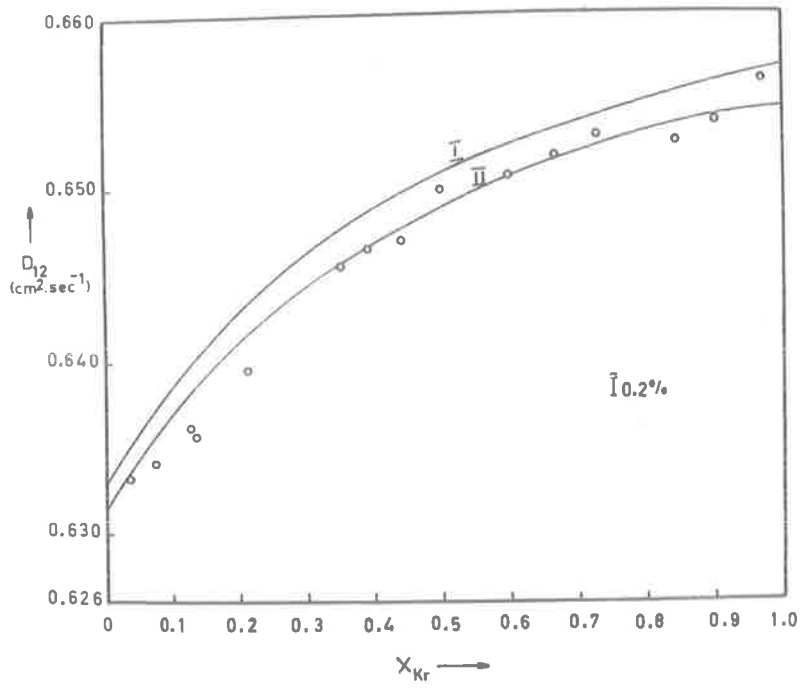

Fig. 1. Composition dependence of mutual diffusion coefficients, $\mathcal{D}_{12}$, for He–Kr at 300°K, 760 mm. o, Present results; Curves I and II calculated for $(\epsilon_{12}/k) = 39.0$°K and $\sigma_{12} = 3.17$ Å (ref. [4]) and $(\epsilon_{12}/k) = 43.5$°K and $\sigma_{12} = 3.14$ Å (ref. [5]), respectively.

dence studies, obtained rather similar parameters. Using quantum collision integrals [6], both these sets of parameters predict our composition dependence assuming the Lennard-Jones (12–6) potential and Kihara's second approximation to the Chapman–Enskog theory [7]. In fig. 1 our experimental points are compared with the composition dependences calculated with the parameters reported in refs. [4, 5]. Since both these groups of workers [4, 5] although using quite different techniques from each other and from us, obtained results over the range 5–15 mm pressure, and since our results were obtained at approximately 660 mm, the fact that over the whole concentration range all results agree within 3% seems to justify our use of the assumed linear dependence of $\mathcal{D}_{12}$ on $1/P$.

Table 2 compares some quantities derived from our results with the corresponding quantities of refs. [4, 5 The values of ϵ_{12} and σ_{12} are relatively insensitive to the absolute values of $\mathcal{D}_{12}$; a constant error of 0.2% in $\mathcal{D}_{12}$ results in an error of 0.05% in ϵ_{12} and an error of

Table 2

	ϵ_{12}/k (°K)	σ_{12} (Å)	$\mathcal{D}_{12}(x_2 = 0)$ [a]	$[\mathcal{D}_{12}(x_2 = 1)/\mathcal{D}_{12}(x_2 = 0)]$ [a]
expt [b]	37.6 ± 8.4	3.19 ± 0.06	$0.630_1 \pm 0.001_3$	1.039 ± 0.002
ref. [4]	39.0 ± 5.0	3.17 ± 0.04	$0.63_{28} \pm 0.00_{40}$	$1.038 \pm 0.001_5$
ref. [5]	43.5 ± 3.0	3.14 ± 0.02	$0.63_{16} \pm 0.00_{32}$	$1.036_9 \pm 0.000_8$

a) Columns 3 and 4 present quantities derived from columns 2 and 3.
b) Our errors have 95% fiducial limits.

0.1% in σ_{12}. On the other hand, an error in $[\mathcal{D}_{12}(x_2 = 1)/\mathcal{D}_{12}(x_2 = 0)]$ of 0.2% gives rise to errors of 22% in ϵ_{12} and of 2% in σ_{12}.

This work was supported in part by a grant from the Australian Research Grants Committee.

References

[1] P.J. Carson, T.N. Bell and P.J. Dunlop, J. Chem. Phys. 56 (1972) 531.
[2] E.A. Mason and T.R. Marrero, Advan. At. Mol. Phys. 6 (1970) 155.
[3] E.P. Ney and F.C. Armistead, Phys. Rev. 71 (1947) 14.
[4] R.J.J. van Heijingen, J.P. Harpe and J.J.M. Beenakker, Physica 38 (1968) 1.
[5] W. Hogervorst, Physica 51 (1971) 59.
[6] R.J. Munn, F.J. Smith, E.A. Mason and L. Monchick, J. Chem. Phys. 42 (1965) 537.
[7] E.A. Mason, J. Chem. Phys. 27 (1957) 75.

Yabsley, M. A., Carson, P. J. & Dunlop, P. J. (1973). Binary diffusion coefficients for the system helium-chlorotrifluoromethane at 300°K and 1 atmosphere. A test of the Chapman-Enskog theory. *Journal of Physical Chemistry, 77*(5), 703–704.